

pubs.acs.org/CR Review

Phase Transitions of Associative Biomacromolecules

Rohit V. Pappu,* Samuel R. Cohen, Furqan Dar, Mina Farag, and Mrityunjoy Kar



Cite This: https://doi.org/10.1021/acs.chemrev.2c00814

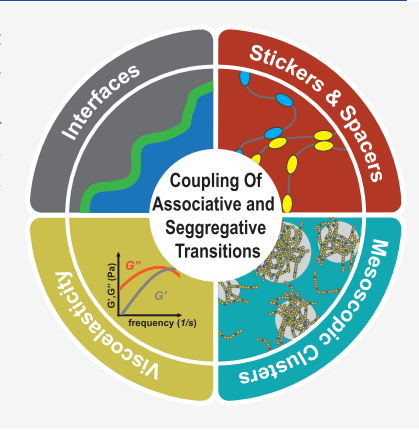


ACCESS

III Metrics & More

Article Recommendations

ABSTRACT: Multivalent proteins and nucleic acids, collectively referred to as multivalent associative biomacromolecules, provide the driving forces for the formation and compositional regulation of biomolecular condensates. Here, we review the key concepts of phase transitions of aqueous solutions of associative biomacromolecules, specifically proteins that include folded domains and intrinsically disordered regions. The phase transitions of these systems come under the rubric of coupled associative and segregative transitions. The concepts underlying these processes are presented, and their relevance to biomolecular condensates is discussed.



CONTENTS

1.0. Introduction	
	6
1.1. Physical Gelation of Biomacromolecules	E
1.2. Defintion of Physical Gels	Е
 1.3. Intrinsically Disordered Proteins and Solvent Quality 	(
•	•
1.4. The Importance of Phase Separation in Live Cells	(
1.5. Phase Separation Combined with Physical	
Gelation	(
1.6. Multivalent Associative Macromolecules and Their Phase Transitions	(
1.7. Associative Macromolecules Drive the For-	
mation of Condensates	С
1.8. Scope of the Review	E
2.0. Phase Separation: One-Component Systems	
2.1. Systems of Hard Molecules	E F
2.2. Phase Separation in One-Component Sys-	
tems with Repulsive and Attractive Inter-	
actions	F
2.3. Purely Entropically Driven Phase Separation	
Can Drive Spatial Organization in Cells	C
3.0. Phase Separation in Complex Mixtures	
3.1. Mean-Field Theories for Free Energies of	
Mixing and the Interaction Parameter χ	
3.2. Phase Separation Becomes a Formal Possi-	
bility When χ Is Positive	F
3.3. χ , Osmotic Second Virial Coefficients, and	
Excluded Volumes	

3.4. Interactions that Drive Phase Separation in n-Nary Mixtures in a Complex Solvent

3.5. Gibbs Phase Rule and Mean-Field Models for	ı
Phase Separation in <i>n</i> -Nary Mixtures	_
3.6. Thermoresponsive Phase Behavior	K
4.0. Associative Macromolecules	L
4.1. Percolation Transitions in Solutions of	
Associative Macromolecules	L
4.2. Mean-Field Models for Percolation	М
5.0. Coupling of Associative and Segregative Tran-	
sitions	N
5.1. The Stickers-and-Spacers Framework	0
5.2. Mapping Stickers and Spacers onto Archi-	
tectures of Associative Macromolecules	0
5.3. Separable Contributions to Segregative and	
Associative Transitions	Р
5.4. Associative Macromolecules Form Preperco-	
lation Clusters in Subsaturated Solutions	0
5.5. Implications of Prepercolation Clusters for	_
Dynamics of Phase Transitions	S
5.6. Examples of Systems That Undergo Phase	,
Separation Coupled to Percolation	S
5.7. Complex Coacervation	T
·	
5.8. The Sweatman Model of Short-Range At-	
tractions and Long-Range Repulsions	U

Special Issue: Liquid-Liquid Phase Separation

Received: November 18, 2022



6.0. Full Phase Diagrams for Associative Macro-	
molecules	١
6.1. Single Type of Macromolecule in a Solvent	١
6.2. Annotating Measured Coexistence Curves	
with Percolation Lines	١
6.3. Spinodals and Critical Points	W
6.4. Phase Behavior near Critical Points	W
6.5. Mixtures of Two Types of Macromolecules in	
Complex Solvents	١
6.6. Extending to Complex Mixtures of Macro-	
molecules	١
7.0. Distinguishing Binding from Phase Transitions	Z
7.1. Binding without Phase Transitions Gives Rise	
to Complexes of Fixed Stoichiometries	Z
7.2. Rigidity Is Not Sufficient to Suppress Phase	
Separation	AA
7.3. High Affinity Disordered Complexes Can	
Suppress Phase Separation	AA
7.4. Impact of Site-Specific Ligand Binding on	
Phase Equilibria	AA
8.0. Interfaces and Material Properties	AE
8.1. Interfaces between Phases and Interfacial	
Free Energies	AE
8.2. Adsorption to Solid Substrates and Wetting	AC
8.3. Wetting Transitions and Phase Separation	ΑC
8.4. Adsorption Transitions, Prewetting, and the	
Connection to Prepercolation Clusters	ΑD
8.5. Summary of Key Concepts Pertaining to	
Interfaces	ΑE
8.6. Condensates Are Viscoelastic Materials	ΑE
8.7. Internal Environments of Condensates	AF
9.0. Overall Summary and Conclusions	AF
9.1. Addressing Critiques of Phase Transitions in	
Cell Biology	AF
9.2. Concluding Remarks	ΑH
Author Information	Αŀ
Corresponding Author	Αŀ
Authors	ΑH
Author Contributions	ΑH
Notes	Αŀ
Biographies	Αŀ
Acknowledgments	Α
References	Α

1.0. INTRODUCTION

There is growing recognition that cellular matter and physiologically relevant biochemical reactions are organized in space and time via the formation, regulation, and dissolution of mesoscale bodies known as biomolecular condensates. These mesoscale membraneless assemblies, comprising hundreds of distinct macromolecules, are concentrated into small volumes, and delineated by internal and external interfaces. 1,2 Here, mesoscale refers to the scale that straddles the molecular (nanometer) and cellular (micrometer) scales. Biomolecular condensates—or just condensates from now on—have distinct molecular compositions that are organized inhomogeneously, and into a range of stoichiometries.4 Measurements to date suggest that the material properties of condensates are akin to those of viscoelastic materials⁵ with either terminally viscous or terminally elastic properties.⁶ Here, terminal refers to the longtime behaviors of condensates.

Importantly, the emerging consensus is that spontaneous phase transitions contribute either directly, or in concert with active processes, to the formation and dissolution of condensates. This has prompted a growing interest in the physical chemistry of phase transitions; specifically the topics of phase separation and gelation. Key results, through the period of 2006–2012, helped catalyze the surge of interest in spontaneous and driven phase transitions in cell biology and biophysical chemistry. In this review, we describe the conceptual underpinnings that pertain to the equilibrium phase transitions of macromolecules that drive the formation and dissolution of condensates in cells, and of simple facsimiles of condensates *in vitro*.

1.1. Physical Gelation of Biomacromolecules

The importance of phase transitions such as physical gelation, ¹³ generalized in the mathematical literature as bond percolation, 14 was recognized by Görlich and co-workers in their efforts to reconstitute and describe the sieve-like selective permeability of nuclear pore complexes.¹⁵ Physical gelation is a continuous, reversible networking transition 16 driven by the physical, noncovalent cross-linking of specific motifs.¹⁷ Key nuclear pore proteins, 18 specifically intrinsically disordered regions (IDRs) within these proteins, feature cohesive motifs known as stickers that enable gelation. ^{15,18,19} The relevant stickers are Phe-Gly motifs or Gly-Leu-Phe-Gly motifs. Accordingly, above protein-specific threshold concentrations, known as percolation thresholds, the IDRs in question form system-spanning networks known as physical gels. These are also known as hydrogels because more than 95% of their volume is water. In reconstituted systems, the hydrogels consist of macromolecules forming reversible physical (noncovalent) cross-links with one another. Growing evidence points to the selectivity of partitioning into nuclear pore facsimiles being determined by the specific chemistries within the IDRs of nuclear pore proteins.²⁰

Proteins and peptides can undergo sequence- and structurespecific physical gelation, providing they feature the requisite number of cohesive motifs or stickers that enable networking through reversible physical cross-links. Thermoreversible gelation was demonstrated by Schneider and co-workers in the context of various peptide-based hydrogels.²¹ Likewise, several researchers in the biomaterials community have demonstrated that reversible hydrogels can form through the incorporation of multiple alpha helical elements²² and other types of structures.²³ Reversible gelation driven by IDRs from RNA binding proteins was demonstrated by McKnight and colleagues.²⁴

1.2. Defintion of Physical Gels

Physical gels are defined by physical cross-links, whereas chemical gels are defined by chemical (covalent) cross-links. ¹⁶ Physical gels can be strong or weak, and this depends on the strengths of the physical cross-links vis-à-vis thermal energy $(k_{\rm B}T)$. ¹⁶ From a formal, conceptual standpoint a gel should *never* be automatically conflated with a solid ²⁵ or a glass. ²⁶ Further, the process of physical gelation, which is a manifestation of bond percolation in the systems of interest for this review, ²⁷ is not something that only happens when a material hardens or vitrifies. Of course, the ability of a material to form system-spanning networks of physical cross-links creates the possibility of vitrification. ²⁸ This would be true if the time scales of molecular transport are intrinsically faster than the time scales associated with the making and breaking of physical cross-links.

This scenario can also arise as a function of age of the material, leading to the phenomenon of aging. ^{26,29}

A clear case for not automatically conflating a physical gel with a hardened or vitrified state of matter comes from what we know about liquid water. In its liquid form, water forms a systemspanning network defined by networks of intermolecular hydrogen bonds, with each water molecule being able to physically cross-link with at least four other molecules on average. And yet, except for aficionados of hydration phenomena, no one speaks of the gel-like structure of water. This "error of omission" is not a major concern for most processes of interest because the time scales for making and breaking hydrogen bonds are faster than the time scales for the self-diffusion of water.

To summarize, a physical gel is a percolated, system-spanning network defined by a network of physical cross-links. The rheological properties of gels will be determined by the interplay between at least two competing time scales, viz., the time scales for molecular transport and the time scales associated with the making and breaking of physical cross-links. Therefore, our use of the term gel, which adheres to Flory's original usage ¹³ and refers to the system forming a percolated network, focuses purely on connectivity.

1.3. Intrinsically Disordered Proteins and Solvent Quality

The relevance of the physics of associations among polymers in aqueous solvents and the interplay between chain-chain and chain-solvent interactions was further appreciated with the realization that many proteomes encompass conformationally heterogeneous regions that are intrinsically disordered.³¹ This realization highlighted the importance of solvent quality and the sequence-specific modulation of solvent quality for describing conformational and phase equilibria of intrinsically disordered proteins/regions (IDPs/IDRs).32 A major surprise was the discovery that water is a poor solvent for homopolypeptides such as polyglutamine³³ and polyglycine.³⁴ The latter is a perfect mimic of the polypeptide backbone without any side chains.³⁵ The observations for polyglutamine were also found to be true of prion-like low complexity domains that are enriched in glutamine, asparagine, and glycine.³⁶ These findings indicated that IDRs bereft of both charged residues and canonical hydrophobic residues adopt conformations that minimize interactions with aqueous solvents.³⁷ Accordingly, such domains are prime candidates to study drivers of phase separation, 37,38 which is a segregative phase transition, whereby molecules separate from one another. Three synergistic studies, namely, those of Mao et al.,³⁹ Marsh and Forman-Kay,⁴⁰ and Müller-Späth et al., 41 showed that charged side chains can modulate the intrinsic preferences of polypeptide backbones, thus contributing to conformational expansion and increased solubility of IDRs with requisite sequence features. These findings demonstrated that the composition-specific balance of chainsolvent, solvent-solvent, and chain-chain interactions can generate distinct flavors of IDRs in terms of their conformational equilibria.42,43

1.4. The Importance of Phase Separation in Live Cells

In cells, interest in segregative transitions such as *liquid—liquid* phase separation⁴⁴ grew out of work by Brangwynne, Hyman, and co-workers.⁴⁵ They showed that the formation of ribonucleoprotein bodies known as P granules in the germline of *Caenorhabditis elegans* could be rationalized using the physics of phase separation. Specifically, P granules were shown to form and dissolve as protein and RNA concentrations rose above or

fell below distinct thresholds. Further, the P granules were relatively round, flowed in response to external forces, and fused with one another as a function of time. These observations were used to propose that P granules behave like viscous Newtonian fluids wherein the stresses arising from flow are directly proportional to the flow velocity. Recent measurements, in live cells, have provided convincing evidence for the thermodynamics of phase separation being directly relevant for how specific P-granule proteins set up facsimiles of these bodies.¹⁰

1.5. Phase Separation Combined with Physical Gelation

In 2012, Rosen and co-workers demonstrated the importance of the coupling between physical gelation, i.e., percolation and phase separation for describing assemblies formed by multivalent proteins comprising folded domains connected by disordered linkers. The physical properties of disordered linkers that connect folded domains contribute to controlling the extent of coupling between percolation and phase separation. Linkers between stickers, intrinsically foldable domains in the cases they studied, encode a preference for being well solvated or they were purely Gaussian chains. While well-solvated linkers act to suppress phase separation and weaken percolation, the purely entropic linkers enhance percolation by coupling this process to phase separation.

1.6. Multivalent Associative Macromolecules and Their Phase Transitions

Macromolecular solutions are mixtures of different types of macromolecules dissolved in a complex solvent. ⁴⁹ The overall free energy of the macromolecular solution can be parsed as a sum of two terms, viz., (i) the free energy of mixing ^{50,51} and (ii) the free energies of reversible associations among macromolecules. ⁵² Phase separation is defined by segregation of macromolecules from an incompatible solvent or from other incompatible macromolecules. ^{50,51} Therefore, we refer to phase separation as a segregative transition that gives rise to two or more compositionally distinct phases that coexist with one another.

Macromolecules can undergo reversible associations mediated by physical, noncovalent interactions among specific types of cohesive motifs. These motifs enable intra- and intermolecular hydrogen bonds, a hierarchy of electrostatic interactions, and interactions among aromatic and/or hydrophobic groups.⁵ Above a system-specific threshold concentration, known as the percolation threshold, multivalent associative macromolecules can form system-spanning networks. 13,52-54 This process is a continuous, purely geometric transition known as percolation.¹⁴ On its own, percolation does not give rise to distinct coexisting phases, but instead it generates a single, highly connected network known as a gel. 55 In fact, even simple hard sphere fluids can undergo a percolation transition, depending on the density of the fluid. Here, the system-spanning network is formed by two types of species, viz., the hard spheres and the voids that are created by the packing of hard spheres.⁵⁶ We refer to percolation, which is a purely geometric transition, as an associative or networking transition because the associating species are included into a system spanning network.

The cellular milieu comprises different types of macromolecules in a complex solvent. In such systems, associative and segregative transitions will be coupled to one another. Accordingly, a solution of multivalent associative macromolecules can undergo **co**upled associative and segregative phase transitions. We abbreviate these coupled transitions as

COAST. Phase separation is a segregative transition because it leads to the segregation of the system into two or more separate, albeit coexisting phases. Phase transitions that are associative are continuous transitions and they do not create distinct coexisting segregated phases. Instead, they are defined either by purely geometric or topological considerations. They can also be driven by conformational changes or self-assembly, which we will lumped under the general category of symmetry breaking. For systems of multivalent associative macromolecules, the relevant associative transitions are percolation or symmetry breaking caused by collective and continuous changes, with concentration, to the extent of physical cross-linking. These can be further coupled to continuous symmetry breaking operations such as conformational changes or changes to oligomerization states.

At this juncture, it is worth emphasizing that the distinction between segregative and associative phase transitions that we introduce here, 52 is different from a recent definition introduced by Minton. ⁵⁹ In the Minton picture, phase separation driven by attractive interactions versus repulsive interactions are distinguished as being associative versus segregative, respectively. This is a simplifying definition that becomes imprecise because it excludes any considerations of solvent-mediated effects and reduces interactions among macromolecules as being effectively attractive or repulsive. Such simplifications are only possible if the interactions are reduced to a single energy scale that is captured by a Flory χ parameter ⁵⁰ or the equivalent second virial coefficient. 16 In complex mixtures such as ternary or *n*-nary mixture of macromolecules in a solvent, we must consider the interplay between homotypic and heterotypic interactions between macromolecules, and the mutual (in) compatibility of macromolecules with the solvent and with one another. As noted by Tanaka, 60 the effective two-body interactions, viz., χ , which capture the two types of free energies that prevail in macromolecular solutions, can be parsed into a solvation term that drives segregative transitions and an associative term that drives networking. Therefore, COAST-like processes in solutions of multivalent associative macromolecules are driven by a combination of macromolecular and solvent (in) compatibility, which contributes to the free energy of mixing, and reversible associations, which drive percolation.

In multivalent associative macromolecules 9,61 the term associativity refers to the presence of stickers that enable either isotropic or anisotropic site- or chemistry-specific interactions that are more favorable and larger in magnitude than the isotropic solvent-mediated interactions. ^{60,61} In soft matter systems, multivalent associative macromolecules can be modeled as patchy colloids featuring patches or stickers of defined sizes and orientations that enable site-specific interactions among the colloidal particles.⁶² Intrinsically folded domains of proteins⁶³ that feature hotspots for specificity of binding are exemplars of patchy particles. Flexible linear polymers can feature stickers that enable specific intra- or interpolymer cross-links. Such systems are known as linear associative polymers. Although biologists tend to conflate the term sticky or stickers to imply nonspecific interactions, the term stickers, which was introduced almost four decades ago in the polymer literature, refers to motifs that enable site- or sequencespecific interactions. The strengths of specific interactions involving reversible sticker-sticker cross-links can span at least an order of magnitude (or more) vis-à-vis thermal energy. 3,64-67 The surfaces of folded domains and regions that are interspersed between stickers in IDRs act as spacers. While stickers enable

site-specific interactions, spacers influence the overall solubility while also influencing the cooperativity of networks of sticker—sticker interactions.

The partitioning of the sequence of a linear associative polymer or the surface of a patchy colloid into stickers versus spacers often becomes a matter of operational convenience intended to capture the fact that the interaction energies feature hierarchies that are also context dependent. The polypeptide backbone and the phosphodiester linkages along nucleic acid backbones are ubiquitous in protein versus nucleic acid systems, respectively. These provide the background against which amnio acid side chain or nucleobase interactions are to be referenced. The direct interactions of backbones will be influenced by side chain or nucleobase chemistries. Therefore, the stickers-andspacers formalism is not exact or complete in that the identities of stickers and spacers are neither immutable, nor is the binary classification truly rigorous. Instead, the formalism provides a useful abstraction to compare sequence-specific driving forces for phase transitions. Further, the parsing of amino acid side chains and nucleobases into stickers versus spacers for a given context allows one to perform separation of function mutagenesis analysis, querying the contributions of distinct chemistries to the segregative versus associative phase

Site- and sequence-specific interactions of stickers enable for the formation of reversible cross-links. Different types of stickers will encode a hierarchy of specific interactions depending on the types of stickers that are incorporated into the sequence of an IDR 65,66 and where they land on the surfaces or interiors of folded domains. Among the relevant, specific sticker—sticker interactions are hydrogen bonds, salt bridges, solvent-mediated ionic interactions, the hierarchies of interactions among groups with multipole moments, associations among hydrophobic residues, and the range of interactions that involve π systems, which include stacking, cation— π interactions, and orienting π systems by combining these systems with hydrogen bonds.

Most condensates also include a range of nucleic acid molecules. ⁶⁹ The delineation of stickers versus spacers can be applied to nucleic acids as well. ^{70,71} Here, the specificity of base pairing and base stacking drive secondary structure formation within the nucleic acid polymers, and the specificity of intermolecular cross-linking. ⁷² Sequence regions that disrupt the specificity of interbase interactions will act as spacers.

1.7. Associative Macromolecules Drive the Formation of Condensates

Facsimiles of condensates and bona fide condensates in live cells appear to form and dissolve through phase transitions described by order parameters.⁷³ The order parameter for purely segregative transitions is the density for a one-component system or the compositional vector for complex mixtures of macromolecules, solutes, and a solvent. For purely associative transitions such as percolation, the order parameter describes the connectedness of molecules, the topology of the network that forms, the extent of cross-linking, and the number densities of connected clusters. 16,17,52,55 Changes in conformation across the phase boundary or the onset of crystalline or semicrystalline order are defined by distinct order parameters.⁵⁸ For processes that combine segregative, associative, and transitions that involve the breaking of symmetry, the order parameter will be a vector or a tensor. Components of order parameters change abruptly at the onset of a phase transition.⁷⁴ However, the

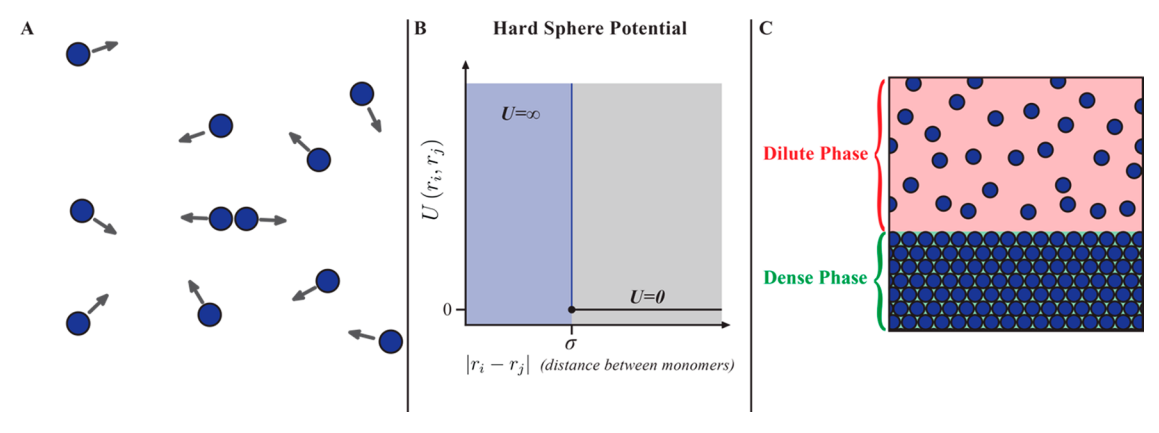


Figure 1. Hard sphere fluids can undergo density transitions, viz., phase separation. (A) System of hard spheres. The arrows indicate that the collisions among the molecules are purely elastic. (B) Potential for a pair of hard spheres. (C) A segregative *density* transition gives rise to two coexisting phases of different densities separated by an interface, as depicted here.

different components of order parameter vectors or tensors might be differently responsive to changes in stimuli that drive phase transitions.

Processes such as phase separation coupled to percolation (PSCP)⁷⁵ and complex coacervation⁷⁶ are exemplars of processes that come under the rubric of COAST. As such, there is no formal distinction between PCSP and complex coacervation. However, we make the distinction for two reasons: First, complex coacervation is an established term and second, it requires the consideration of electrostatic interactions and their attendant complexities such as the range of the interactions and the competing effects of macroions and solutions ions. In many systems, one can get away without worrying about these complexities. Therefore, we reserve PSCP for systems where charge effects are likely to play either a minor role or can be treated without consideration of the spatial range or correlation effects of electrostatic interactions. Other COAST-like processes include polymerization induced phase separation, 4,77 micellization,^{78,79} surfactant influenced,⁸⁰ and thermodynamically controlled microphase separation,⁸¹ which can also be realized when stickers are clustered into linear blocks along the sequence of interest. 61,82

Other processes that can give rise to condensates include active processes that are coupled to COAST-like spontaneous processes or purely active processes such as reaction, or motility-controlled phase separation and active emulsification. Spontaneous cooperative processes that are likely contributors are clustering via short-range attractions and long-range repulsions (so-called SALR-controlled processes). Additionally, condensate formation can also be under dynamical control, and these processes include homogeneous or multistep nucleation-mediated growth, or spinodal decomposition, a variant of which is viscoelastic phase separation.

1.8. Scope of the Review

This review focuses on spontaneous phase transitions that come under the rubric of COAST. The primary focus is on PSCP. Any model for the spontaneous process of condensate formation and dissolution must integrate the contributions of associative effects originating from site- or sequence-specific interactions and segregative effects originating from the interplay of configurational and solvation effects that have both entropic and enthalpic components. Biomacromolecules, specifically the protein and nucleic acid components of nuclear and cytosolic condensates, are complex mixtures defined by finite sizes,

heterogeneity and hierarchies of sequence-encoded interactions, conformational heterogeneity, and thermodynamic consequences of post-transcriptional and post-translational modifications. While simple concepts provide a useful starting point for describing how condensates form and dissolve, the complexity of these systems also necessitates the development of new physics, even for describing spontaneous phase transitions. This is especially true for multicomponent systems.

Our focus on spontaneous phase transitions comes from the fact that it highlights the intrinsic, evolutionarily selected, sequence-encoded, and solution-condition-mediated processes that are likely to be co-opted and modulated by active processes and the diverse components within cellular milieus. 90 COASTlike processes are intrinsic consequences of the information written into protein and nucleic acid sequences. These are likely to be leveraged by a blend of equilibrium and nonequilibrium processes that are operative in live cells.^{7,90,91} Our objective is to provide clarity regarding phase transitions that come under the rubric of COAST. To start, we will introduce the foundations of purely segregative and purely associative phase transitions. We will then segue to descriptions of how these processes are coupled, and why this coupling appears to be important for describing the how condensates form and dissolve through reversible phase transitions.

2.0. PHASE SEPARATION: ONE-COMPONENT SYSTEMS

Phase separation is a segregative transition whereby the system of interest separates (segregates) into two or more coexisting phases. Note that segregative transitions can also be referred to as demixing or immiscibility transitions. The nomenclature of X-Y phase separation is reserved for the formation of two coexisting phases X and Y. Here, X-Y specifies the types of coexisting phases that can form. Phase separation that gives rise to two coexisting phases can come in different flavors, such as liquid-liquid phase separation, liquid-solid phase separation, liquid-liquid-crystalline phase separation, etc. In binary mixtures, such as a single type of macromolecule in a solvent, segregative transitions arise due to macromolecule-solvent interactions that, on average, are unfavorable compared to the arithmetic mean of macromolecule-macromolecule and solvent-solvent interactions.⁵⁰ In multicomponent systems, segregative transitions are governed by a blend of pairwise favorable versus unfavorable interactions among the different components.⁹² In systems with only one type of molecule,

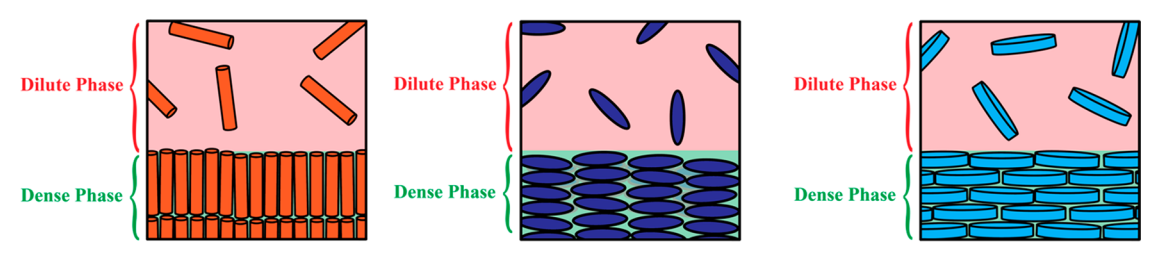


Figure 2. Systems of hard aspherical molecules including rods, ellipsoids, and discoids can also undergo segregative transitions.

segregative transitions are density transitions, and we discuss these first.

2.1. Systems of Hard Molecules

One-component fluids comprising spherical particles are the simplest systems that one can use to develop an atomistic description of phase separation. Consider the case of a system of hard spheres, each of diameter σ that cannot interpenetrate. These particles interact via purely elastic collisions (Figure 1A). For a pair of particles with position vectors \mathbf{r}_i and \mathbf{r}_j , the interaction potential (Figure 1B) can be written as

$$U(\mathbf{r}_{i}, \mathbf{r}_{j}) = \begin{cases} 0 \text{ if } |\mathbf{r}_{i} - \mathbf{r}_{j}| \geq \sigma \\ \infty \text{ if } |\mathbf{r}_{i} - \mathbf{r}_{j}| < \sigma \end{cases}$$
(1)

Note that systems of purely repulsive hard molecules, irrespective of their shape, will lack attractive interactions. Molecular dynamics simulations by Alder and Wainwright ⁹³ and Monte Carlo simulations by Wood and Jacobson ⁹⁴ showed that a fluid of hard spheres undergoes a freezing transition that can be described as liquid—solid phase separation. This is because, above a critical density, the hard sphere fluid minimizes its free energy, purely entropic in this case, by separating into two coexisting phases. The coexisting phases are a low-density liquid and a high-density solid.

The onset of the equilibrium freezing transition can be anticipated by the density dependence of the radial distribution function g(r). This function quantifies the relative probability of realizing a specific interparticle distance r referenced to the relevant probability in a noninteracting, and hence ideal, gas. A typical profile for g(r) shows the characteristic short-range order and long-range disorder that one expects for a liquid. However, above a critical density, the face-centered cubic packing of spheres is manifest on all length scales, leading to an equilibrium freezing transition. The separation of a hard sphere fluid into species of two distinct coexisting densities (Figure 1C) is described using a coexistence curve.

The density dependence of the phase transition of a fluid of N hard spheres can be rationalized using the configuration integral, which is written as

$$Z_{N} = \frac{1}{V^{N}} \int \exp \left[\frac{\sum_{i,j < i} U(\mathbf{r}_{i}, \mathbf{r}_{j})}{k_{B}T} \right] d^{3N}r$$
(2)

Here, V is the system volume, $k_{\rm B}$ is the Boltzmann constant, and T is the temperature of the system. For a hard sphere fluid, where the pair potential is described by Equation 1, the configuration integral in Equation 2 is independent of temperature. Thus, the thermodynamic properties, correlation functions, and structural properties depend only on the number density given by the prefactor in Equation 2. At high densities, a hard sphere fluid undergoes an equilibrium freezing transition to increase its accessible volume. This is an example of an

entropically driven segregative transition, which for a one-component system is a *density transition*.

Density transitions can also be realized for fluids of hard rods, ⁹⁷ hard ellipsoids, or hard discs ⁹⁸ (Figure 2). In such systems, which have served as touchstones for the description of phase behaviors of lipids, ⁹⁹ the spherical symmetry in hard sphere fluids is broken by the aspherical geometries of the molecules. ¹⁰⁰ Accordingly, the density transition gives rise to various liquid crystalline phases that depend on the shapes of the underlying molecules. The segregative transitions one observes in systems of hard molecules are entropically driven and are a consequence of the bulk densities of molecules crossing specific, shape-dependent thresholds.

2.2. Phase Separation in One-Component Systems with Repulsive and Attractive Interactions

The simplest generalization of a fluid of hard spheres is that of a van der Waals fluid. The hard-core repulsions are softened via a short-range repulsive potential, and a cohesive, longer-range term is included to capture dispersive interactions, which are attractive in nature. A typical pair potential for a van der Waals fluid is the 12-6 Lennard-Jones potential written as

$$U_{\mathrm{L}j}(\mathbf{r}_{i}, \mathbf{r}_{j}) = 4\varepsilon_{ij} \left[\left(\frac{\sigma_{ij}}{|\mathbf{r}_{i} - \mathbf{r}_{j}|} \right)^{12} - \left(\frac{\sigma_{ij}}{|\mathbf{r}_{i} - \mathbf{r}_{j}|} \right)^{6} \right]$$
(3)

Here, ε_{ij} is the well depth of the minimum in the Lennard-Jones potential and σ_{ij} is the effective hard-core diameter for a pair of particles.

As shown by Weeks, Chandler, and Andersen, ¹⁰¹ the short-range repulsive forces completely determine the equilibrium structure of the van der Waals fluid. ¹⁰² The interaction potential for a pair of particles effectively consists of hard spheres in an attractive, uniform background that mimics the longer-range attractive interactions known as van der Waals forces. Inclusion of the attractive interactions allows for temperature-dependent responses of the fluid. As a result, there exists a combination of pressures and temperatures for which the system of Lennard-Jones particles can separate into coexisting liquid and vapor phases. Additionally, the separation into distinct coexisting solid phases can be observed by modulating the exponent of the repulsive arm of the Lennard-Jones potential. ¹⁰³

The main point is that simple models describe how segregative density transitions arise and give rise to distinct pairs of coexisting phases. Further, there are singular combinations of pressure and temperature, known as triple points, where three distinct phases can coexist. Therefore, even a one-component system can be spatially organized to achieve phases of distinct densities coexisting with one another. The interactions in these simple models are isotropic, and changes to pressure and temperature engender density transitions. Alternatively, changes to the bulk density for fixed pressure

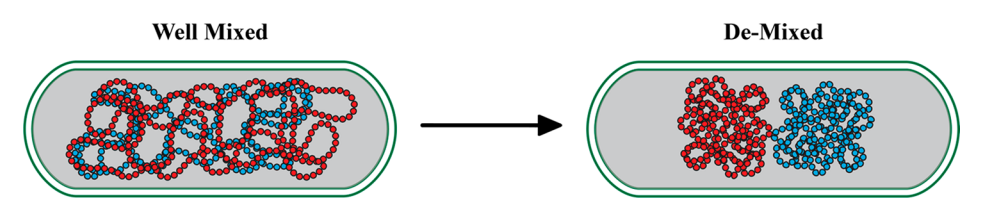


Figure 3. Entropically driven phase separation helps explain bacterial chromosomal segregation.

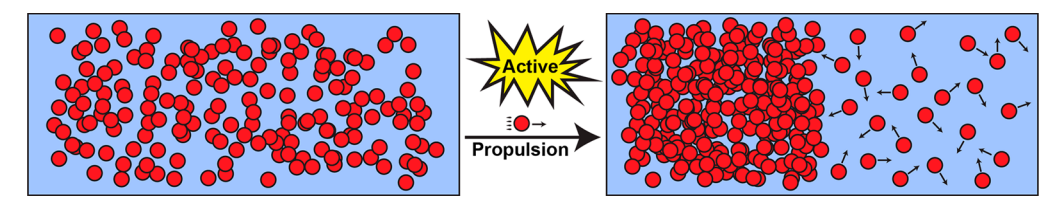


Figure 4. Example of movement-induced (motility-induced) phase separation. ⁸³ The figure shows active Brownian particles that are self-propelled in an external field. Propulsion creates flows and local inhomogeneities that can drive segregative transitions.

and temperature also engender segregative transitions, giving rise to different types of coexisting phases.

2.3. Purely Entropically Driven Phase Separation Can Drive Spatial Organization in Cells

The universal requirement of steric exclusion can give rise to entropically driven phase separation and the formation of distinct coexisting phases. The repulsive forces at short-range are orders of magnitude larger than the intermediate or long-range attractions. ^{102,104} Accordingly, if one were to be naive and view a cell as a bag of hard molecules and self-avoiding polymers of different shapes and sizes, then distinct segregative transitions are likely to be realized as the densities of different molecules cross threshold values. ⁸ Biochemical activity would control the production and degradation of the molecules of interest, and changes to cellular volumes that accompany the production or degradation of molecules would enable spatial organization via purely segregative transitions.

Indeed, the physics of entropically driven segregative transitions of self-avoiding polymers has proven to be effective at explaining chromosomal segregation in rod-shaped bacteria under the right conditions. ¹⁰⁸ In this model, circular DNA molecules are treated as self-avoiding, ring-like polymers. The well-mixed state limits the configurational degrees of freedom of the self-avoiding ring-like polymers, thus extracting an entropic penalty. 105 This penalty is alleviated by separation into two distinct chromosome-rich territories that coexist with one another (Figure 3). The role of specific protein cofactors and specific geometries observed as part of bacterial chromosomal segregation can be explained using models whereby protein binding enables physical cross-linking, thereby generating topological constraints that are layered upon the entropically driven segregative transitions. ¹⁰⁶ In a similar vein, segregative transitions of rod-like molecules, captured by Onsager's model for liquid-liquid-crystalline phase separation, 97 has had a profound impact on our understanding of membrane phase behavior.¹⁰

The preceding discussion makes the point that the physics of entropically driven phase separation, which only considers the density transitions of hard molecules, can explain many of the basic foundations of spatial organization in cells. Here, hard molecules refer to generalizations of hard spheres that include complex shapes and sizes. Such systems do not have any attractive interactions. And yet, phase separation can be realized based purely on the absolute densities of hard particles in a

single-component fluid or the relative densities of different types of hard particles in multicomponent mixtures. This point was made in the 1960s by A. G. Ogston, who noted that "any system of two solutes which interact only entropically will satisfy the conditions for "incompatible" phase separation providing only that the molecules are of different size". There will be the inevitable criticism of the logic in this paragraph because biological organization must be about relative affinities and the specificities they engender. This is undeniable. However, the keypoint is that spatial sorting and compartmentalization are emergent properties in even the simplest systems, viz., collections of hard molecules. In such systems, the steep energetic penalties for steric overlap, and the maximation of entropy through shape complementarity are sufficient to enable phase separation above a density threshold. These discussions highlight why phase separation is logical rather than "implausible" 109 as a route for compartmentalization or spatial organization in cells.

In the soft matter literature, segregative transitions of hard spheres have been studied in the presence of active processes that either steer particles in specific directions ⁸³ (Figure 4) or account for the presence of chemical reactions. ¹¹⁰ In the simplest instantiations of active segregation, an external force augments the intermolecular interactions, and generates local density fluctuations to enable local density transitions. Active processes can be drivers of segregative transitions, and this topic has received considerable attention in the physical ^{83,110,111} and chemical literatures. ¹¹²

3.0. PHASE SEPARATION IN COMPLEX MIXTURES

3.1. Mean-Field Theories for Free Energies of Mixing and the Interaction Parameter χ

From a physical chemistry standpoint, cells may be viewed as complex mixtures of an assortment of macromolecules, solutes, and metabolites, all dissolved in a nonideal aqueous milieu. Here, complexity refers to the different molarities, stoichiometries, and volume fractions of the different molecules. How does one describe the thermodynamics of mixing and segregation in complex mixtures? The mean-field theories of Hildebrand, 113 generalized by Flory 50 and Huggins 115 for polymer solutions and blends, provide a useful starting point.

For mixtures of molecules, the fundamental quantity of interest is $\Delta\mu_{\rm mix}$, which is the free energy density of mixing. This quantifies the change in free energy per molecule of the system

that is associated with transferring molecules that make up the mixture from their pure, single-component, homogeneous phases to a mixture defined by the volume fractions of $\phi_{\rm i}$ for each of the species i. We consider a binary mixture of molecules of type A and B dispersed randomly on a cubic lattice. For simplicity, one ignores three-body and higher-order interactions. Further, we shall assume that there are no volume changes upon mixing. 16 In this scenario, the free energy of mixing is written as

$$\Delta \mu_{\text{mix}} = k_{\text{B}} T \left[\frac{\phi_{\text{A}}}{N_{\text{A}}} \ln \phi_{\text{A}} + \frac{\phi_{\text{B}}}{N_{\text{B}}} \ln \phi_{\text{B}} + \chi \phi_{\text{A}} \phi_{\text{B}} \right]$$
(4)

Here, $\phi_{\rm A}$ and $\phi_{\rm B}$ are the volume fractions of molecules of type A and B. $N_{\rm A}$ and $N_{\rm B}$ are ≈ 1 if A and B are rigid, roughly spherical macromolecules such as stable globular proteins, colloidal particles, or small molecules such as solutes, metabolites, or drugs. If A and B are flexible, linear macromolecules, then $N_{\rm A}$ and $N_{\rm B}$ refer to the degree of polymerization quantified as the number of chemical or Kuhn monomers within the molecules. The interaction parameter χ is a dimensionless parameter that quantifies the differences among the magnitudes of the pairwise interactions in the mixture. It is defined as

$$\chi = \frac{z}{2} \frac{(2u_{AB} - u_{AA} - u_{BB})}{k_{B}T} \tag{5}$$

Here, z is the coordination number of the lattice used to model macromolecules as gases of monomers. The free energy of mixing is a sum of entropic and energetic contributions. In an ideal mixture, $\chi=0$, and this can arise from a counterbalancing of the pairwise interactions energies, namely, $2u_{AB}$ and the sum $u_{AA}+u_{BB}$. The free energy of mixing is purely entropic when $\chi=0$, and this entropy always favors mixing. In an ideal mixture, the composition in any volume element within the system will match the overall composition. Therefore, such a system will be homogeneous and is described as a random mixture. Unlike a one-component system, where density alone can generate a segregative transition, in a mixture, there is the added consideration of mixing of the degrees of freedom. In this case, entropy always favors mixing.

The mixing of A and B molecules can be enhanced beyond the ideal case if χ is negative. In this scenario, the one-phase system is always preferred. Even so, there will be compositional inhomogeneities with respect to volume elements that correspond to the molecular scale. This is because the system will strive to enhance favorable, pairwise A–B interactions over the less favorable or even unfavorable A–A or B–B interactions. An ionic liquid, 114 comprising a mixture of oppositely charged ions sans a solvent, would be an exemplar of such a mixture.

3.2. Phase Separation Becomes a Formal Possibility When χ Is Positive

In a binary mixture of A and B molecules, we can set $\phi_A = \phi$, and $\phi_B = (1-\phi)$ because of conservation of mass, i.e., $\phi_A + \phi_B = 1$. The system is closed, and hence the overall composition of the mixture is a conserved order parameter. If χ is positive, then there exists some threshold volume fraction $\phi = \phi_{\rm sat}$ above which the one-phase, homogeneous mixture is no longer thermodynamically stable. The one-phase mixture becomes saturated, and to minimize the overall free energy of mixing, the system separates into coexisting dilute and dense phases. For a fixed temperature, the value of $\phi_{\rm sat}$ depends on the magnitude of χ and the relative molecular weights of the A and B molecules. The compositions of the coexisting phases, denoted as $\phi_{\rm sat}$ and $\phi_{\rm dense}$

will be temperature dependent. Phase separation leads to an interface between the two coexisting phases. If A is a macromolecule, such as a linear polymer, with each molecule being defined by N chemical monomers, and B is a lowmolecular weight solvent, then there will be the transport of the solvent across the interface to help equalize the chemical potentials. This scenario describes an osmotic solution, whereby the exchange of the solvent across the phase boundary will be opposed by the increased pressure within the dense phase. This pressure, known as the osmotic pressure, is a colligative property that quantifies the free energy difference between a polymer solution and a pure solvent, and at equilibrium it must be equalized between the two coexisting phases. 115,116 Therefore, the compositions ϕ_{sat} and ϕ_{dense} are set by equalizing chemical potentials and the osmotic pressures across the two phases. 115 If we denote the chemical potential of the macromolecule at temperature T as $\mu_{m,T}$ and the osmotic pressure as Π_T , then the requirements for chemical and osmotic equilibrium are

$$\mu_{m,T}(\phi_{sat}) = \mu_{m,T}(\phi_{dense})$$
and
$$\Pi_{m,T}(\phi_{sat}) = \Pi_{m,T}(\phi_{dense})$$
(6)

In theoretical work, the preferred units for concentration are volume fractions, ϕ , which quantify the amount of the system volume that is taken up by the polymers. However, experimentalists prefer molar units or mg/mL denoted as c. And so, analysis of experimental data is usually performed in molar units. For an A-B mixture that is a polymer solution, A is a linear polymer and B is the solvent.

The determinants of $\phi_{\rm sat}$ or $c_{\rm sat}$ are the solution temperature, the degree of polymerization $N_{\rm A}$, and the value of χ . Following Flory, 16,64 one can write $\chi \approx u + u'/T$. Here, u is an athermal entropic term, and u' is an effective pairwise energy determined by the interplay of polymer-solvent, polymer-polymer, and solvent-solvent interactions. Therefore, the value of χ is determined by the solution temperature, and the relevant parameters are T and N_A . Above c_{sat} , the overall free energy of the system is minimized by separation of the system into a dense, polymer-rich phase that coexists with a dilute, polymer-deficient phase. The compositions of the dense and dilute phases quantified by $c_{\rm dense}$ and $c_{\rm dilute}$, respectively refer to the temperature-dependent concentration of polymers in the dense versus dilute phases. The precise values of $c_{\rm dense}$ and $c_{\rm dilute}$ are governed by the equalization of chemical potentials and osmotic pressures across the phase boundary. Since the dilute phase is saturated at c_{sat} , the value of c_{dilute} is the same as c_{sat} . The value of c_{dense} will depend on the amount of solvent that is present in the dense phase. If the dense phase is akin to a polymer melt, then the volume fraction of the dense phase will approach unity, i.e., $\phi_{\mathrm{dense}} \approx 1$. This is clearly not the case for biomolecular condensates as shown first by Gall and co-workers in their measurements of mass densities in nucleoli, Cajal bodies, and nuclear speckles. 117 Their estimates suggest that $\phi_{\rm dense}$ is less than 0.1. Clearly, condensates encompass considerable amounts of solvent, and this has become clear from several in vitro and in *vivo* measurements. 11,64,66,118,119

Given the mean-field, lattice gas nature of the Flory—Huggins theory, the simplest description of the coexisting phases is that of a dilute gas of chemical or Kuhn monomers derived from each polymer that coexists with a dense melt of polymers. This is rather like liquid—vapor phase separation. However, this

description ignores the abundance of the solvent in the polymer-deficient dilute phase. As a result, the coexisting phases are better described as a dilute polymer solution, rich in a low-molecular weight solvent, that coexists with a polymer-rich phase. This has given rise to the term liquid—liquid phase separation for the phase behaviors of biopolymer solutions that are described using the Flory—Huggins theory. 44,49

3.3. χ , Osmotic Second Virial Coefficients, and Excluded Volumes

We shall consider an A–B mixture, which comprises a macromolecule A in a solvent B. If the macromolecule is a linear polymer with n_p chemical monomers or n_k Kuhn monomers, then the volume occupied by the chemical or Kuhn monomers (i.e., residues in a protein sequence) is proportional to b, where b is the size of each monomer. The effective work done to bring a pair of monomers to within a distance r of one another is the potential of mean force W(r). The excluded volume per monomer (v_{ex}) , which has also been referred to as the effective solvation volume (v_{es}) , is the effective volume that is set aside for interactions of each monomer with the surrounding solvent. It is quantified by averaging over all intermonomer distances in the entire solution volume. Accordingly, v_{ex} is computed as

$$\mathbf{v}_{\rm ex} = -\int_0^\infty \left[\exp\left(-\frac{W(r)}{k_{\rm B}T}\right) - 1 \right] r^2 dr \tag{7}$$

The excluded volume can be positive, zero, or negative. ¹⁶ Therefore, a positive excluded volume implies that the polymer is in a good solvent, and the effective pairwise interactions among the monomers are, on average, repulsive. If, on average, the effective monomer—solvent interactions are counterbalanced by the monomer—monomer and solvent—solvent interactions, then the excluded volume is zero. This situation corresponds to a theta or inert solvent for the polymer. Finally, the excluded volume is negative if the monomer—monomer interactions are, on average, attractive. In this scenario, the polymer is in a poor solvent. The conformations of polymers in dilute solutions, ⁴³ and the overall phase behavior in polymer solutions are determined by the sign and magnitude of v_{ex}. ³⁷

The osmotic second virial coefficient B_2 is a well-known, and well-established measure of the effective strengths of pairwise macromolecular interactions in a solvent. It can be defined using $B_2' = B_2 M_w^2$ as

$$B_{2}' = -2\pi \int_{0}^{\infty} \left[\exp\left(-\frac{W(r)}{k_{\rm B}T}\right) - 1 \right] r^{2} dr$$
 (8)

As in Equation 7, the term W(r) captures the distance-dependent solvent-averaged potential of mean force between a pair of macromolecules that are a distance r apart from one another in the solvent, and M_w is the molecular weight of the macromolecule. The value and sign of B_2 will vary with solution conditions such as the temperature, pH, or concentration of solution ions. Negative values of B_2 imply net attractions among the macromolecules. Conversely, positive values of B_2 imply net repulsions among the macromolecules. In an ideal mixture, B_2 is zero, and the attractions and repulsions are counterbalanced, on average. The integrands of Equations 7 and 8 that lead to $v_{\rm ex}$ and B_2 , respectively, are identical to one another implying that $v_{\rm ex} = 2\pi B_2'$.

In an A—B mixture, the osmotic pressure can be computed as the partial derivative of the free energy of mixing as

ı

$$\Pi = \frac{\phi_{\rm A}^2}{b^3} \frac{\partial \Delta \mu_{\rm mix}}{\partial \phi_{\rm A}} \bigg|_{n_{\rm A}} \tag{9}$$

Here, n_A is the number of macromolecules of type A in a solvent of type B. Note that n_A is kept constant. In a dilute mixture of A and B molecules, where N_A and N_B are the number of chemical or Kuhn monomers per A and B molecules, respectively, the osmotic pressure can be written in terms of the virial expansions as

$$\Pi = \frac{k_{\rm B}T}{b^3} \left[\frac{\phi_{\rm A}}{N_{\rm A}} + \frac{\phi_{\rm A}^2}{2} \left(\frac{1}{N_{\rm B}} - 2\chi \right) + \frac{\phi_{\rm A}^3}{3N_{\rm B}} + \dots \right]$$
Setting $c_n = \frac{\phi_{\rm A}}{b^3}$

$$\Pi = k_{\rm B}T \left[\frac{c_n}{N_{\rm A}} + \left(\frac{1}{N_{\rm B}} - 2\chi \right) \frac{b^3 c_n^2}{2} + \frac{b^6 c_n^3}{3N_{\rm B}} + \dots \right];$$
Because, $v_{\rm ex} = \left(\frac{1}{N_{\rm B}} - 2\chi \right) b^3$, it follows that:
$$\Pi = k_{\rm B}T \left[\frac{c_n}{N_{\rm A}} + \frac{v_{\rm ex}c_n^2}{2} + wc_n^3 + \dots \right]$$
(10)

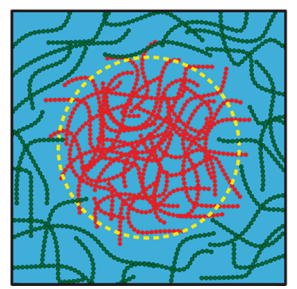
If A is a linear polymer with $N_{\rm A}$ monomers, and B is a low molecular weight solvent with $N_{\rm B}\approx 1$, then ${\rm v_{\rm ex}}=(1-2\chi)b.^3$ In Equation 10, c_n is the number density of macromolecular monomers in molar units. The prefactors of each of the higher-order terms are known as virial coefficients. In dilute solutions, terms beyond the ${\rm v_{\rm ex}}$ term become negligibly small. Accordingly, using what is known as a Zimm plot, 122 which is a plot of: $\frac{\Pi}{ck_{\rm B}T}$ versus c, one can estimate the magnitude and sign of the osmotic second virial coefficient denoted as B_2 .

There are a few ways to generate a Zimm plot. The traditional approach uses static light scattering, 123 which was recently used by Safari et al., to study the effective interactions between TPX2 molecules. 124 To access a broader range of B_2 values, one can use static laser light scattering. 118 These measurements are performed as a function of polymer concentration. Other approaches include direct measurements of osmotic pressure, which is a readily accessible colligative property of polymer solutions. Given the challenge of expressing and purifying large amounts of biomacromolecules, one can also use fluorescence correlation spectroscopy, and the concentration-dependent deviation in diffusion coefficients to back-calculate the second virial coefficient. This approach was demonstrated by Wei et al., 118 and it requires that certain hydrodynamic criteria be satisfied. In the next section, we describe the inferences one can glean from knowledge of second virial coefficients.

3.4. Interactions that Drive Phase Separation in *n*-Nary Mixtures in a Complex Solvent

Cells are complex mixtures comprising an assortment of macromolecules in a solvent that is itself rather complex. The Flory—Huggins theory can be generalized for a mixture of more than two molecules. There are now multiple χ parameters, one for each pair of molecules in the mixture. Accordingly, in compact notation, for a system with n macromolecules in a complex solvent, one can write the free energy of mixing in terms of a compositional vector $\mathbf{\Phi}$ and an interaction matrix \mathbf{X} . The





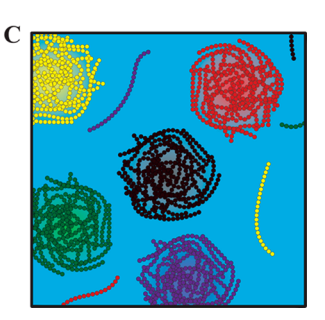


Figure 5. Scenarios for phase separation. (A) The coexistence of two phases, one that is polymer-rich and another that is solvent-rich. (B) A scenario that is reminiscent of the ternary PEG, dextran, water system whereby two phases, rich in different types of polymers, coexist with one another. (C) The formation of distinct phases, each enriched in a specific type of polymer.

free energy of mixing is written as $\Delta \mu_{\text{mix}} = k_{\text{B}}T(\mathbf{\Phi}_{\text{N}}' \ln \mathbf{\Phi} + \mathbf{\Phi}'\mathbf{X}\mathbf{\Phi})$. Here, $\mathbf{\Phi}' = (\phi_1, ..., \phi_n)$ is the compositional row vector, $\mathbf{\Phi}$ is the transpose of this vector, and $\mathbf{\Phi}_{\text{N}}'$ is the vector $(\phi_1/N_1 ..., \phi_n/N_n)$ where each N_i is the number of chemical or Kuhn monomers in species *i*. Finally, the X-matrix is written as

$$\mathbf{X} \equiv \begin{pmatrix} \chi_{11} & \chi_{12} & \chi_{13} & \cdots & \chi_{1n} \\ \chi_{21} & \chi_{22} & \chi_{23} & \cdots & \chi_{2n} \\ \chi_{31} & \chi_{32} & \chi_{33} & \cdots & \chi_{3n} \\ \vdots & \vdots & \vdots & \ddots & \vdots \\ \chi_{n1} & \chi_{n2} & \chi_{n3} & \cdots & \chi_{nm} \end{pmatrix}$$
(11)

In the notation used here, each χ_{ii} term quantifies the effective strengths of solvent-mediated homotypic interactions. Each of the χ_{ii} terms will be as defined in Equation 5 where we shall now set A to be the solvent, and B to be macromolecule *i*. Knowing the elements of the X-matrix will help in identifying the macromolecular drivers—or scaffolds—of phase separation in complex mixtures. As we will discuss below, each element of the X-matrix is directly related to a measurable parameter, viz., the appropriate osmotic second virial coefficient. Therefore, the combination of measurements and computations that allow one to populate the elements of the X-matrix will provide a direct route to identifying macromolecular scaffolds 1,126 that are the main drivers of phase separation.

Notice that each element of the X-matrix is a pairwise interaction parameter and is therefore proportional to the corresponding second virial coefficient such that $\chi_{ij} \propto B_{ij}$. Therefore, the X-matrix and the matrix of second virial coefficients, denoted as B, are equivalent. Since the phase behavior of the mixture, including the numbers of coexistence phases are, to first order, determined by the signs and magnitudes of the elements of the B matrix, it helps to be able to measure or estimate each of these elements. One approach would be to measure the diagonal elements B_{ii} using the Zimm plot and estimate 127 B_{ii} as $B_{ii} = (B_{ii}B_{ii})^{1/2}$. Note that this only works if the net charge for each of the macromolecules is close to zero because excess charge creates imbalances requiring an accounting for the preferential effects of counter- and co-ions drawn from the solution. For macromolecules with a net charge, it becomes imperative to measure B_{ii} , B_{jj} , and B_{ij} separately. These measurements will need to be performed as a function of pH and salt concentration.

When B_{ij} needs to be measured, one can do so by fixing the concentrations of solvent components, and one of species i or j, and measure either scattering or osmotic pressure as a function of the concentration of species j or species i. The relevant B_{ij} can

then be extracted from application of the Zimm analysis to the data. These measurements will need to be performed in the presence of the solvent of interest, which makes it imperative that the contribution of the solvent to each B_{ij} term be dereferenced through separate measurements of B_{ii} and B_{jj} in the solvent of interest. Computations can help with the generation of estimates of each of the elements of the B-matrix, ¹²¹ although the effects of components of the complex solvent, which is never just deionized water, can contribute in nontrivial ways. Therefore, computations must account for the complex solvent in computationally tractable ways, and this remains a persistent challenge.

Why and how does a **B**-matrix help with describing the overall phase behavior of a complex mixture? Given a **B**-matrix, an empirical route to identifying scaffolds and coscaffolds is to compute the norm using all elements that are negative and identifying the fraction of the elements that contribute to at least 90% of this norm. This is an *ad hoc* maximum-likelihood threshold that is based on the consideration that the relative contributions of scaffolds or coscaffolds with respect to nonscaffolds must exceed thermal energy $k_{\rm B}T$. Given its central importance, a defining challenge for physical chemists in the condensate field is to compute the **B**-matrix elements from sequence and structure information on macromolecules that make up the complex mixture of interest.

3.5. Gibbs Phase Rule and Mean-Field Models for Phase Separation in *n*-Nary Mixtures

For mixtures, with n distinct types of macromolecules in a solvent, there are n(n-1)/2 distinct χ parameters that contribute to the overall phase behavior. Note that the elements of the B-matrix will change with temperature, pressure, and changes to solution conditions. By the Gibbs phase rule, if there are n components in the system, and p coexisting phases, then the number of thermodynamic degrees of freedom is defined as F = n - p + 2. The maximal number of phases that can coexist with one another is computed by setting F to be zero and solving for p. Therefore, the maximum number of phases that can coexist with one another will be n + 2. Accordingly, for a onecomponent system, such as a fluid of van der Waals spheres, n =1 and the maximum number of coexisting phases is three where a vapor, liquid, and solid coexist at a triple point defined by a specific value of the temperature and pressure. For a system where we fix the temperature and pressure, and $n \geq 2$, a maximum of *n* phases can coexist with one another. Accordingly, at a fixed temperature and pressure, a mixture with n-distinct types of macromolecules in a solvent will have n + 1 distinct components, and in theory, such a system can feature a maximum of n + 1 coexisting phases. The most trivial scenario

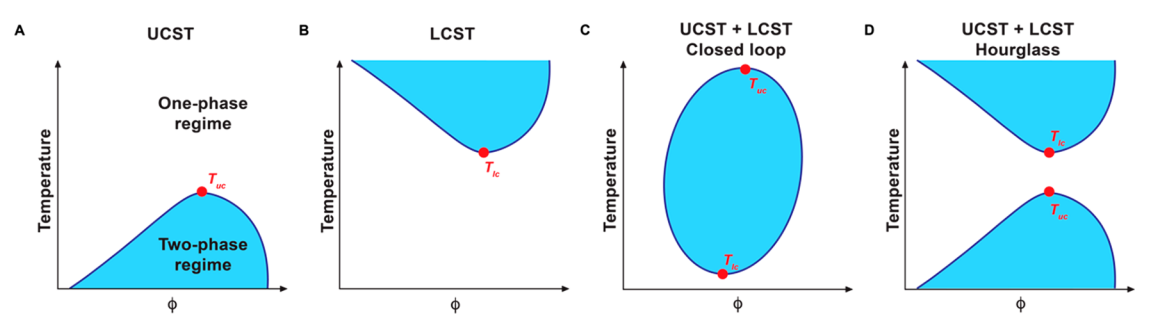


Figure 6. Coexistence curves for different types of thermoresponsive phase transitions. The systems depicted in (A) and (B) have an upper critical solution temperature (UCST) and a lower critical solution temperature (LCST), respectively. (C) A system with both a UCST and an LCST, where the two-phase regime exists between these critical temperatures, resulting in a closed loop. (D) A system with both a UCST and an LCST, with a two-phase regime above the UCST and below the LCST, resulting in an hourglass shape.

pertains to a macromolecule-rich phase and a solvent-rich phase coexisting with one another ¹²⁸ (Figure 5A).

Jacobs and Frenkel¹²⁸ developed a mean-field model that rests on the variance of the distribution of pairwise interaction energies, which we shall denote as σ_2 . This quantity is used to predict the expected phase behaviors of a mixture of n-macromolecules. Note that the distribution of pairwise interactions is the same as the distribution of elements that make up the **B**-matrix. In the formalism of Jacobs and Frenkel, if σ_2 is small, essentially less than k_BT , and n, the number of distinct types of macromolecules is large (n being larger than the limit below which the central limit theorem does not apply), then the prediction is of the scenario depicted in Figure 5A.

If σ_2 is large (greater than $2k_BT$) and n is finite, being ~ 10 , then Jacobs and Frenkel predict that one or a small set of mutually compatible macromolecules will form a phase that coexists with a second dense phase enriched in a distinct set of mutually compatible macromolecules. 128,129 Examples such as these are "water-in-water" systems, 130 where the solvent composition will be roughly the same across the two coexisting phases. This scenario is readily illustrated in synthetic systems comprising the polymers polyethylene glycol (PEG) and dextran. 130 Here, one observes the separation into coexisting PEG-rich and dextran-rich phases (Figure 5B). PEG and dextran are water-soluble polymers that are incompatible with one another. Accordingly, $\chi_{\rm PD}$ is positive, whereas $\chi_{\rm PW}$ and $\chi_{\rm DW}$ are negative. Note that χ_{PD} , χ_{PW} , and χ_{DW} are measures of the effective two-body interactions in the ternary mixture for PEG and dextran, PEG and water, and dextran and water, respectively. In the ternary mixture of PEG, dextran and water, the molecular components can separate into a PEG-rich and dextran-rich phase coexisting with one another. The solvent content in these phases will be determined by the favorable solvation of both polymeric systems.

If the sets of n(n-1)/2 values for the different χ parameters in the X-matrix are dominated by the diagonal elements both in terms of magnitude and their sign, then, from a formal standpoint, n distinct phases, each enriched in one type of macromolecule, can coexist with one another and a dilute phase that is enriched in the solvent (Figure 5C). In cells 131 and even in vitro, 132 one observes multilayered condensates 133 with significant spatial inhomogeneities. Such spatially organized structures, which are also observed in synthetic polymer mixtures 135 and designed systems, 136 cannot be described by mean-field models because the order parameter Φ as used in such models only quantifies the compositions of coexisting phases, not their spatial inhomogeneities.

Overall, an assessment of the ability of a mixture of nmacromolecules to undergo segregative transitions that give rise to two or more coexisting phases will be determined by the elements in the B- or X-matrix. The preceding discussions highlight the importance of measuring second virial coefficients in binary (macromolecule plus solvent) and ternary mixtures (pairs of macromolecules in the solvent of interest). Being able to compute the elements of the relevant B- or X-matrix would represent a major advance in the field. There are serious efforts underway to make this happen, and building on these efforts for the assortment of associative macromolecules of different chemistries and architectures is imperative. Of course, a key challenge is that cellular milieus are complex solvents comprising an assortment of mono- and multivalent ions, region-specific concentrations of protons, osmolytes, metabolites, and small molecule solutes, and finite concentrations of seemingly inert entities that can act as macromolecular crowders. These complexities of the solvent require the accounting of coefficients that quantify preferential interaction or preferential exclusion effects. Further, crowders that are inert will take up volume and this will deplete the macromolecules of free volume, thereby inducing what is known as depletionmediated attraction. The effects of confinement into tight spaces will also have a direct impact on the apparent solvent quality. And finally, the presence of surfaces of membranes, cytoskeletal networks, and other scaffolds of cellular structures can impact the overall solubility profiles in ways that require descriptions in terms of the Gibbs adsorption isotherm. 137 Perturbations or large-scale changes to cellular volumes or components of the cellular milieu, either through active regulation or spontaneous changes in response to stimuli, will have a direct bearing on solvent quality and the driving forces for phase separation. One such physiologically relevant parameter, especially in single cell organisms or in plant systems, is temperature. Changes to temperature will drive thermoresponsive phase transitions, as we describe next.

3.6. Thermoresponsive Phase Behavior

Phase separation in macromolecular solutions will be responsive to changes in solution conditions. ¹³⁸ In aqueous solutions, one of the parameters of interest is temperature, and the phase behavior of interest is referred to as *thermoresponsive phase behavior*. A polymer solution can have an upper critical solution temperature (UCST) (Figure 6A) or a lower critical solution temperature (LCST) (Figure 6B). ¹³⁸

For systems featuring a UCST, the macromolecular solution separates into two coexisting phases below a critical solution temperature denoted as $T_{\rm uc}$. For a system exhibiting a lower

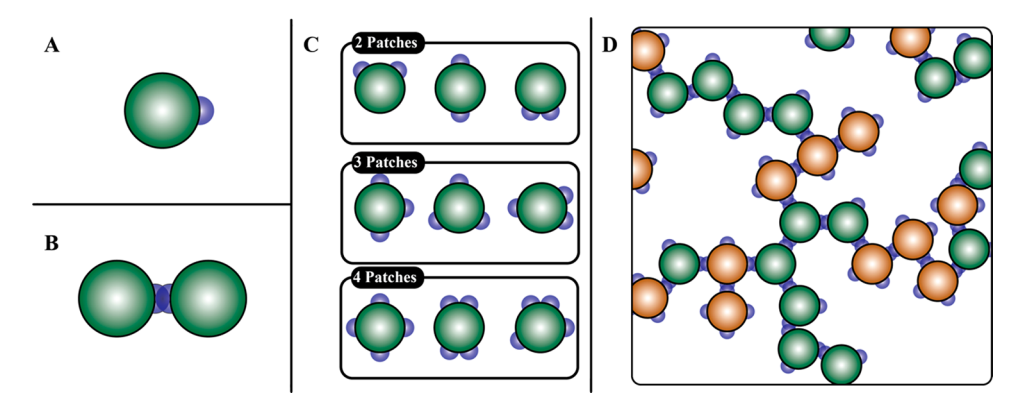


Figure 7. Patchy particles and the structures they form through site-specific interactions. (A) Particle with a single patch. (B) Dimer formed by the interaction of particles, each with a single patch. (C) Particles with two, three, and four patches. (D) System spanning network formed by particles with three and four patches.

critical solution temperature, the polymer solution separates into two phases above a critical solution temperature denoted as $T_{\rm lc}$. The two segregative transitions are driven by different considerations. UCST phase behavior is primarily an enthalpically driven process. As $T_{\rm uc}$ is approached, χ approaches zero because the effective polymer—polymer interactions become less attractive, implying that χ becomes less positive.

LCST phase behavior is entropically driven and enthalpically stabilized. 138,139 The entropic penalty associated with organizing solvent molecules around functional groups along the chain will increase with increasing temperature. This penalty is reduced by the release of solvent, and the segregation of polymers into a solvent-deficient phase. The interactions within the solvent-deficient, polymer-rich phase will be a combination of direct interpolymer contacts and bridging contacts wherein components of the single or multicomponent solvent act as bridges between functional groups of the polymers. 139 Since the two types of transitions have different driving forces, it follows that a polymer solution can have access to both USCT and LCST types of segregative transitions. For homopolymers, this can be achieved by changing the composition of the solvent. 140 For heteropolymers, this can be achieved by the inclusion of sequence features that encode both types of transitions.

We propose, based on a growing corpus of data, 71,139 that binary solutions comprising biopolymers and/or synthetic polymers in an aqueous solvent will likely have access to both UCST and LCST phase behavior 141 (Figure 6C). Whether the upper and lower critical solution temperatures, viz., $T_{\rm uc}$ and $T_{\rm lc}$ are in the accessible range between 0 and 100 °C will depend on a combination of the solution conditions, specifically the prospect of "co-(non)solvency", 142 salt concentration, pH, and hydrostatic pressure, and the types of chemistries that are dominant within the macromolecule. 140,142 Some systems may even feature two closed loops, and this will give rise to apparent hourglass shapes for the coexistence curves in the accessible temperature range 138,140 (Figure 6D).

4.0. ASSOCIATIVE MACROMOLECULES

The preceding discussions focused mainly on segregative transitions, i.e., phase separation of macromolecules. However, biomacromolecules engage in site- and sequence-specific interactions. These interactions enable reversible associations known as binding ¹⁴³ that give rise to complexes of defined structures and numbers/stoichiometries of components. ¹⁴⁴ Accordingly, we describe the networking transitions, which are

purely associative in nature, that arise from accounting for site-specific or chemistry-specific interactions alone. This leads us to the concept of percolation. Once we have introduced the concepts of percolation and demonstrated how percolation thresholds are computed for systems with different numbers and types of cohesive motifs, i.e., stickers, we will segue to considering the coupling between phase separation and percolation or more generally, the coupling of associative and segregative transitions.

4.1. Percolation Transitions in Solutions of Associative Macromolecules

The simplest instantiation of an associative molecule is a hard sphere with an attractive patch (Figure 7A). The patch contributes three features, namely, its size vis-à-vis the size of the spherical particle, the interaction strength, and range of interaction between pairs of patches. ¹⁴⁵ Attractive interactions between pairs of patches enable site-specific reversible crosslinks that form between particles. In a gas of patchy particles, the strengths of attractive interactions with respect to $k_{\rm B}T$ will be the main determinant of the lifetimes of interparticle cross-links. In a fluid of patchy particles, the density of particles will make an additional contribution to the lifetimes of cross-links.

Janus particles have single attractive patches located at precise locations on the surfaces that are otherwise repulsive. Such systems can make dimers through the site-specific cross-links (Figure 7B). However, these systems can also form an assortment of spatial or linear clusters that depend on the size of the attractive patch with respect to the surface area of the particle. For example, cooperative linear polymerization can be realized through clusters of intermediate size if the patch covers more than 30% of the surface of the particle. Janus particles that are generators of various spatial or linear aggregates can now be synthesized to generate precise self-assembled geometries. If we presume that the patches are an order of magnitude smaller than the size of the particle, then a system of particles, each with two patches, can make linear polymers.

What if each of the particles has three or more patches, where each patch is an order of magnitude smaller than the size of the particle (Figure 7C)? Clusters of various sizes will form as each particle can make reversible cross-links with up to three different particles.⁶² New particles can be added to grow the network, thereby increasing the average size of clusters. For a given concentration of particles with three or more patches or stickers, there will be a characteristic distribution of cluster sizes defined by the range of attractions between the patches and the locations

of patches on the surface of each particle. The average cluster size will grow continuously with concentration, such that above a threshold concentration known as a percolation threshold ($c_{\rm perc}$), the particles form a system-spanning network ¹⁴⁹ (Figure 7D). As the bulk concentration of particles grows above $c_{\rm perc}$ the network grows until all particles are incorporated into a single large cluster.

Below $c_{\rm perc}$ the concentration of macromolecules within each of the clusters that forms can be higher than the bulk concentration $c_{\rm bulk}$. This difference in local concentration of macromolecules within a cluster and the bulk will likely increase with cluster size, where the cluster size is defined by the number of molecules within the cluster. ¹⁶ Above $c_{\rm perc}$ the incorporation of clusters into the system-spanning network helps reset the concentration within the network to be akin to that of the bulk. The uptake of solvent by the network can cause swelling of the network. The structures of macromolecules, which determine the types and strengths of cross-links that can form, will determine the network architecture and all the relevant material properties of the network, which is a physical gel.

Unlike phase separation, percolation is a continuous and inclusive transition rather than a first-order segregative one. 16 Specifically, percolation is a geometric transition that quantifies the changes to connectivity of molecules. Therefore, the extent of connectivity for a fixed concentration or the concentration for a fixed extent of connectivity are the relevant order parameters. ¹⁶ These change continuously and the transition cannot be described in terms of the coexistence of distinct prepercolation sol and postpercolation gel phases. Therefore, the sol and gel fractions cannot and should not be estimated by equalizing chemical potentials of the sol and gel fraction. Instead, above the percolation threshold, the sol fraction is incorporated into the gel fraction. As a result, a chemically cross-linked gel can swell to include the solvent or shrink to exclude solvent. In contrast, a physically cross-linked gel can form or break apart in response to changes in solvent. The extent of cross-linking, and the topologies this generates, will set up shear stresses within the cross-linked network.⁵³ These stresses will contribute to elastic or storage moduli, and enable the generation of nonrandom networking of molecules that can lead to spatially inhomogeneous organizations or sponge-like architectures that have been reported for biomolecular condensates.¹¹

Percolation can happen independently of phase separation. For spherical, patchy particles, the percolation threshold can be estimated by knowing the number of patches per particle, which we refer to as the *valence*. The percolation threshold is also determined by the strength of each cross-link that forms when patches form reversible cross-links with one another. The topologies of networks that emerge from percolation are determined by the sequence-specific interactions and conformations adopted by the underlying macromolecules. The physics of patchy spherical particles can be transferred, at least via mean-field models, to describe percolation transitions of linear associative polymers. S5,61,151 In such models, a solution of associative polymers can be modeled, to zeroth order, as a gas with a finite concentration of stickers. This is made feasible by modeling polymers above their overlap concentrations. 16

4.2. Mean-Field Models for Percolation

In biochemical reactions, the totality of reversible associations can give rise to two types of species, viz., a homogeneous distribution of clusters with precise numbers of molecules per cluster or a heterogeneous distribution of clusters, featuring

clusters of different numbers of molecules per clusters. Both types of end products can be described using the formalism of binding polynomials. The number of molecules within a cluster is referred to as the molecularity of the cluster. A microscopic binding reaction consists of clusters that form through reversible associations whereby x number of molecules come together to form a cluster via homotypic associations or x numbers of molecules of type A come together with y numbers of molecules of type B to generate a cluster with x molecules of type A and y molecules of type B. Both scenarios refer to reactions of precise stoichiometries. In the opposite limit, one can also have what are known as isodesmic associations. 152 In such processes, there is an elementary association constant, and the average molecularity of a species in solution increases monotonically with concentration. 153 Macroscopically, such processes are not the same as binding, because the numbers of molecules per cluster do not have a precise upper bound, even though each microscopic step can be modeled as a binding reaction. ¹⁵⁴

We now consider a system of associative macromolecules such as patchy particles in a solvent or linear polymers with $n_{\rm s}$ stickers interspersed by spacers. The macromolecules can associate via sticker–sticker interactions. The mean-field model considers a gas of stickers. This is applicable for describing spherical particles with stickers as patches. It is also applicable for describing the sticker–sticker interactions between linear associative polymers for concentrations that lie above the overlap regime. In this regime, there is no formal distinction between intra- and intermolecular interactions. ¹⁶ To keep matters simple, we shall assume that all sticker–sticker interactions are intermolecular in nature.

In the system of associative macromolecules, where each molecule features three or more stickers, each molecule can make different types of physical cross-links pictured in Figure 8.

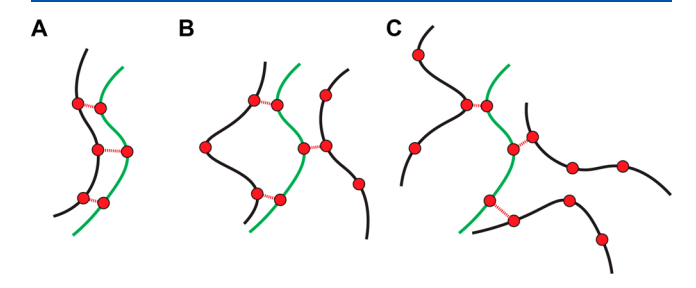


Figure 8. Clusters versus percolation. (A) A dimer forms that cannot grow into a network. (B and C) Trimers of different topologies featuring unsatisfied stickers that poise the system to grow and become a percolated network.

Formally, all three cross-links can be between the same pair of molecules, giving rise to a dimer that cannot grow (Figure 8A). This network-terminating scenario will minimize the entropy of cross-linking. However, there are other options to consider. Every option that is not a closed dimer can seed a network that can grow to a certain size (Figure 8B,C). Accordingly, for a fixed concentration of polymers, there is a threshold extent of association denoted as $p_{\rm perc}$ above which the polymers form a system-spanning network due to the network of specific physical cross-links. If each molecule has $n_{\rm s}$ stickers and each sticker can make up to k bonds or cross-links, then the Flory–Stockmayer criterion 13,54 for $p_{\rm perc}$ is written as $p_{\rm perc} = (n_{\rm f}-1)^{-1}$. Here, $n_{\rm f} = kn_{\rm s}$ is the functionality of each sticker. If k=1, then $n_{\rm s}=3$ is the

minimum number of stickers per molecule that is required to realize a percolation transition.

For a fixed set of sticker types, there is a threshold concentration denoted as $c_{\rm perc}$ above which the polymer solution forms a percolated, system-spanning network. The network size grows continuously above $c_{\rm perc}$ until all molecules are incorporated into the network. The topology of the network will be governed by the structures or architectures of the underlying molecules that make up the network. The value of $c_{\rm perc}$ will be determined by the numbers of stickers and the interaction strengths of stickers. The estimation of $c_{\rm perc}$ can be generalized to consider multiple sticker types such that the hierarchy of interaction strengths and valences of different sticker types will contribute directly to $c_{\rm perc}$.

Binding reactions can drive percolation transitions, which is a geometric transition characterized by a networking of multivalent macromolecules. However, percolation cannot be described using binding isotherms. Instead, percolation requires the formal description of a networking transition—a problem that has been solved for various topologies and dimensions in mathematical theories of percolation. Below, we summarize models that are in the spirit of the original Flory—Stockmayer formalism for percolation. Our summary is of the model developed by Choi et al. Our summary is of their work.

We consider a set of N associative macromolecules, each with n_i stickers of type i. For simplicity, we shall assume that each sticker can engage in a single physical cross-link. We consider a pair of stickers i and j that form a physical cross-link denoted as $i \leftrightarrow j$. This leads to a gain in energy of ε_{ij} . The formation of a $i \leftrightarrow j$ cross-link will constrain the sticker pairs i and j to a "bond volume" v_{ij} . We introduce a parameter $\lambda_{ij} = v_{ij} \exp\left(-\varepsilon_{ij}/k_{\rm B}T\right)$. In the Flory—Stockmayer framework, 13,54 a macromolecule that is part of a network can only make a cross-link to a free macromolecule. We shall write the free energy of the system as $F = -k_{\rm B}T \ln Z$. Here, Z is the partition function that is computed by assuming a mean-field model for a gas of stickers. It is written as

$$Z = \Omega \prod_{i,j} \exp \left(-\frac{N_{ij} \varepsilon_{ij}}{k_{\rm B} T} \right) \left(\frac{\nu_{ij}}{V} \right)^{N_{ij}}$$
(12)

In Equation 12, i and j are the indices of the sticker types, N_{ij} is the total number of paired stickers of type i and j, V is the volume of the system, and Ω is a factor that quantifies the number of unique combinations of stickers that yield N_{ij} sticker pairs of type i-j. Minimization of F, the mean-field free energy, with respect to N_{ii} , the number of homotypic pairs of stickers, and N_{ij} the number of heterotypic pairs of stickers, subject to the assumption of weak interactions, i.e., λ_{ij} $(Nn_i - N_{ij})/V \ll 1$ and λ_{ij} $(Nn_j - N_{ij})/V \ll 1$ leads to an estimate for the average number of interacting stickers per macromolecule p, which becomes

$$p \approx c \frac{\sum_{i} \lambda_{ii} n_{i}^{2} + 2 \sum_{i \neq j} \lambda_{ij} n_{i} n_{j}}{\sum_{i} n_{i} - 1}$$
(13)

Here, c is the concentration of macromolecules. According to the Flory–Stockmayer criterion, 13,54 the average number of interacting stickers per macromolecule at the percolation threshold $p_{\rm perc}$ is estimated using

$$p_{\text{perc}} = \frac{1}{\sum_{i} n_i - 1} \tag{14}$$

Inserting the expression for p_{perc} shown in Equation 14 into the left-hand side of Equation 13, we obtain the following expression for c_{perc} :

$$c_{\text{perc}} \approx \frac{1}{\sum_{i} \lambda_{ii} n_{i}^{2} + 2 \sum_{i \neq j} \lambda_{ij} n_{i} n_{j}}$$
(15)

Knowledge of the number of stickers of type i, the bond volumes v_{ij} , and the interaction strength ε_{ij} is sufficient for a mean-field estimate of the percolation threshold c_{perc} .

5.0. COUPLING OF ASSOCIATIVE AND SEGREGATIVE TRANSITIONS

In multivalent systems, there is always the formal possibility of percolation above a threshold concentration $c_{\rm perc}$. Conversely, in a poor solvent, where $v_{\rm ex}$ is negative and χ is positive, the one-phase, well-mixed solution can become saturated, and the free energy of mixing is minimized by phase separation of the macromolecular solution that is realized beyond a χ -dependent threshold concentration designated as $c_{\rm sat}$. The key questions are 2-fold: Can phase separation (the segregative process) and percolation (the associative process) be coupled to another? And what is the nature of this coupling, i.e., how do the segregative and associative transitions influence one another?

A fluid of patchy particles can undergo segregative transitions if the density crosses a threshold value. The strengths of site-specific, interpatch interactions, and the sizes of the patches will rescale the density threshold for segregative transitions when compared to the hard sphere fluid. Accordingly, the phase transitions of a square-well fluid consisting of hard sphere molecules with a single patch are the simplest examples of systems featuring site-specific interactions that also undergo phase separation.

Phase transitions of spherical patchy particles will come under the rubric of COAST if at least a fraction of the particles have at least three patches. The system will undergo phase separation and this will depend on the sizes of particles, the densities of particles, the sizes of the patches vis-à-vis the particles, and the ranges as well as strengths of interactions between patches. 155 This is also true for solutions of linear or branched associative polymers where each polymer has at least three stickers that can engage in intermolecular interactions. Indeed, as shown in the literature on associative polymers, there is always the formal possibility that phase separation can be coupled to percolation. 47,52,55,156 In a binary mixture, if we denote the threshold concentration for phase separation as c_{sat} , then the system will separate into two coexisting phases of concentrations c_{sat} and $c_{
m dense}$ if the bulk concentration $c_{
m bulk}$ is greater than $c_{
m sat}$. There are two realistic possibilities for the interplay between phase separation and percolation. 47,156 If c_{bulk} is greater than c_{sat} and $c_{\rm sat} < c_{
m perc} < c_{
m dense}$, then phase separation and percolation are coupled. Conversely, if $c_{perc} < c_{sat}$ then percolation is realized without phase separation.

Dense phases or condensates that form via PSCP are gel-like because percolated networks form within the dense phases. Whether the condensates have the rheological properties of solids, glasses, or liquids will depend on the interplay between the time scales for the making and breaking of cross-links and the time scales for mobility and transport of molecules within the dense phase and across the phase boundary. ¹⁵⁷

5.1. The Stickers-and-Spacers Framework

The amplitudes of the conformational fluctuations of flexible macromolecules, a feature we do not consider when discussing rigid patchy particles, will contribute directly to the behaviors of flexible polymers in different concentration regimes. 16 A key parameter is the overlap volume fraction, 158 which is the concentration above which the likelihood of realizing intermolecular interactions is higher than the likelihood of realizing intramolecular interactions. ¹⁶ The overlap concentration changes with solvent quality, decreasing significantly in a good solvent where χ is negative, and increasing to a plateau value in a poor solvent where χ is positive. ¹⁵⁸ Despite the decreased overlap concentration for a homopolymer in a good solvent, the increased likelihood of intermolecular associations is offset by the relatively repulsive intermolecular interactions. 159 Conversely, homopolymers in poor solvents typically undergo associative transitions and phase separation at concentrations that are well below the overlap concentration. Accordingly, the overall phase behavior is determined mainly by the magnitude of

For associative polymers, there is an intricate interplay between the effects of γ and the contributions of sticker–sticker interactions. As a result, segregative transitions can be realized even for slightly negative, zero, or slightly positive values of χ . Here, slightly negative values refer to slightly positive values of v_{ex} , where v_{ex} is less than 10% the volume of the chemical or Kuhn monomer. The realization of segregative transitions for zero, or slightly positive values of vex is a consequence of three contributions, viz., (i) the multivalence of associative interactions involving stickers, (ii) the cooperativity of sticker-sticker interactions in dense phases, and (iii) the fact that configurational entropy of spacers can still be maximized through a mixing of chain degrees of freedom (a consequence of being above the overlap concentration) within dense phases. As a result, segregative transitions are feasible for weak stickersticker interactions (vis-à-vis k_BT) if the sticker valence is high when compared to the minimal value of three. Conversely, for strong sticker–sticker interactions (again with respect to k_BT), lower sticker valencies will be sufficient to enable segregative transitions. Additionally, for zero, slightly positive or even slightly negative values of v_{ex} the overlap concentration will be low, and it can be lowered further by increasing the degree of polymerization. What emerges is not only percolation through the network of sticker-sticker interactions, but phase separation through the effects of nonsticker regions, known formally as spacers, and synergy between associative and segregative transitions. The resultant phase transition is referred to as phase separation coupled to percolation (PSCP).

At this juncture, it would be useful to provide a brief nonchronological overview of the stickers-and-spacers framework for molecular liquids, patchy colloids, and linear associative polymers. The theory of molecular association in liquids dates to the 1950s at least. These theories were developed to explain deviations of colligative properties such as freezing point depression from expectations based on the assumption of ideal mixtures. This led to the development of models that accounted for strong, anisotropic effects in hydrogen-bonding liquids. These were added to augment the regular solution theories of Hildebrand, on which the Flory—Huggins model is based. In the 1970s, considerable attention was focused on the development of polymeric materials that showed shear-thickening behaviors for application as adhesives and coatings. In such systems, the intrinsic viscosity of polymers

increases with time and concentration. 163 These rheological properties were traced to specific features of polymers, namely, the presence of multiple strong, self-associating functional groups known as stickers. 163–165 Ionomers, i.e., polymers featuring a small number of uniformly spaced ionic groups along otherwise neutral scaffolds, were among the first systems studied that came under the rubric of associating or associative polymers. 162 These systems were shown to form strong physical gels. They also exhibited a range of microphases such as spherical or cylindrical micelles, the ability to form aggregates of specific size, ¹⁶⁶ and the ability of micelles or aggregates to crosslink into higher order macrophases or gels. ¹⁶⁷ In the 1990s the theories of associative polymers focused intensely on the roles of spacers, the regions interspersed between stickers, as modulators of percolation thresholds, and the determinants of the extent of coupling between phase separation and percolation. The key finding was that polymers with an overall $\chi \approx 0$ or even slightly positive could undergo phase separation due to the influence of the strong associative nature of stickers. This picture deviated from expectations based on homopolymers in a solvent. There were animated discussions regarding the merits of certain assumption, the most important being the treatment of the sol and gel as coexisting phases and the equalization of chemical potentials across the sol-gel "boundary". These issues were satisfactorily resolved, and by 2010 a mature framework emerged, 53,168 based on mean-field models, for describing associations among polymers in the overlap regime, and the coupling of these associations to phase separation, which continues to be described by a Flory-Huggins formalism. Generalizations were made to describe polyelectrolytes crosslinked by multivalent counterions. 169 The contributions of Cates, ¹⁷⁰ Freed, ¹⁷¹ Halperin, ¹⁷² Joanny, ¹⁷³ Khokhlov, ¹⁷⁴ Rubinstein, ^{55,61} Semenov, ⁵⁵ Tanaka, ^{52,60,175} Wertheim, ^{165,167,176} Witten, ¹⁷⁷ and many others have inspired computational and theoretical approaches 29,178 aimed at explaining a growing corpus of experimental data in the condensate field and regarding observations made for soft materials.17

5.2. Mapping Stickers and Spacers onto Architectures of Associative Macromolecules

Colloidal particles range in size from nanometers to micrometers, and they are collections of atoms held together by strong cohesive interactions rather than by covalent bonds. In the early literature, proteins were viewed as being akin to colloidal particles. Advances in structural biology rendered such coarsegrained descriptions as being moot. However, the colloidal picture is still useful for structure-based coarse graining that enables analytical or semianalytical descriptions of segregative transitions. The addition of attractive patches onto colloidal particles generates a mapping from high-resolution structural descriptions to a coarse-grained model that preserves the feature of proteins engaging in site-specific interactions. In this mapping, the patches that enable site-specific interactions are known as *stickers* because they enable highly specific, reversible cross-links. The remaining surface features are collectively known as spacers. The hard versus soft interactions of spacers (which refers to the steepness of the repulsive potentials used to model steric exclusion) and the possible presence of uniform attractions mediated by spacers will be the main contributors to segregative transitions. Rigid or semirigid folded domains of proteins can be mapped onto patchy colloids (Figure 9A).

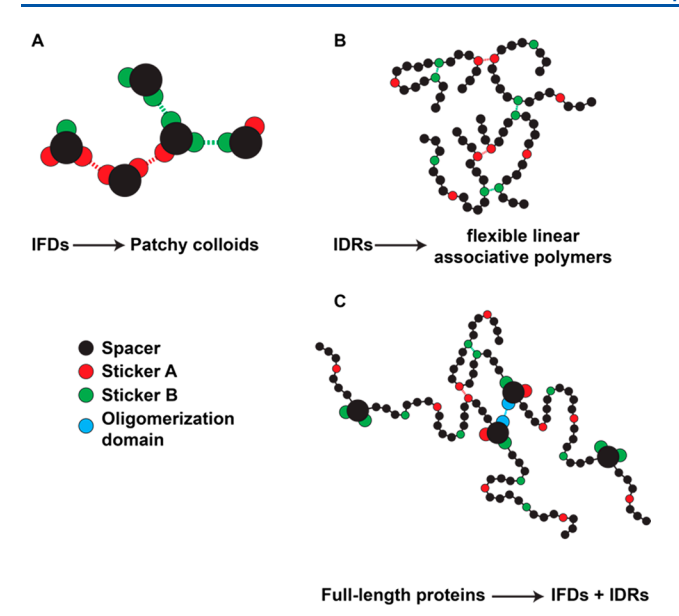


Figure 9. Mapping of proteins onto different physical instantiations of associative macromolecules. (A) How intrinsically foldable domains (IFDs) may be mapped onto patchy colloids. (B) How intrinsically disordered regions (IDRs) may be mapped onto flexible, linear associative polymers. (C) How full-length proteins with IFDs and IDRs may be mapped onto specific combinations of patchy colloids and linear polymers. In all cases, black regions indicate spacers, and red and green regions indicate different types of stickers. Blue regions in (C) indicate oligomerization domains that behave as strong stickers.

IDRs modeled as autonomous units can be mapped onto flexible, linear associative polymers as shown in Figure 9B. Here, the stickers enable specific intra- and intermolecular cross-links. These stickers can be short linear motifs, specific types of molecular recognition features, ¹⁸¹ or individual residues. An IDR can feature many different sticker types. These include different chemistries, different sizes of stickers, and differences in the structures of the motifs that make up stickers.

In IDRs, the stickers can be uniformly distributed along the sequence, randomly distributed along the sequence, or arranged into distinct blocks. Depending on the number of distinct types of stickers, the segregation of stickers into distinct blocks gives rise to polymers with block copolymeric architectures. Such systems typically form microphases, such as spherical or cylindrical micelles or lamellae that have fixed sizes and molecularities. 78,79,183

Associative macromolecules, specifically proteins, often feature a combination of folded domains and IDRs. Depending on whether there is oligomerization through the folded domains, the architectures can be linear, branched, or a combination thereof (Figure 9C). Further, reversible associations that give rise to oligomers of precise or variable molecularities can also enable many combinatorial options for generating associative macromolecules.

5.3. Separable Contributions to Segregative and Associative Transitions

Both patchy particles and associative polymers can undergo phase transitions that come under the rubric of COAST. The concentration regimes where these transitions become accessible can be fundamentally different for the two types of architectures. This is tied to the fact that flexible systems enable overlaps of molecules at macromolecular concentrations that are orders of magnitude lower than for rigid molecules. As a result,

hybrid molecular architectures, featuring patchy colloids interspersed by flexible polymers, will provide tunability of the overall phase behavior.¹⁸⁴ The underlying architectures of associative macromolecules also affect the network topologies of dense phases formed by phase separation.

Processes that come under the rubric of COAST are driven by a combination of solubility-determining interactions, encapsulated in the osmotic second virial coefficient, and specific interactions between stickers. Formally, it is easy to prescribe a clear separation between the two types of interactions, but in practice this is difficult. To clarify this point, we first ask if there is a connection between the dissociation constant for dimer formation and the second virial coefficient. As a thought experiment or in a computer simulation, one can perform the following assessments: First, we quantify the free energy of association by an alchemical replacement of the stickers, where, for simplicity, all units along the chain are identical to one another. This free energy of association, which we refer to as $\Delta\mu_{\scriptscriptstyle a}$, is attributable solely to the contribution from the second virial coefficient. Next, we consider dimerization by adding one sticker at a time. The free energy of association that results from addition of each of the stickers is referred to as $\Delta \mu_s$, where s refers to the number of stickers that have been incorporated into the calculation. The difference denoted as $\Delta \Delta \mu_{\rm excess} = (\Delta \mu_{\rm s} \Delta \mu_a$) quantifies the difference between the contributions of specific associations from s stickers versus solvent-mediated associations of the sticker-free system.

Solvent-mediated interactions, which drive segregative transitions, have been referred to as "non-specific" interactions. 59,60,109,185 We do not subscribe to this type of simplification because solvent effects can be rather complex and highly specific to the macromolecules being studied. Instead, the contributions of different interactions that we attempt to capture in our prescription of $\Delta\Delta\mu_{\rm excess}$ can be cast as a rescaling of χ , whereby the rescaled version is written as $(\chi' = \chi + \chi_{\rm assoc.})$. Here, χ is the polymer-specific, sticker-free contribution of pairwise interactions to the free-energy density of a polymer solution, and $\chi_{\rm assoc.}$ quantifies how χ is augmented by the contributions of specific sticker–sticker interactions.

Although the contributions to χ and $\chi_{assoc.}$ are formally separable, this can be nontrivial from an experimental standpoint. One way of approaching this is to use two distinct assays. A scattering-based assay or measurements of colligative properties, which averages over all configurations of the polymer and solvent, yields an estimate of B_2 and hence χ . This can be complemented by a site-specific assay for binding, such as one that quantifies the change in quantum yield of the intrinsic fluorescence or changes in fluorescence lifetimes of locations proximal to the site of interest, coupled to mutagenesis, which can be used to infer $\chi_{assoc.}$ by referencing it to the measurement of B_2 for the mutant that lacks the sticker(s). In this approach, the contribution of specificity is the contribution to the pairwise dissociation constant that cannot be explained by the contribution from B_2 alone. Alternatively, one can compare calorimetric enthalpies to enthalpies derived from the measured osmotic second virial coefficients. The difference between these enthalpies represents the contribution from specific interactions.

Importantly, for a fixed set of solution conditions, the osmotic second virial coefficient is a quantification of the effective strength and nature of pairwise associations of macromolecules in solution. It quantifies an effective free energy of dimerization in solution and can only describe the formation of higher-order assemblies based on pairwise interactions among the molecules.

However, higher-order associations whereby the assembly cannot be thought of as a sum of dimers, will require the consideration of higher-order terms in the virial expansion. Accordingly, in the rescaling of χ , the $\chi_{\rm assoc.}$ term often features a concentration dependence to account for higher-order species that can be generated by site- or residue-specific intersticker interactions. 52,53

Overall, the addition of stickers, i.e., associative groups to a macromolecule, will rescale the effective two-body interactions and require that we consider more than just the second virial coefficient, which, as we have discussed, is the primary determinant of polymer solubility. 52,53 These considerations are incorporated into $\chi_{\rm assoc}$, which will also be concentration-dependent to allow for the prospect of prepercolation clusters forming and growing continuously with concentration. 52,53

The most tractable and well-studied system for understanding PSCP transitions are linear multivalent proteins (Figure 9C). Here, pairs of multivalent proteins make complementary, sitespecific interactions through their folded domains. Wellestablished examples include the poly-SH3 and poly-PRM as well as the poly-SUMO and poly-SIM systems in aqueous solvents. 1,46-48,126,187 The folded domains encompass stickers at specific sites. These sites make complementary heterotypic interactions, viz., SH3 with the PRM and SUMO with the SIM. The linkers are the primary spacers that contribute to the excluded volume and hence to the coupling between segregative and associative transitions. 188 The surfaces of folded domains, specifically their electrostatic features governed by both homotypic and heterotypic interactions, can also contribute to the osmotic second virial coefficient. 46,48,187,188 Therefore, the surfaces of folded domains may be viewed as auxiliary spacers. These surfaces can also contribute as auxiliary stickers based on the presence of complementary motifs within the linkers and the surface of the folded domain.

Harmon et al. studied the simple example of a patchy-colloidlike folded domain and a disordered linker that lacks any auxiliary motifs.⁴⁷ Further, the excluded volume, which they referred to as the *effective solvation volume* (v_{es}) , of the linkers was set to be zero or greater than zero. Harmon et al. showed that linkers for which $v_{es} = 0$ will undergo PSCP-like transitions. They discerned this using two distinct order parameters, one for detecting segregative transitions and the other for associative transitions. For the former, the relevant order parameter is the concentration of macromolecules. For the latter, the relevant order parameter is the connectivity of molecules and hence the number of molecules within the single largest cluster. Choi et al. later formalized the distinction of the two order parameters, using radial distribution functions to detect the onset of spatial inhomogeneities and the presence of two phases of two different macromolecular densities, namely, a dense and a dilute phase. 189

The coupling of segregative and associative transitions can be quantified by computing $c_{\rm perc}$ using generalizations of Flory—Stockmayer theory. ^{13,54} The mean-field theories for gelation put forth by Flory ¹³ and Stockmayer ⁵⁴ allow one to estimate $c_{\rm perc}$ just by knowing the valence and intrinsic affinity of the stickers. In particular, the Flory—Stockmayer theory allows one to estimate the threshold concentration above which a system-spanning network is formed by a gas of stickers as described above in section 4.0.

Harmon et al. computed a ratio they referred to as c', which they defined as the ratio of the percolation threshold estimated from their simulations to the percolation threshold estimated based on the mean-field Flory—Stockmayer theory. ^{13,54} If c' < 1,

then tethering the stickers to linkers enables a positive cooperativity of the percolation transition. This positive cooperativity implies that the percolated network is realized at concentrations that are lower than would be feasible for a gas of stickers. This comes about due to a coupling of associative and segregative transitions and the formation of a dense phase that is in essence gel-like. Further, the probability of forming a new intersticker cross-link is enhanced in the presence of an extant cross-link, and this positive cooperativity is enabled in the dense phase and is facilitated by the linkers of zero effective solvation volume.

Essentially, the segregation into dense and dilute coexisting phases is an emergent property of the coupling between the flexible nature of the spacers, their solvation preferences, and the associative, specific interactions of the stickers. Although Harmon et al. did not study what transpires when $v_{\rm es}$ is negative (i.e., $\chi>0$), the expectation for this scenario is intuitive in that segregative transitions can be enhanced by the properties of the spacers. Such a scenario can lead to precipitation if the spacers become strongly segregative, which would happen if the positivity of χ increases substantially vis-à-vis the dissociation constant of sticker—sticker interactions.

For linkers of zero or slightly negative v_{es} , the segregative and associative transitions can be fully decoupled if the linkers are long, or if the intrinsic sticker–sticker interactions are not much stronger than $k_{\rm B}T$. In this scenario, percolation, in accord with Flory–Stockmayer theory, will occur without phase separation.⁴⁷

Interestingly, up to a point, the PSCP behavior is preserved even for positive values of $v_{\rm es}$ (i.e., negative values of χ). However, depending on the interplay between the affinity of sticker—sticker interactions and the magnitude of the positive $v_{\rm es}$ (negative χ), the segregative transition can become significantly destabilized. Large positive values of $v_{\rm es}$, specifically those that approach the upper limit of $v_{\rm es}$, will suppress phase separation. Further, the high effective solvation volumes of the spacers will also hinder the networking transitions, thus causing an upshift of $c_{\rm perc}$ when compared to the Flory—Stockmayer limit.

Taken together, the domain-linker plus motif-linker systems allow for a clear delineation of stickers versus spacers. This has allowed for the extraction of rules that enable the design of systems where the associative percolation transition and segregative phase separation can be strongly coupled or fully decoupled. The relevant parameters are the sticker valence, the sticker—sticker interaction strengths, the effective solvation volumes of spacers, and the flexibility and length of spacers/linkers.

Recent work has shown that the findings can be transferred onto IDRs studied as autonomous units. This requires more elaborate efforts to delineate stickers and spacers, bringing to bear the combination of experimental and computational methods that are also deployed for the study of sequence-ensemble relationships of IDPs. The overall approach to identifying stickers versus spacers leverages the one-to-one correspondence between the interactions that contribute to collapse transitions of individual polymers in ultradilute solutions and the multichain interactions that contribute to phase separation. 3,63,64,66

5.4. Associative Macromolecules Form Prepercolation Clusters in Subsaturated Solutions

In their work on the phase transitions of linear multivalent proteins, Li et al. described their observations as being **Chemical Reviews** Review pubs.acs.org/CR

"macroscopic liquid—liquid phase separation that is thermodynamically coupled to sol-gel transitions in the droplet phase". 46 This phrasing describes PSCP, which is a process that comes under the rubric of COAST.

Depending on the strengths and valence (number) of stickers, associative macromolecules can form clusters at very low concentrations. Clusters that form below c_{sat} are referred to as prepercolation clusters that form in the sol or pregel when describing gelation or percolation decoupled from phase separation. For a given bulk concentration c_{bulk} that is below the saturation concentration ($c_{\text{bulk}} < c_{\text{sat}}$), the distribution of cluster sizes, $p(n_{\text{cluster}}|c_{\text{bulk}})$ will be determined by the sticker valence, the sticker-sticker interaction strengths, and the macromolecular concentration c_{bulk} or, more precisely, the degree of subsaturation defined as $s_{\text{sub}} = \ln(c_{\text{bulk}}/c_{\text{sat}})$. The reversible associations will be describable by a series of microscopic reversible steps. 52

The expectation of polydisperse clusters in a sol provides a definitive test for whether the process of condensate formation is purely segregative or if it comes under the rubric of COAST. 52 For purely segregative transitions, the subsaturated solutions defined by the bulk concentration being below c_{sat} are best described as a disperse gas of unassociated macromolecules. 190 The key point is that for purely segregative transitions, the only relevant energy scale in a binary mixture will be prescribed by χ . Clustering in subsaturated solutions will be bounded, because the likelihood of cluster formation, which will change with s_{sub} , will become zero for clusters comprising small numbers of molecules. 190 However, if associative and segregative transitions are coupled, then the subsaturated solution is a sol, defined by an assortment of clusters characterized by reversible cross-links. The size distribution of prepercolation clusters is typically heavy tailed (Figure 10), implying that, while most of the species in

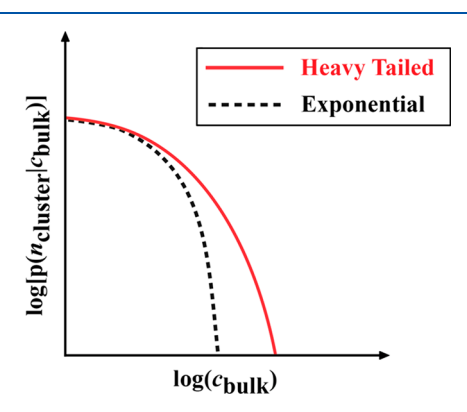


Figure 10. Schematic of an exponentially bounded (black dashed curve) versus heavy-tailed (red solid curve) version of $p(n_{\text{cluster}}|c_{\text{bulk}})$.

solution are likely to be dispersed monomers and oligomers, there is a finite, albeit small likelihood of observing mesoscale clusters. 190

In a sol-like description for the coexisting dilute phase, the likelihood of forming polydisperse clusters will increase with increasing concentration. Recent in vitro studies haved provided definitive evidence for the presence of heterogeneous distributions of prepercolation clusters in subsaturated solutions. 190 Detecting these species requires the use of a combination of methods in vitro that allows one to access the totality of species that form in subsaturated solutions. 190 Each of the methods used by Kar et al. 190 has distinct advantages and limitations. Dynamic light scattering (DLS) is sensitive to the

most abundant species and the largest, least abundant species. However, the abundance of distinct species cannot be quantified using DLS. Instead, nanoparticle tracking analysis (NTA) was needed to quantify abundance. 190 However, this too is a scattering-based method, and hence only the abundance of the largest species, which is in the 1% range or lower depending on bulk concentration, could be quantified. Methods based on measurements of fluorescence anisotropy or fluorescence correlation spectroscopy (FCS) were also used, and these relied on the use of mixtures of unlabeled and fluorescently tagged proteins. 190 However, anisotropies plateau past a certain size, as explained by Kar et al., 190 and the ability to detect species that grow becomes increasingly challenging using FCS because of the low mobilities and low abundance of such species. These limitations were overcome using methods based on ultrafast mixing and confocal detection in microfluidic channels. 191 In these methods, one separates mixing of species from transport, and hence one can get a full readout of the entire size distribution. Fluorescence anisotropy measurements using freeto-move molecular rotors 192 coupled to fluorescence intensity distribution analysis provided the most definitive assessments of the continuous evolution of size distributions and the heavytailed nature of these distributions as a function of protein concentration. Kar et al. 190 brought all these methods to bear on the quantification of species distributions in subsaturated solutions of the protein FUS and other FET family proteins. These measurements, performed at a series of concentrations in sub-saturated solutions, provided definitive evidence of the presence of monomers, oligomers, and mesoscale clusters. 190

A recent complementary study focused on the distribution of species formed in subsaturated solutions of the proteins Rubisco and EPYC1. 193 These studies largely corroborated the findings of Kar et al. with one discrepancy. The authors noted the absence of a heavy tailed distribution and an absence of mesoscale species. They proposed that this might be due to differences in the cluster landscape organized by heterotypic interactions versus purely homotypic interactions. This may well be true, and ongoing studies will help clarify the role of the interplay between homotypic and heterotypic interactions as determinants of cluster distributions. However, it is worth emphasizing that the work of He et al. 193 used only FCS, and this has intrinsic limitations as explained above and in detail by Kar et al. 190

In vivo, the clearest example of prepercolation clusters comes from work on the nuclear protein negative elongation factor (NELF) that forms condensates in response to stress, thereby arresting transcription thus functioning as intranuclear stress granules. 194 Using confocal microscopy, Lan et al. noted a uniform distribution of NELFs in the nucleoplasm when stress is absent. 195 However, using highly inclined and laminated optical sheet microscopy, Lan et al. discovered that NELF proteins form a polydisperse distribution of clusters in the nucleus. ¹⁹⁵ The size distribution of clusters has a heavy-tailed shape. At the onset of stress, the clusters coalesce to form condensates that sequester essential transcription factors. The sol that coexists with condensates features distributions that are reminiscent of what they observe at ultralow expressions. When the MAP kinase P38 is inhibited, condensates do not form, but the clusters persist. This work demonstrates a clear separation of interactions that drives clusters versus condensates. One of the key takeaways is that the free-energy profiles for condensate formation, which they extract from their data, are rather flat. 195 Further, the *in vitro* and in vivo studies that use multipronged approaches highlight

the weaknesses of drawing definitive conclusions based on one set of methods, especially when the methods in question have diffraction limited spatial resolutions. There is clearly much to learn by integrating measurements that probe the nano-, meso-, and micro-scales. And the integrated contributions of segregative and associative effects are likely to become clear only through interrogations that span the multitude of length scales. A recent study highlights the importance of multiscale, multiresolution studies of condensate structures and the fact that networks of interactions undergird condensate structures. The sponge-like structures observed by Gall and colleagues for nucleoli and Cajal bodies 117 are evident even for the simplest of condensates, both computationally and experimentally.

5.5. Implications of Prepercolation Clusters for Dynamics of Phase Transitions

The local concentration of macromolecules within clusters will be higher than c_{bulk} . Notice that such concentration inhomogeneities are also present in atomic and molecular liquids as is evident in the peaks and troughs of radial distribution functions. ^{30,102} The concentration inhomogeneity within a cluster comprising $n_{\rm cluster}$ molecules can be defined as ψ = $(c_{\text{bulk}}/c_{\text{cluster}})$. Here, c_{bulk} and c_{cluster} are the concentrations of macromolecules within the bulk and cluster, respectively. An inhomogeneity refers to values of ψ being less than or greater than one. Values of ψ < 1 are realizable through intermolecular associations. The expectation is that the inhomogeneity ψ becomes more pronounced, decreasing to be below one, as cluster sizes increase. While this is not what we expect for a distinct phase of uniform density, the finite sizes of clusters allow for this scenario as a formal possibility. Further, the overall solubility sets up c_{sat} , the threshold concentration above which the one-phase regime is saturated. Accordingly, the buildup of local concentration inhomogeneities through cluster formation will be governed by the "structure" (functional form or shape) of the cluster distribution $p(n_{\text{cluster}}|s_{\text{sub}})$, which quantifies the probability of realizing a cluster with $n_{cluster}$ molecules for a given subsaturation s_{sub} .

The combination of the system becoming supersaturated for $c_{\text{bulk}} > c_{\text{sat}}$ and the concentration inhomogeneities engendered by prepercolation clusters of size n_{cluster} will drive a combination of segregative and associative (networking) transitions. The dynamics of the coupling between clustering and macroscopic phase separation were recently measured by Kar et al. using dynamic light scattering and time-resolved microscopy. These data provide a qualitative picture of the transition from prepercolation clusters in the subsaturated sol to a coexistence of the sol with dense condensates featuring percolated networks of macromolecules.

The presence of prepercolation clusters appears to rule out homogeneous nucleation and growth as the operative mechanism for a COAST-like process. Homogeneous nucleation rests on the notion of a single energy scale defined by χ . This can only be operative for a purely segregative transition that lacks any surface defects or seeds. Instead, describing the dynamics of a COAST-like process such as PSCP requires that one accounts for the presence of prepercolation species that form and dissolve on time scales that are considerably more rapid than the time it takes for condensate formation via homogeneous nucleation, coarsening, or some variation thereof.

A reasonable postulate is that prepercolation clusters enhance the rates for phase separation in supersaturated solutions because the clusters poise the system for segregative transitions. It is also conceivable that prepercolation clusters erect a sort of kinetic proof-reading barrier if the clusters are to undergo significant rearrangement within the condensate, or new interactions must be added to drive condensate formation. The latter has been reported recently to explain the transition of NELF clusters to NELF condensates in the context of forming condensates that sequester essential transcription factors in response to nuclear stresses. ¹⁹⁵

5.6. Examples of Systems That Undergo Phase Separation Coupled to Percolation

The importance of multivalence was established in the domain-linker-domain systems interacting with motif-linker-motif systems that Li et al. studied. His work showed how valence matters for associative transitions. It also showed that the result of phase transitions are spherical droplets that are now referred to as condensates. These dense phases cannot come from percolation alone. However, the formation of dense phases can be explained by understanding the roles of linkers, which were resolved by Harmon et al. Harmon et al.

A clear prediction for PSCP would be the observation of prepercolation clusters conforming to a heavy-tailed distribution that should form in subsaturated solutions. Li et al. 46 reported what they termed as oligomers. Kar et al. showed that polydisperse clusters form in subsaturated solutions. 190 Their observations were concordant with a heavy-tailed distribution. Support for these observations *in vivo* comes from the work of Lan et al., 195 which we have already summarized.

In their recent molecular cartography inside cells, Cho et al. ¹⁹⁸ made an interesting observation. They found that components of stress granules, specifically ATXN2L, NUFIP2, and FXR1, which are all RNA binding proteins, have "texture" in terms of their cytoplasmic colocalization even in the absence of stress. In their parlance, texture refers to detectable preferential localization. Given the resolution of their approach, colocalization refers to the types of prepercolation clusters observed by Kar et al., *in vitro*, and Lan et al., in the nucleus. RNA binding proteins with multiple RNA recognition motifs tethered by a combination of prion-like low complexity domains and Argrich IDRs seem to be prominent drivers of prepercolation clusters via homotypic interactions. Heterotypic interactions with RNA transcripts likely modulate the cluster distributions and/or coopt prepercolation clusters to form condensates.

Work on the UBQLN2 system has identified stickers that contribute to modulating the phase boundary, whereas spacers alter the material properties. These results build on the findings of Wang et al. The FET family proteins. They observed a clear correlation between joint valence of Arg and Tyr stickers and the percolation threshold, which also tracks with the saturation concentration (a measure of phase separation). However, changes to spacers largely left $c_{\rm sat}$ and the percolation thresholds unchanged. They did, however, have a direct impact on the material properties of condensates, including their aging dynamics. This work led to the development of a generalized theory to account for the presence of multiple sticker types within associative macromolecules. The strategy of the presence of multiple sticker types within associative macromolecules.

Direct experimental evidence for PSCP and the fact that PSCP leads to network structures within condensates comes from work of Bremer et al.⁶⁶ and Farag et al.³ A recent computational study leverages the findings of Bremer et al.⁶⁶ to show that the internal structures of macromolecules within condensates follow graph theoretical expectations of small-

world percolated networks.³ These features result directly from the hierarchy of interactions that are encoded by the stickers and the very different interactions, namely, solubility-determining ones, that are controlled by the spacers.³ The predictions of spatial inhomogeneities within condensates formed by PLCDs and other low complexity domains were borne out in recent single molecule imaging studies reported by Wu et al.¹⁹⁶

A common method by which spacer properties are leveraged to modulate PSCP in biology appears to be post-translational modifications. These modifications can change the driving forces for segregative transitions by enabling significant changes to ves, especially if the modifications add or delete charged residues that increase the overall net charge per residue. 47 Posttranslational modifications can also impact associative transitions and the overall coupling inherent to processes defined by COAST by modulating sticker valences or sticker diversity, and hence impacting the hierarchy of sticker-sticker interactions. For example, phosphorylation of spacer residues, namely, serine and threonine residues, has been observed to impact phase behavior, activity, and function for RNA Polymerase II (Pol II).²⁰⁰ These multisite phosphorylation reactions place negative charges on the corresponding spacer residues, thereby increasing their contributions to ves and adding de novo electrostatic interactions.

In the context of Pol II, Guo et al. 200 found that the conversion from hypo-phosphorylated Pol II to hyper-phosphorylated Pol II is associated with a shift from Pol II integrating into transcriptional condensates, which contain high concentrations of mediator complex proteins, to Pol II integrating into splicing condensates, which contain high concentrations of serinearginine dipeptide rich (SR-rich) proteins. 201 The implication is that hypo-phosphorylated Pol II interacts with mediator complex proteins, such as MED1, via specific IDR-IDR interactions, whereas hyper-phosphorylated Pol II interacts with SR-rich proteins, such as SRSF2, via electrostatic interactions. Importantly, hypo-phosphorylated Pol II is not recruited to splicing condensates and hyper-phosphorylated Pol II is not recruited to transcriptional condensates, suggesting that these changes to spacer residues, and hence the driving forces for segregative transitions, as well the coupling between associative and segregative transitions, change the interactions that dominate Pol II PSCP and the specificity of recruitment into condensates.

Other post-translational modifications that modulate the effects of spacer residues include acetylation, which, unlike phosphorylation, neutralizes charged residues. For example, Bock et al. discovered that N-terminal acetylation of the FUS protein had a negligible effect on monomeric conformations but they still promoted phase separation. ²⁰² These and other studies focus mainly on quantitative assessments of the order parameter for phase separation. The consequences of the coupling to associative transitions, namely, percolation, are seldom if ever investigated in vitro or in live cells. This requires an investigation of the spatial organization of molecules within condensates. 131,196 In this context, the findings of Qamar et al. 203 highlighted the polydispersity of FUS sequences that are generated by monomethylation, symmetric dimethylation, and asymmetric dimethylation of Arg residues in FUS. Even though these modifications do not alter the charge of Arg, they likely influence the hierarchy of sticker-sticker interactions involving Arg residues from disordered Arg-rich regions within FUS and other FET family proteins.

5.7. Complex Coacervation

Aqueous solutions of oppositely charged macromolecules can undergo spontaneous phase transitions that are known as *complex coacervation*. ^{76,204} Although the formation of a dense coacervate phase is usually associated with phase separation alone, a percolation transition will also occur, due to the macromolecules interacting via reversible physical cross-links. Here, the cross-links are primarily ionic interactions. We distinguish complex coacervation from PSCP that is based on short-range interactions, because the focus in the former is on long-range electrostatic interactions that drive the intermolecular associations among oppositely charged macromolecules and the contributions of counterion release to the driving forces for phase transitions.

Complex coacervation involves different types of linear, flexible oppositely charged polymers. ²⁰⁵ It can also be realized by interactions involving low-molecular weight surfactants and/or nanoparticles. Studies of synthetic polymeric complex coacervates have been useful for mapping out the phase behavior as a function of salt, pH, and temperature. ²⁰⁵, ²⁰⁶ For example, in recent work, Neitzel et al. ²⁰⁵ studied the coacervation of copolyelectrolytes with equivalent fractions of charged and neutral ethylene oxide monomers incorporated into the sequences of the polymers. This provides a titration of the charge content and its effect on the properties of coacervates and the salt dependence of complex coacervation.

We are starting to learn more about the complex interplay of complementary charge—charge interactions, the release of counterions (Figure 11A), the preferential accumulation or depletion of solution ions (Figure 11B), the impact of linear patterning of ionic groups (Figure 11C), and the effects of charge regulation whereby proton uptake and release can

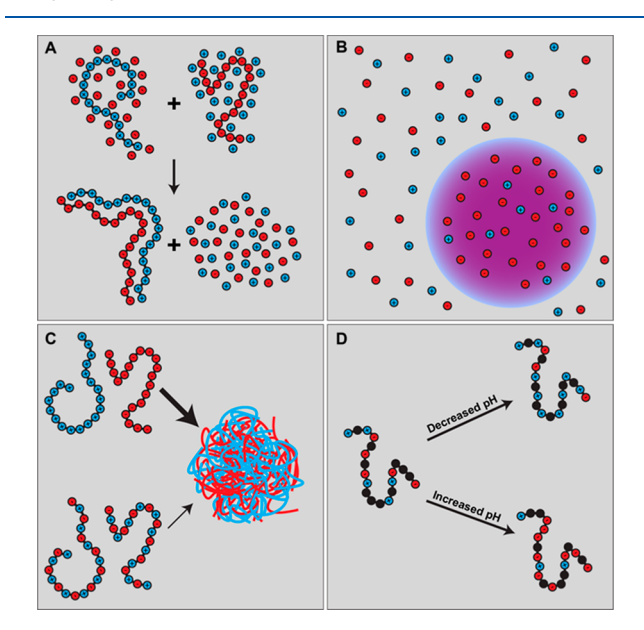


Figure 11. Schematics summarizing the physical principles of complex coacervation. (A) Two polyelectrolytes, a polycation (left) and polyanion (right) can form a complex driven by a combination of complementary electrostatic interactions and the release of counterions. (B and C) The formation of coexisting dilute and dense phase (coacervate) from the vantage point of the salt (B) and the polyelectrolytes (C). (D) The charge states of ionizable residues will be sensitive to pH and this can affect the complexation and coacervation of polyelectrolytes and polyampholytes (schematic shows the latter).

modulate the charge densities of associating macromolecules (Figure 11D). In their thermodynamic characterization of complex coacervation of poly(ethylene-imine) with either poly aspartic acid and/or poly glutamic acid, Priftis et al. 207 discovered that complex coacervation is driven by the release of counterions and enthalpically disfavored. Further, the water content of coacervates was found to be dependent on the salt concentration, highlighting the modulation of water activity as an important feature of coacervation.

Complex coacervation is a phenomenon wherein association via complexation drives segregative behavior. Simple theories such as the mean-field theory of Voorn and Overbeek have provided a useful starting point, even if the tenets of this theory have not held up to close scrutiny. The Voorn—Overbeek theory provides a prescription for the free-energy of mixing. It simply adds to the Flory—Huggins formalism by including a Debye—Hückel term for the electrostatic interactions. The overall expression for the free energy $\Delta F_{\rm VO}$ has the following form:

$$\frac{l^3 \Delta F_{\text{VO}}}{V k_{\text{B}} T} = \sum_{i} \frac{\phi_i}{N_i} \ln \phi_i + \frac{1}{2} \sum_{i,j} \chi_{ij} \phi_i \phi_j - \alpha \left(\sum_{i} \sigma_i \phi_i \right)^{3/2}$$
(16)

In a system of volume V, the first two terms on the right-hand side of the equation correspond to the entropy of mixing and the energy of mixing. The third term incorporates the contributions from electrostatic interactions for Kuhn monomers of length l. The summand in the third term involves σ_{ij} which is a ratio of the number density to the volume fraction of the charges for the i^{th} type of macromolecule. The proportionality constant α modulates the strength of the electrostatic interactions as a function of the thermal energy.

For a three-component system consisting of two oppositely charged polyelectrolytes and a complex solvent comprising water and solution ions, the theory predicts demixing, as given by the negative curvature of the free energy as a function of the volume fraction ϕ . Including the effects of salt requires a description of the phase behavior now in terms of three order parameters, namely, the volume fractions of the two polymers, ϕ_{P1} and ϕ_{P2} , and the volume fraction of the salt in question, ϕ_S . Assuming a 1:1 ratio of the complexing polyelectrolytes, it follows that $\phi_{P1} = \phi_{P2} = \phi_P$, and the phase diagram of interest becomes a projection onto the plane (ϕ_P, ϕ_S) .

Progress is being made to incorporate the effects of correlations, which are expected to be significant, given that ionic groups are tethered to make polymers. Perry and Sing adapted liquid-state integral equation theories, specifically the polymer reference interaction site model to account for excluded volume and chain connectivity in their descriptions of complex coacervation.²⁰⁹ The transfer matrix model of Sing and coworkers²¹⁰ incorporates the effects of proton binding and release²⁰⁶ as well as the release or preferential uptake for solution ions as drivers of coacervation. By enumerating all possible adjacent pairwise interactions, they calculate the grand canonical partition function for a polymer chain in an ionic solution, thereby accounting for pH effects. Their model can also be applied to study the effects of charge patterning on the phase behavior.²¹¹ Separate studies by de Pablo, Tirrell, and coworkers have analyzed the importance of charge blockiness for cooperativity in polyelectrolytic coacervates. 211 The more biologically relevant cases involving polyampholyte mixtures are not well understood, even though polyampholytes are useful models for many IDRs.²¹²

The importance of complex coacervation, especially for understanding the formation and regulated dissolution of various nuclear bodies, cannot be understated.²¹³ In fact, one can think of the nucleus as a set of coexisting phases, each forming under the regulation of a network of complex coacervation processes. Therefore, each nuclear body may be viewed as a distinct complex coacervatome, a term that emphasizes the fact that these bodies form via the collective phase behaviors of networks of polyelectrolytes and polyampholytes that are further regulated by solution ions (charge renormalization), proton uptake and release (charge regulation), 213 and active processes such as enzyme catalyzed posttranslational and post-transcriptional modifications. Never has it been more imperative that we go beyond simple synthetic systems, even though they are already quite challenging, 214 and study complex mixtures of multivalent associative macromolecules that undergo networked complex-coacervation-type phase transitions.

Pak et al. interrogated the complexities of complex coacervation in live cells. ²¹⁵ Their findings uncovered numerous surprises, including the discovery of stickers, which they referred to as *charge interacting elements*. The recent works of Greig et al. ²⁰¹ and King et al. ²¹⁶ point to some of the advances that are underway to interrogate complex coacervatomes in live cells and as reconstitutions.

5.8. The Sweatman Model of Short-Range Attractions and Long-Range Repulsions

Sweatman has proposed an alternative to macrophase separation that is based on a model that invokes the interplay of short-range attractions and long-range repulsions (SALR). This SALR model is intended to describe how *in vivo* facsimiles of condensates might come about. So Inspiration for the SALR model comes from the behaviors of charged colloidal particles in aqueous solutions. As noted by Sweatman, SALR allows for the formation of size-limited, liquid-like, or solid-like clusters within a gas or liquid.

For systems characterized by short-range attractions and longrange repulsions, the free energy of the system is minimized for finite cluster sizes.⁸⁵ The merits of this proposal were tested using Monte Carlo simulations based on local and cluster moves. The simulations were performed with single-component systems in an implicit solvent. The main tenets of SALR can be mapped onto models introduced to distinguish diffusionlimited colloidal aggregation²¹⁷ from reaction-limited colloidal aggregation. 218 In diffusion-limited colloidal aggregation, uniformly sticky particles form open, fractal-like structures because the rate of influx in the nonequilibrium system is considerably faster than the reconfiguration times of clusters and the particles therein. Conversely, in reaction-limited colloidal aggregation, the cluster growth and hence the resultant morphologies are tied to whether the colloidal particles are in the right orientation to associate or react.

Sweatman's model introduces the competing effect of longrange repulsions. The presence of the latter engenders an instability for clusters that go beyond a certain size. Accordingly, associative particles with a net charge can grow to a certain size via short-range attractions. Beyond a certain size threshold, which depends on the valence of patches that drive attractive interactions and the magnitude and range of the repulsions among collections of particles, an instability sets in, and this leads to clusters of fixed size. It appears that the recent

observations of Petry and co-workers²¹⁹ might well fit into the SALR framework.

Sweatman has argued that the SALR-like behavior of colloidal systems is likely to be a plausible explanation, as compared to macrophase separation, for the observation that condensates within cells do not grow beyond a certain size. The suppressor of coarsening behavior in cells that comes from SALR-like behavior is proposed to involve crowding-induced depletion-mediated attractions at short-range.²²⁰ However, the source of the emergence of long-range repulsions is unclear, although the assumption is that this comes from the buildup of clusters of molecules that have a net charge. Early work by Potemkin et al. 221 showed that in solutions of associating polyelectrolytes, an interplay between the energetics of sticker-sticker interactions and the translational entropy of counterions can create regimes in the space of temperature and salt concentration where macrophase separation is suppressed and clusters of optimum sizes are formed. Importantly, the Sweatman model and variations thereof imply that the balancing of forces is always a possibility in solutions of different types of associatve macromolecules without requiring invoking active processes to achieve clusters of optimal sizes.84

6.0. FULL PHASE DIAGRAMS FOR ASSOCIATIVE MACROMOLECULES

6.1. Single Type of Macromolecule in a Solvent

We now turn to the topic of constructing phase diagrams and interpreting relevant features. To start, we shall consider the example of an associative macromolecule in an aqueous solvent. Of course, the solvent is never just deionized water. Instead, it comprises a complex mixture of solutes, ions, and buffering agents, in addition to water. All components will have an influence on the overall phase behavior, especially the segregative transition, via the Flory χ parameter. For a fixed set of solution conditions, one can assess how the phase behavior changes with temperature. This is readily achieved in vitro, 66,118,136,222 and recently, Fritsch et al. measured a full phase boundary in the (ϕ, T) plane in live cells. To reach of the temperatures one can access, measurements have been reported that quantify c_{sat} and c_{dense} for a variety of systems. The locus of these points constitutes the coexistence curve. For a given temperature, a tie line connects the concentrations of the coexisting phases. Since the temperature is uniform across the system, the tie line is horizontal for a coexistence curve that is plotted on the (c, T) plane, where $c = c_{\text{bulk}}$ is the bulk macromolecular concentration. Note that c_{sat} and c_{dense} will vary with temperature. Measurements for various systems with UCST behavior show that c_{sat} increases by orders of magnitude as temperature increases. 66 In contrast, c_{dense} changes minimally with temperature.

Coexistence curves have been reconstructed from measurements in live cells. ^{10,73,223} Some of these measurements have been aided by the development and deployment of optogenetic methods. ^{47,159} In this case, the ordinate is no longer the temperature. Instead, it is either the strength of light activation or the effective valence enabled by a high local concentration through light activation. In a recent study, a *bona fide* phase boundary was generated for the P-granule protein PGL3 by manipulating the local temperature. This work demonstrated that P-granule assembly was tied to the generation of a temperature gradient, and that its formation and dissolution,

in a live cell, could be explained by thermoresponsive phase separation of PGL3.³³

One can also fix temperature and measure the local concentrations of coexisting phases at different salt concentrations, ²²² different pH values, or even different concentrations of other small molecule solutes. Across the phase boundary the concentrations of macromolecules and the concentrations of analytes (salt, protons, metabolite, or solute) will be determined by the equalization of macromolecular chemical potentials and osmotic pressure, as well as the equalization of chemical potentials of the analyte in question. In this case, coexistence curves are mapped on a (c_{am}, c_{an}) plane, where c_{am} and c_{an} refer, respectively, to the bulk concentration of the associative macromolecule and c_{an} is the bulk concentration of the analyte. Tie lines on the (c_{am}, c_{an}) plane are not constrained to be horizontal, although this is possible under special circumstances. Differences in solvent-mediated interactions across the phase boundary will lead to ties lines that have nonzero slopes (Figure 12). A positive slope would imply an increased concentration of the analyte in the dense phase, when compared to the dilute phase, whereas a negative slope implies the opposite.

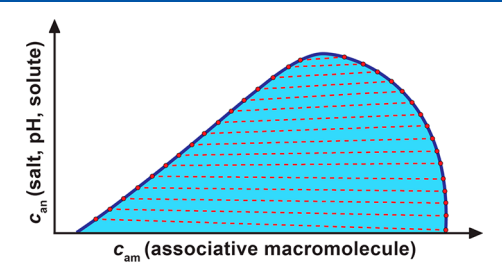


Figure 12. Coexistence curve or phase boundary in the (c_{am}, c_{an}) plane. The phase boundary is in blue, the two-phase region is in pale blue, and the coexisting phases are joined by dashed red lines, which are tie lines. Tie lines may have positive slopes, implying an accumulation of the analyte in the dense phase, negative slopes, implying a depletion of the analyte from the dense phase, or horizontal slopes, implying equal preference of the analyte for the dense and dilute phases. Note that the slopes of tie lines can change sign as the critical point is approached, which is what we depict in this schematic.

Recent advances have allowed for the direct and highthroughput measurements of the slopes of tie lines, ²²⁴ and this will open the door to measuring concentrations of analytes within dense and dilute phases of associative macromolecules. As noted above, solvents in vitro are complex mixtures of small molecules and ions. In cells, the complexity of the solvent increases due to the presence of other macromolecules that act as crowders that are preferentially excluded from condensates. Crowders could also be codrivers of condensates through preferential interactions with the associative macromolecule of interest.^{224,225} Being able to measure tie lines provides direct inferences regarding the preferential interactions or preferential exclusion of macromolecular components of complex mixtures. In vitro, such measurements of dilute and dense phase concentrations and of the slopes of tie lines are likely to be aided by recent advances in HPLC-based methods. 226

6.2. Annotating Measured Coexistence Curves with Percolation Lines

Measuring the percolation threshold invariably involves a combination of extrapolation and computations. As shown in Figure 13, one can map the coexistence curve and perform measurements outside the two-phase regime at macromolecular

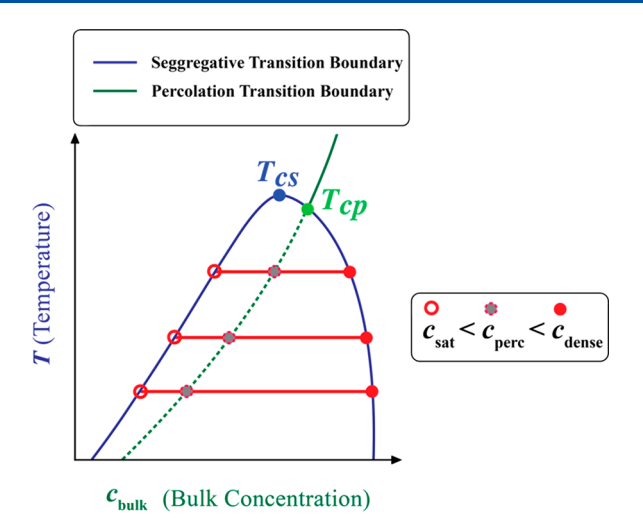


Figure 13. Coexistence curve (blue) and percolation line (dashed and solid green) for a solution of associative polymers undergoing UCST-style phase separation coupled to percolation. The red lines are tie lines (see section 6.1) that connect coexisting dilute and dense phases. There are two critical temperatures, $T_{\rm cs}$ for the segregative transition and $T_{\rm cp}$ for the percolation transition. For temperatures below $T_{\rm cs}$ and above $T_{\rm cp}$ there is the formal possibility of phase separation without percolation. Whether this regime is accessible or not will depend on the gap between the two critical temperatures $T_{\rm cs}$ and $T_{\rm cp}$.

concentrations above the overlap concentration. The results of these measurements, which query the onset of turbidity without the formation of coexisting phases, can be performed for a series of macromolecular concentrations above the overlap regime and extrapolated into the two-phase regime using a suitable theory. Bracha et al. have used the onset of hysteretic behavior as a proxy for mapping the percolation line in live cells. This arises from the realization that because $c_{\rm dense}$ is greater than $c_{\rm perc}$ percolation can dynamically arrest phase separation. Therefore, cycles of light activation and deactivation, performed in a pulsatile manner, afford a dynamic route to map the percolation line.

The generalized percolation model developed by Choi et al.²⁷ provides a joint theoretical and experimental route for quantifying percolation lines. If one measures the apparent dissociation constant of site- or sequence-specific binding for the macromolecules to themselves in a concentration regime that is outside the two-phase regime, then this information, combined with knowledge of the sticker valence can be used to compute the percolation line. Alternatively, one can map how phase boundaries shift with titrations of sticker valence or sticker strengths, while keeping the identities and positions of spacers fixed. This provides a handle on the effective strengths of sticker—sticker interactions. Zeng et al.²²⁷ used this information, combined with the theory of Choi et al.²⁷ to compute percolation lines for a series of variants of the prion-like low complexity domain of the hnRNP-A1 protein.

In computations that rely on coarse-grained and architectureor sequence-specific models of associative macromolecules, one can deploy two sets of order parameters that, when quantified independently, provide a direct readout of the coexistence curves and percolation lines. Choi et al. have introduced these order parameters as part of their LaSSI model, a lattice-based engine for computing architecture- and/or sequence-specific coexistence curves and percolation lines. The order parameter for computing coexistence curves is based on analyses that detect the onset of spatial inhomogeneities in pair distribution functions. The order parameter for computing the onset of percolation is based on quantification of the number of molecules that make up the single largest cluster in the system.

6.3. Spinodals and Critical Points

Below the coexistence curve, referred to as a *binodal* for a system of two coexisting phases, lies the *spinodal* or instability line. Between the binodal and spinodal, the one-phase system is metastable. In contrast, below the spinodal, the one-phase system is unstable. Accordingly, below the spinodal, the dynamics of phase separation and/or PSCP are governed purely by the dynamics of macromolecular transport and the dynamics of making and breaking physical cross-links. The spinodal line is typically well above the overlap regime. As a result, below the spinodal, the system makes bicontinuous structures, whereby spines of macromolecular regions are connected to one another, leaving small, solvent-rich regions embedded within them. Evidence for spinodal decomposition has been observed in live cells, both for artificial systems⁷³ and for a system that forms foci at membranes in response to hypertonic stress.⁸⁸

The binodal and spinodal coincide at the critical point. At this point, one expects so-called ultraviolet divergence, featuring large-scale fluctuations in the system. An intriguing suggestion is that some systems, in live cells, might be close to the critical point. In vitro, near-critical behavior has been observed for systems such as the Laf-1 protein in the presence of RNA molecules. The challenge at this juncture is measuring the onset of criticality both *in vitro* and in live cells. Most biophysical measurements are confounded by the large fluctuations encountered in the vicinity of critical points. However, the universality of critical exponents, and the applicability of theories of critical phenomena pave the way for joint experimental, computational, and theoretical studies that quantify the phase behaviors near critical points.

6.4. Phase Behavior near Critical Points

Prior to discussing phase behavior at the critical point, we clarify the distinctions between discontinuous and continuous transitions. This is relevant because the concept of a critical point is only applicable for a continuous transition. First, we shall consider a one-component system that can be in a liquid, solid, or vapor phase (Figure 14). As noted by Widom, ¹⁰⁴ there are two distinct equilibrium regimes to consider. At the triple point, which is defined by a specific temperature and pressure, the liquid coexists with the vapor and solid phases. The densities of the one-component system in the liquid, solid, and vapor phase are set by equalization of the chemical potentials, such that μ_{liquid} = μ_{solid} = μ_{vapor} . However, there is a second equilibrium regime of the liquid, defined by the existence of a critical point. This is the point where the vapor-liquid coexistence curve terminates. Past the critical point, the system forms a single fluid phase, and one cannot speak of coexisting liquid and vapor phases. Equilibrium states of the liquid in the vicinity of the triple point are very different from the equilibrium state of the liquid at the critical point. In the vicinity of the triple point, the liquid is "ordinary" in the parlance of Widom, 104 because the equilibrium state of the simplest liquids (see section 2.2) is defined mainly by shortrange repulsions. In contrast, at the critical point, long-range attractions make substantive contributions, and this engenders fluctuations whose wavelengths are considerably larger than the dimensions of the constituent molecules. The upshot is that at there are two distinct types of interactions that contribute to the liquid state at the triple point versus the critical point. Near the triple point, the equilibrium phase transitions, be they solid-to-

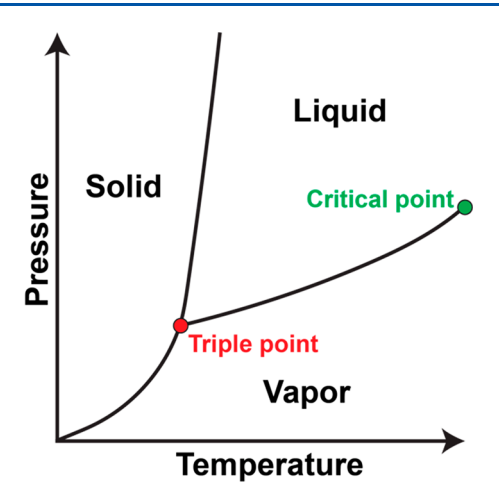


Figure 14. Pressure—temperature phase diagram of a substance that can be in a liquid, solid, or vapor phase. The red circle indicates the triple point where all three phases coexist. The green circle indicates the critical point where the vapor—liquid coexistence curve terminates. Beyond this critical point, the system forms a single fluid phase.

liquid (melting), vapor-to-liquid (condensation) or vapor-tosolid (sublimation), or their converse, are first-order transitions, accompanied by a latent heat and discontinuous changes in the specific heat capacity. However, at the critical point, the phase transition is continuous and does not involve a latent heat. Instead, it involves some sort of symmetry breaking operation with respect to the underlying physical laws.

If we extend the framework laid out above to the problem of phase separation in binary mixtures, it follows that away from the critical point, phase separation is a first-order, compositional and/or density transition. Therefore, whether condensation via processes that come under the rubric of COAST, specifically the segregative transition, is being measured in the vicinity of or

away from the critical point will dictate how the phase behavior must be analyzed. This brings us to analyses that have guided recent efforts on the computational^{229,230} and experimental side of the condensate literature.⁸⁷ These analyses gloss over the physical considerations outlined by Widom.¹⁰⁴

In the (ϕ, T) or (c, T) plane, the critical point is defined in terms of a critical volume fraction ϕ_c and critical temperature T_c . In a system that undergoes a UCST-type phase transition, the width of the two-phase regime for a given temperature T can be written as $(\phi_{\text{dense}} - \phi_{\text{sat}}) \propto (T_c - T)^{\beta}$. Here, β is the relevant critical exponent that describes how the order parameter vanishes as T_c is approached. For phase separation, the order parameter is the $(\phi_{\text{dense}} - \phi_{\text{sat}})$, which is the width of the two-phase regime. The critical exponent is thought to be universal in its applicability to any system undergoing phase separation.

The classical mean-field theory of Landau²³¹ predicts a value of $\beta = 0.5$. In accord with its mean-field nature, the Flory-Huggins theory also yields a value of $\beta = 0.5$. Simulations of the Ising model show that $\beta \approx 0.3264$ for $d = 3.^{74}$ Many computational studies have assumed, without proof, that phase separation belongs to the same universality class as an Ising model in d = 3.^{229,232} This leads to an imposition of a model that the order parameter will scale as $(T_c - T)^{0.33}$, which is then used to extract T_c through numerical fitting²³³ of the computed binodals. ^{229,230,232} In direct contrast, data for polystyrene in methylcyclohexane²³⁴ show the presence of two regimes, a mean-field regime below T_{cl} where the order parameter scales as $(T_c - T)^{0.5}$, and a critical regime, where the order parameter scales as $(T_c - T)^{0.33}$. These data also show a clear crossover between the two regimes. The implication is that there are two different regimes for the density fluctuations, one where short-range, Flory-style interactions dominate, and another regime near the critical point, where the density fluctuations are likely to be large enough to be divergent.

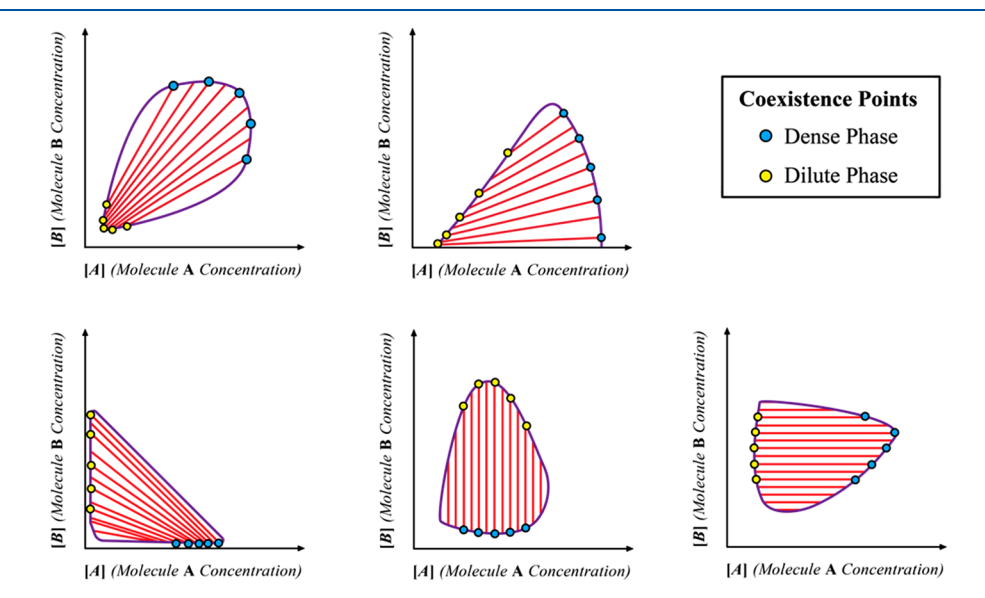


Figure 15. Shapes of phase boundaries for systems with A and B macromolecules. The solution conditions are fixed. The top left panel shows the case of a system where the phase behavior is driven purely by heterotypic interactions. The top middle panel shows the case where homotypic interactions among A molecules are equivalent to or outcompeting the heterotypic interactions. The bottom left panel shows the converse scenario. The bottom middle and bottom right panels show phase boundaries for the mixture where the drivers of phase transitions are purely A—A or B—B homotypic interactions. In all cases, the yellow circles designate coexisting dilute phases, and the blue circles are coexisting dense phases. Intercepts drawn from the yellow and blue circles to the abscissa and ordinate will quantify the concentrations of the coexisting dilute and dense phases, respectively. In each panel, the red lines are the tie lines, and the phase diagrams for precisely two coexisting phases.

Unlike the data for polystyrene in methylcyclohexane, ²³⁴ none of the measurements reported in the literature for finite-sized, multivalent associative biomacromolecules show a crossover behavior. Instead, the data appear to be well described by the mean-field exponent of 0.5.⁶⁴ Therefore, the data to date suggest that the width of the two-phase regime scales as $(T_c - T)^{0.5}$ and not with an Ising-like exponent of 0.33. Further, as shown in Figure 13, there will be two critical points in a PSCP-type process, namely, one corresponding to the terminus of the liquid—liquid phase transition and one corresponding to the terminus of the percolation line. What is currently missing is a rigorous description of how these critical temperatures are determined and how the gap between these values changes based on polymer architectures and interaction strengths.

6.5. Mixtures of Two Types of Macromolecules in Complex Solvents

The simplest extension that goes beyond an associative macromolecule in a complex solvent is that of two types of associative macromolecules in a complex solvent. Examples of such ternary systems are two different multivalent proteins in a solvent ^{126,187,235} or a protein and RNA molecule in a solvent. ²³⁶ We shall consider a mixture of associative macromolecules, labeled A and B, in a solvent. For fixed solution conditions, the ternary system can be treated as a pseudo binary system. The phase behavior, which refers to the coupling of phase separation and percolation, will be governed by the relative strengths of homotypic (A-A versus B-B) and heterotypic (A-B) interactions. As is always the case for associative macromolecules, the homotypic and heterotypic interactions will be influenced by solubility-determining contributions, i.e., χ_{AA} , χ_{BB} , and χ_{AB} , and the effects of site- or sequence-specific binding, which contribute to $\chi_{assoc.}$. Note that $\chi_{assoc.}$ will also be a matrix of coefficients, except the elements of the matrix will be dependent on concentration.

We shall consider the shapes of phase boundaries drawn in the (c_A, c_B) plane. Here, c_A and c_B are the concentrations of macromolecules A and B, respectively. The shapes of coexistence curves will depend on the blend of homotypic versus heterotypic interactions (Figure 15). Likewise, the slopes of tie lines will depend on the interplay between homotypic versus heterotypic interactions and the stoichiometric ratios of A to B. Perfectly horizontal or perfectly vertical tie lines imply the dominance of A-A or B-B homotypic interactions, respectively. If and only if the tie lines are horizontal or vertical can we expect there to be a single macromolecular c_{sat} that contributes to the segregative phase transition. For systems with sloped tie lines, both the slopes of the tie lines and the intercepts at the coexistence curve will determine the concentrations of the coexisting phases. 92,189,224 These concentrations will change as the stoichiometry of A and B change. Therefore, it is incorrect to expect fixed c_{sat} values for the A and B molecules. ^{109,237}

Can the concentrations of A and B molecules in dilute and dense coexisting phases be measured? The answer is yes, and doing so requires the quantification of concentrations of A and B molecules in the coexisting dilute and dense phases, or measurement of one of these concentrations, and the simultaneous measurement of the slopes of tie lines. Recent methods have shown precisely how these can be extracted. Importantly, these measurements must be performed for different ratios of A and B molecules. The simplest way to approach this would be to fix the concentration of one of the macromolecules and map the onset of phase separation as a

function of the concentration of the second macromolecule. The geometry of elliptical versus parabolic phase boundaries provides readymade constraints for the spectrum of measurements that are to be performed. These measurements are neither challenging nor impossible. ¹⁰⁹ They are, however, imperative. ⁷⁵

6.6. Extending to Complex Mixtures of Macromolecules

At first glance, the complexities of multidimensional phase diagrams, which are highly informative regarding the driving forces for the phase transitions of associative macromolecules, might seem too daunting to navigate, let alone measure. However, it is entirely tractable via advances in experiments, theory, and computations. The recent works of Yang et al., ¹² Sanders et al., ²³⁸ and Guillén-Boixet et al. ¹¹ directed at cytosolic stress granules provide a telling illustration of how one can proceed.

Using a combination of selective knockdown and knockout experiments, Yang et al. identified 34 essential proteins that constitute the core network of stress granules. 12 Of these, a pair of proteins, G3BP1/2, proved to be necessary and sufficient for assembling bona fide stress granules in live cells. Sanders et al. 238 were able to uncover the roles of other members of the G3BP1/2 network, showing that their stoichiometric ratios contribute directly to the modulation of G3BP1/2 phase behavior. Guillén-Boixet et al. 11 showed that stress granules form mainly through heterotypic interactions among G3BP1/2 and naked, unfolded RNA molecules that are released via stress-induced polysomal runoffs. The blend of heterotypic and homotypic interactions determines the overall shapes of phase boundaries and the responsiveness of stress granules to other macromolecular components. These components act as ligands that modulate phase boundaries, and as codrivers of phase behavior that impart spatial organization onto stress granules through their homotypic interactions.

Similar successes have been reported for *in vitro* reconstitutions of facsimiles of P-bodies comprising at least seven different macromolecular components.²³⁹ Recently, King et al. demonstrated the reconstitution of facsimiles of fibrillar centers and dense fibrillar components of nucleoli using a systematic approach that involves a collection of different macromolecular components.²¹⁶ Importantly, their work demonstrates that the blend of interactions and interactors, discerned using unbiased approaches, ensures that facsimiles of nucleolar layers can form at concentrations of associative macromolecules that are below the endogenous levels. This requires the reconstitution of synergistic networks of homotypic and heterotypic interactions.

There is no doubt that a lot needs to be done in terms of interrogating multicomponent condensates to uncover the drivers of these condensates. Recent studies show how the interplay of substrate-binding folded domains, the network of condensate-specific IDRs, and the distinctive features of constituent nucleic acids contribute thermodynamically to the formation of selective, coexisting phases within nuclei. 194,201,216 Therefore, the physical principles underlying the phase behaviors of networks of associative macromolecules are clearly operative in describing how different condensates form, coexist with one another, and mutually regulate one another. Naïve extrapolations of the physics of simple systems cannot explain the complexities of multicomponent mixtures. A few of the considerations that need attention are listed below.

The Gibbs phase rule sets the upper bound on the number of coexisting phases. We consider a system with $n_{\rm am}$ associative macromolecules. Let there be $n_{\rm con}$ constraints on the system.

The constraints refer to concentrations that cannot change due to the nature of the system. If there are $n_{\rm ph}$ possible coexisting phases, 240 then for fixed temperature and pressure, there are $n_{\rm df}$ thermodynamic degrees of freedom in the system. This is estimated as $n_{\rm df} = n_{\rm am} - n_{\rm con} - n_{\rm ph}$. The degrees of freedom refer to the number of macromolecular concentrations that we can choose freely or that cells can freely titrate. If we have two coexisting phases, $n_{\rm ph} = 2$, then the number of concentrations that can be titrated experimentally or within a cell will be $n_{\rm am} - n_{\rm con} - 2$. Considerations such as copy numbers and expression levels go into determining $n_{\rm con}$.

For a system with $n_{\rm am}$ associative macromolecules featuring three or more stickers that can engage in intermolecular interactions, the question is how many phases can coexist with one another for a given set of conditions. The upper limit on the number of coexisting phases will be $(n_{\rm am}-n_{\rm con})$. Nuclear speckles, nucleoli, stress granules, P-bodies, the mitochondrial nucleoid, and other multilayered structures can be described as structures defined by more than two coexisting phases. For $n_{\rm ph}$ coexisting phases, the tie object is an $(n_{\rm ph}$ -1)-simplex, where a simplex is the mathematical generalization of a tetrahedron to arbitrary dimension (Figure 16). If $n_{\rm ph}=2$, then the tie object is a

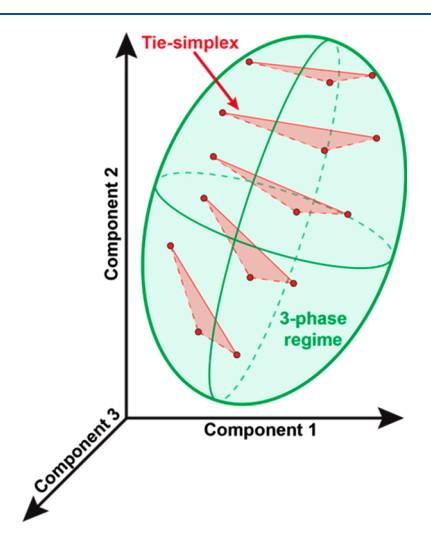


Figure 16. Ellipsoidal phase boundary for a system with three associative macromolecules in a solvent. If three phases can coexist, as would be the case for the nucleolus¹³² or nuclear speckle, ¹³¹ then the tie simplex is a 2-simplex, which is a triangle. The concentrations of the macromolecules in the three coexisting phases will be determined by the direction cosines that define each side of the triangle.

1-simplex or a tie line. However, if we have three coexisting phases, as with a spatially organized condensates that coexists with a dilute phase, then the tie object is a 2-simplex, which is a triangle. Based on the number of layers one observes in a cellular condensate, one can work out the number of coexisting phases. The concept of a tie simplex, combined with efforts such as those of Yang et al. 12 to identify the core scaffolds, and super resolution microscopy used to delineate athe apparent number of coexisting phases or territories, will allow one to map diagrams that combine coexistence curves and percolation lines, in the appropriate $n_{\rm ph}+1$ -dimensional space.

As for the slopes of tie simplexes, this too will depend on the number of coexisting phases. For two coexisting phases, we have a tie line with a certain slope. If there are more than two coexisting phases, the line is generalized to $n_{\rm ph}$ dimensions, i.e., a plane if $n_{\rm ph}$ is three, and instead of a slope we have direction

cosines describing a simplex gradient. The simplex gradient tells us about the relative interplay of homotypic versus heterotypic interactions. These considerations are coming into sharp focus in the condensate field.

7.0. DISTINGUISHING BINDING FROM PHASE TRANSITIONS

It has been argued that the phase behavior in multicomponent systems is highly complex and imparts fragility unto a system that organizes via phase transitions. 109 It has also been argued that in contrast to phase transitions, the collective properties of complex networks of macromolecules can be reduced to binding isotherms governed by networks of site-specific interactions defined by precise stoichiometries and structures. 109 As noted at the outset, measurements of stoichiometries directly contradict this line of thinking. 4,241 There are two additional challenges with the arguments being made in the literature. 109 First, sitespecific binding in complex systems cannot be described by simple binding constants. Instead, it requires the description of linkage effects, the construction, through measurement, of terms that make up all the coefficients of binding polynomials and uncovering nested hierarchies of interactions that contribute to allosteric regulation. ^{143,144,242} This is just as difficult, ²⁴³ if not more so, than studying phase behaviors in complex mixtures. Importantly, the presence of molecules exhibiting high degrees of conformational heterogeneity and measurements demonstrating the presence of distributions of stoichiometries in condensates combined with polydisperse distributions of prepercolation clusters, essentially rule out a simple, bindingisotherm-based description for condensate formation and dissolution. It is also worth noting that one seldom sees binding isotherms for complex mixtures and if they are presented, all sitespecific interactions are lumped into a single, apparent dissociation constant.

Are processes that come under the rubric of COAST even necessary, or can all the processes we have described to this point be lumped under the rubric of binding;¹⁰⁹ Binding defines the formation of assemblies of precise molecularities.¹⁴³ This would be true at all concentrations, with the populations of the specific species being modulated by the overall concentration.²⁴⁴ However, phase transitions are infinitely cooperative transitions²⁴⁵ that give rise to emergent properties whereby specific equilibria are only accessible beyond specific concentration thresholds.

7.1. Binding without Phase Transitions Gives Rise to Complexes of Fixed Stoichiometries

We reiterate the results of Harmon et al., who showed that the properties of spacers help delineate the distinctions among reversible binding reactions on the one hand versus coupled/decoupled associative and segregative transitions on the other. The properties of spacers that tether domains together determine whether phase separation and percolation are coupled, or if phase separation is suppressed and percolation is fundamentally altered by the effective solvation volumes of spacers.

For spacers of zero effective solvation volume, there is an optimal regime for spacer lengths where the coupling of phase separation and percolation is most pronounced. Above this window of optimal spacer lengths, percolation is realized without phase separation. What happens below this window? If the spacers are too stiff or too short, then percolation is suppressed, and phase separation will not be realized at most

physiologically relevant concentrations, no matter the value of the excluded volume. Instead, complexes of precise molecularities will form, and describing their formation will not require the consideration of either phase separation or percolation. Instead, the thermodynamic equilibria of the system can be described fully using binding isotherms, binding polynomials, and analysis of these to extract linkage effects, if any.

In addition to spacer effects, Wingreen and colleagues have generalized the observations of percolation-suppressing interactions by studying the assemblies formed by rigid multivalent particles featuring precise, site-specific interaction modes. 246 They arrived at a prediction they refer to as the *magic number effect*, highlighting how specific sticker valences can lead to a saturation of all binding sites. This suppresses the possibility of percolation. The requirements articulated are 2-fold: The intersticker interactions must be in the realm of 7–10 $k_{\rm B}T$ and the associating particles must be rigid. However, even for systems that satisfy these requirements, the deviations of valence from the so-called magic number will lead to percolation because the binding sites are not saturable through assemblies of precise molecularities despite the clear presence of site-specific interactions.

7.2. Rigidity Is Not Sufficient to Suppress Phase Separation

The fact that rigidity alone is insufficient for suppressing COAST-like processes is manifest in observations that glycolytic enzymes can form condensates in the synapse. 247 The enzymes in question are multivalent proteins that lack any IDRs. However, the binding sites cannot be saturated through the formation of complexes of precise molecularities. Instead, these systems, which fit the description of being patchy colloids, form from an assortment of complexes that drive PSCP transitions above threshold concentrations that can be influenced by solution conditions. This is an example of a seemingly rigid multivalent system that makes networks and condensates through processes based on COAST. Similar effects have been observed for the Speckle-type BTB/POZ protein, ²⁴⁸ and for the auxin responsive factors where polymerization of plant homeodomains⁴ drives multivalence of IDRs that in turn drives PSCP-like transitions. Examples of polymerization induced phase separation, which is a distinct exemplar of a COAST-like process," have been documented for condensate forming systems in plants.²⁴⁹

7.3. High Affinity Disordered Complexes Can Suppress Phase Separation

Counterexamples, where systems feature intrinsic disorder and high multivalence, and do not undergo PSCP transitions, include the high-affinity complex formed by prothymosin Alpha and the histone protein H1. 250 Both molecules are intrinsically disordered polyelectrolytes. 41,250,251 Despite being intrinsically disordered and ionomer-like in terms of their high multivalence of associative groups, prothymosin Alpha and H1 form highly stable 1:1 complexes via charge complexation. 250,251 The measured affinities of these complexes are in the picomolar range. However, the complexes that form are disordered, and this is manifest in the observation that no single binding mode is preferred. 250,251 Disordered complexes are sometimes referred to as being fuzzy complexes. Such complexes need not be weak, as is often asserted in the literature. 109 Instead, as shown by Schuler and co-workers, complementary electrostatic interactions between two oppositely charged polyelectrolytes, combined with the release of large numbers of counterions,

provide the driving forces for the formation of highly stable, albeit disordered, 1:1 complexes that fit the definition of being fuzzy. 250,251

It is now clear that the overall phase diagrams of the prothymosin Alpha and H1 system and related ones are highly sensitive to salt concentrations, salt types, and the strengths of the 1:1 interactions.²⁵³ They can even enable realization of the magic number effect. The latter has been shown to be true for the interactions of H1 with DNA.²⁵⁴ Depending on the valence, i.e., number of complementary nucleotides, H1 and cognate DNA molecules can either form complexes of precise molecularities or undergo phase separation via complex coacervation. So, the magic number effect can be operative even in semiflexible and disordered systems.²⁵⁴

Overall, sections 7.1–7.3 highlight how phase transitions can be suppressed in favor of binding that gives rise to complexes of precise stoichiometries. These sections also discuss how the rules of suppression of phase transitions can be overcome with subtle changes to enable phase transitions that give rise to diverse stoichiometries. The upshot is that the molecular architectures, the interplay of rigidity and flexibility, the overlap concentrations, the valence as well as chemistries of stickers, and the nature of spacers will determine whether a complex has defined stoichiometry that forms via reversible binding or features a multitude of stoichiometries that form via reversible phase transitions. This brings us to the topic of how site-specific binding of ligands can influence phase equilibria.

7.4. Impact of Site-Specific Ligand Binding on Phase Equilibria

Condensates typically contain hundreds of distinct types of macromolecules. However, the current working hypothesis is that only a small number of homotypic and heterotypic interactions, defined by macromolecules that contribute large negative values in the X-matrix will be the likely drivers of condensate formation. The nondriver or nonscaffold molecules can be ligands, solutes, or metabolites. Direct support for this hypothesis comes from the works of Yang et al., Sanders et al., and Xing et al.

Solutes and metabolites can be preferentially excluded from, or they can preferentially interact with, the scaffold macromolecules in either dilute or dense phases. These preferential exclusion or preferential interaction effects, which explain the effects of protective and destabilizing osmolytes on protein stability in dilute solutions, are likely to be important modulators of macromolecular solubility.

Additionally, there are molecules, referred to as ligands, that bind site-specifically and preferentially to scaffold molecules across the phase boundary. Preferential binding through site-specific interactions refers to the relative affinity of ligands to sticker versus spacer sites on scaffold molecules within the dense versus dilute phase. Specifically, phase separation is weakened if the ligand prefers to bind to sites on the scaffold in the dilute phase versus the dense phase. Conversely, phase separation is strengthened if the ligand preferentially binds to scaffold sites in the dense phase as compared to scaffold sites in the dilute phase. The extent to which phase separation is weakened or enhanced by specific types of ligands can be put on a quantitative footing using the framework of polyphasic linkage.

Recent work has uncovered a set of rules for ligands as drivers or enhancers of PSCP of associative macromolecules that drive phase transitions via homotypic interactions. These rules are valid if we assume an absence of ligand-induced conforma-

tional changes or changes to assembly states that alter the intrinsic valence of stickers. The rules that have emerged are as follows: Monovalent ligands weaken the PSCP of scaffolds. This is true regardless of whether the ligands bind site-specifically to scaffold stickers or spacers. If the monovalent ligands bind to scaffold stickers, then suppression of phase separation occurs through direct binding and thus competition with scaffold—scaffold interactions. Conversely, for monovalent ligands that bind to scaffold spacers, the weakening of phase separation is realized by enhancing the excluded volumes of spacers.

A ligand, by definition, has a lower valence of stickers when compared to scaffolds. However, ligands can be multivalent. The site-specific binding of multivalent ligands to scaffold stickers generally weakens scaffold phase separation by replacing some of the interscaffold cross-links with ligand-scaffold cross-links. The effects of multivalent ligands are also determined by the relative strengths of the scaffold-ligand and scaffold-scaffold intersticker interactions. If the scaffold-ligand interaction affinity is greater than that of the scaffold-scaffold interaction, the PSCP-weakening effect of multivalent ligands that bind stickers is lowered, and these ligands can promote scaffold phase separation. Multivalent ligands that bind site-specifically to scaffold spacers will promote scaffold phase separation by contributing additional cross-links among scaffold molecules. However, the magnitude of these effects will depend on ligand concentrations, and whether ligands bind to single or multiple sites on scaffolds. It is also worth noting that the number of binding sites need not be the same across the phase boundary.

The recent work of Dao et al.²⁶³ has demonstrated the veracity of the rules developed by Ruff et al.^{53,186} We propose that the regulatory effects of ligands will likely enable the tuning of driving forces for COAST-like processes in cells. The scenario we envisage is the expression of ligands of various types that contributes to the modulation of the driving forces for phase separation. The effects of networks of ligands, and the effects of ligands on the driving forces for phase transitions in multicomponent systems are areas of active interest.²⁶¹

8.0. INTERFACES AND MATERIAL PROPERTIES

8.1. Interfaces between Phases and Interfacial Free Energies

Coexisting phases are delineated by phase boundaries. For a one-component fluid, the densities of coexisting phases are governed by establishing chemical, mechanical, and thermal equilibrium across the phase boundary. Chemical equilibrium is achieved by equalizing chemical potentials across the phase boundary. Likewise, thermal, and mechanical equilibria are established by equalizing the temperature and pressure, respectively, across the phase boundary. An interface of finite thickness and interfacial free energy will delineate the boundary between coexisting phases. A finite, positive interfacial free energy arises from the drive to minimize the numbers of molecules that lie at the interface between the coexisting phases.

For spherical particles featuring isotropic interactions, a simple molecular model can be deployed to estimate the interfacial free energy density, defined as the free energy cost to increase the interfacial area by one square meter (using MKSA units). For water at 20 °C, the interfacial free energy density at the vapor—liquid interface is $7.28 \times 10^{-2} \, \mathrm{Nm}^{-1}$. This interfacial free energy density, denoted as μ_{int} , can be written as $\mu_{\mathrm{int}} = \frac{w}{2a}$. Here, w is proportional to the heat of vaporization, and a is the area per molecule. For a water molecule, the radius $r = 1.4 \times 10^{-2} \, \mathrm{M}$

 10^{-10} m, $a = 2.46 \times 10^{-19}$ m², and $w = 3.59 \times 10^{-20}$ J. If we assume spherical geometries for the molecules, it follows that μ_{int} decreases as r^{-2} as the radius r of the spherical molecule increases. Accordingly, for macromolecules, substitution of a with the surface areas of macromolecules suggests a substantial lowering of the interfacial free energy density. This simple calculation assumes of an interface with a featureless medium taken to be an ideal gas. Such a model is useful for setting up expectations regarding contributions of molecular length scales to interfacial free energy densities. For condensates, the relevant length scales are those of macromolecules versus those of components of the solvent, including water and solution ions. In this context, it is worth noting that interfacial tensions, a measure of interfacial free energy density that is associated with changes to the shape of the interface, have been measured to be ultralow for synthetic and naturally occurring coacervates as well as condensates. 132,264,265 A simple explanation for the low values of interfacial tensions, vis-à-vis the air-water interface, is the differences in sizes of macromolecules versus those of solvent components. However, there are numerous considerations that are glossed over in this simple, size-based rationalization, one of which we discuss below.

The interfacial free energy density is minimized by reducing the area of the interface. This can happen by shape changes, whereby the interface becomes more spherical. Contributions to changes in interfacial free energy densities that arise purely from changes in the shapes of interfaces are referred to as interfacial tension. 266 This, we denote as γ . For water at the vapor-liquid interface or for the interface between purely viscous liquids, μ_{int} is dominated by the interfacial tension. However, changes to the interfacial free energy density can also come about without a macroscopic change in shape, ^{79,268} as happens at the liquid—ice interface, when compared to the liquid-solid interface in argon. Here, minimization of the interfacial free energy density comes from a compression of the interface, 270 which involves rotational degrees of freedom in the case of water.²⁶⁹ Compression derives from an increase in pressure that is caused by stress in the interface of the coexisting dense phase. If the two coexisting phases are Newtonian liquids, or a liquid and a vapor, then the interfacial stress f will be the same as the interfacial tension γ . However, if the coexisting phases are complex fluids with an elastic component, or one of the phases is some form of solid, then the interfacial stress f will be smaller than the interfacial tension γ . In this scenario, the interfacial area can be minimized through compressive forces that minimize the anisotropic stresses, and the resultant interface need not be spherical. Aspherical interfaces have been reported in several contexts. 4,241 These can result from dynamical arrest, 62,72,133,271 especially when RNA is involved, 272 or equilibrium considerations that define the interfaces of complex materials. Comparative analyses of these interfaces on distinct length scales are imperative to understand the complexities that contribute to the characteristics of interfaces and reactions at interfaces.²⁷³

Recent work has highlighted a feature referred to as *interfacial resistance*.²⁷⁴ This has emerged from careful analysis of molecular flux across interfaces. Specifically, Taylor et al.²⁷⁴ leveraged Fluorescence Recovery After Photobleaching (FRAP) measurements by complete or partial bleaching of condensate regions. They noted that one often assumes that local equilibrium is established at the interface. This implies the absence of resistance across the interface. Taylor et al. estimated interfacial resistance using a series of systematic FRAP

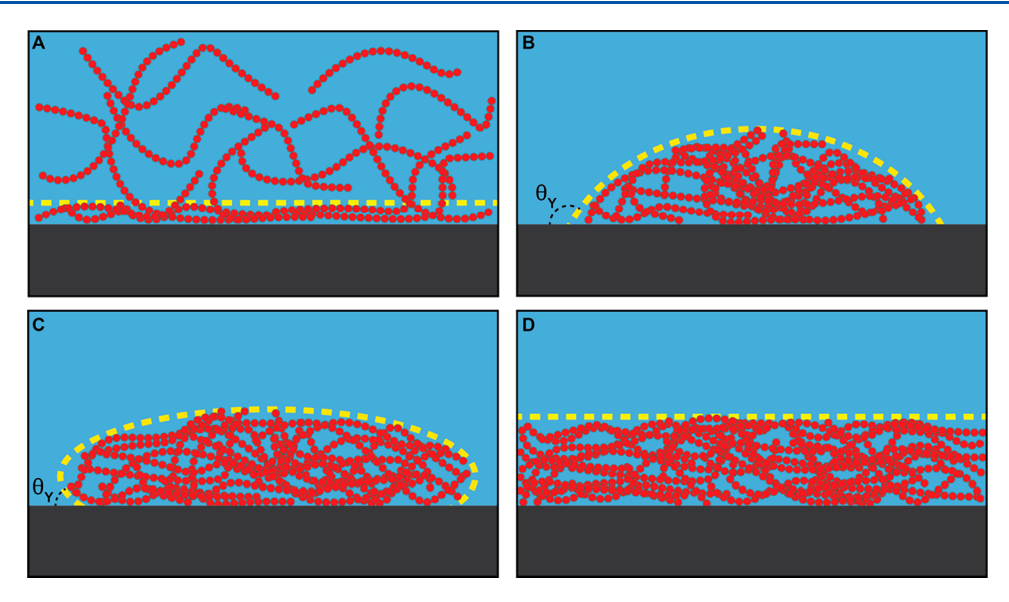


Figure 17. Adsorption and wetting of a polymer onto a solid surface. The solvent is shown in blue and the solid surface is shown in gray. The red chains indicate a polymeric species able to undergo phase separation at the proper conditions. The yellow dashed curves outline the adsorbing or wetting polymers. In (A), the polymer is in the one-phase regime and adsorbs onto the substrate. In (B) and (C), the polymer has undergone phase separation and the nascent dense phase partially wets the surface. The contact angle, θ_Y , may be above 90°, indicating poor wetting (B), or below 90°, indicating good wetting (C). In (D), the polymer-rich dense phase completely wets the surface.

measurements. They recast the equations for flux across interfaces to account for the presence of interfacial resistance. A key question pertains to the relative contributions of interfacial tension versus interfacial stress to the interfacial resistance. How changes in shape versus changes in size of the interface and the distinctive conformational characteristics of interfaces^{3,275} contribute to interfacial resistance remain unresolved.

Overall, the interfacial free energy density is governed by joint contributions from interfacial tension, which is the drive to minimize the interfacial free energy by changing the shape of the interface, and from interfacial stresses, which refer to the drive to minimize the interfacial free energy through compressive forces that do not involve changes in overall shape. Whether we should focus exclusively on interfacial tension or a combination that includes both stresses and interfacial tension will depend on whether the interface is uniform on all length scales beyond the molecular scale. This is also tied to whether the system is purely viscous or viscoelastic on the timescales of interest. In general, nonuniformities due to compressive forces will require that we account for both interfacial tension and interfacial stresses.

Recent investigations have started to probe the molecular aspects of condensate interfaces.²⁷⁷ A key finding is that the thickness of the interface is larger than the average size of a macromolecule within the condensate. Farag et al.³ have predicted, using a computational model of prion-like low complexity domains, that molecules at the interface are likely to be highly expanded and oriented perpendicular to the interface. Their definition of the interface was inspired by the work of Fisk and Widom. ²⁷⁸ The rationale for the observation of Farag et al. ³ is that the interfacial free energy is minimized by having small sections of many chains exposed at the interface, as opposed to large sections of a few chains. This finding also points to the presence of unsatisfied, non-cross-linked stickers being present at interfaces. Accordingly, it is plausible that expanded conformations with unsatisfied stickers are the prime sites for enhancing biochemical reaction efficiencies. Indeed, fibril

formation appears to be significantly enhanced by the presence of cohesive, fibril-forming stickers at interfaces of condensates formed by prion-like low complexity domains. ²⁷⁹

Drawing on observations from the microdroplet literature, Stroberg and Schnell have proposed that the interfaces of condensates might be where reaction efficiencies are enhanced by several orders of magnitude.²⁸⁰ This has to do with the unique properties of interfaces, including interfacial electrostatic potentials, reduced dimensionality, the creation of electric double layers, and the recently uncovered conformational features of interfaces mentioned above. Substrate channeling and product inhibition are likely to be made more efficient at interfaces than in bulk solutions or within condensates. Accordingly, an important area of investigation in condensate research is the nature of internal interfaces within condensates and the properties of interfaces between coexisting dense and dilute phases. Of particular interest is the nature of interfaces formed when the mechanism involves complex coacervation 264 because nuclear bodies, specifically those implicated in transcriptional and post-transcriptional regulation, are likely to be driven by some form of complex coacervation.

8.2. Adsorption to Solid Substrates and Wetting

An interface is a generic term used to describe a region that separates two distinguishable bulk phases. The interface is either a physical slab or a mathematical plane as defined by Gibbs. ²⁸¹ The key point is that properties that distinguish the bulk phases from one another, such as the density, composition, or conformation, are different in the interface from those of the two bulk phases. The term surface is only applicable if the interface involves a vapor on one side.

Wetting, or more precisely, the extent of wetting, is a measure of the interfacial free energy between coexisting bulk phases. It is quantified in terms of a contact angle. Importantly, wetting always involves interactions among *three* separated volumes that meet at a triple line. For example, in the work of Feric et al. ¹³² they measured contact angles by forming a droplet of the protein of interest, nucleophosmin 1 or fibrillarin, at the interface of air

and a solid surface that was coated with a hydrophobic or hydrophilic material. So, the contact angle in this case was the contact angle of Young, 282 denoted as $\theta_{\rm Y}$ and measured as $\cos(\theta_{\rm Y})=(\gamma_{\rm SV}-\gamma_{\rm SL})/\gamma_{\rm LV}.$ Here, the interfacial free energy densities $\gamma_{\rm SV},\gamma_{\rm SL}$, and $\gamma_{\rm LV}$ are the free energy penalties associated with increasing the interfacial areas at the solid–vapor (SV), solid–liquid (SL), and liquid–vapor (LV) interfaces. The droplet formed by the protein is the wetting phase, and the solid substrate with different coatings is the wetted phase. Young's equation applies if and only if the interfacial energy densities are isotropic. 282

Partial wetting is the term used to describe any contact angle between 0° and 180°. Complete wetting refers to the case of the contact angle being zero, whereas nonwetting refers to the case of the contact angle being 180°. Partial wetting interpolates between these limits. Wetting or partial wetting may be enabled by adsorption, which is defined as the adhesion of atoms, small molecules, polymers, colloids, or ions from a gas, liquid, or dissolved solid onto an interface (Figure 17). In the parlance of adsorption, the interface is the adsorbate and the entities that adsorb are the adsorbents. Here, the adsorbate is analogous to the wetted phase in our descriptions of wetting. Unlike wetting, adsorption may occur across only two separated volumes. Hence, if a phase-separable system is in contact with a distinct interface, wetting can only occur above the saturation concentration, in the two-phase regime, whereas adsorption may also occur below the saturation concentration, in the onephase regime. So, one can speak of adsorption in the one-phase system, which becomes relevant in the context of prewetting (see below). Adsorption is central to any analysis of wetting and wetting transitions. Importantly, adsorption at interfaces can modify the interfacial free energy density.

Adsorption and its impact on the interfacial free energy density γ is described by the Gibbs adsorption equation or adsorption isotherm. It relies on invoking a Gibbs dividing surface, which refers to the fact that the interface between coexisting phases has a finite thickness. There is a transition region that separates the two phases. In the transition region, the density is between that of the dense and dilute coexisting phases. The Gibbs dividing surface is a mathematical plane onto which all thermodynamic variables pertaining to the extensive quantities of the interface are projected. The value of the variable of interest is computed by subtracting out the value obtained from a reference that consists of the contributions from the two bulk phases. This becomes an interfacial excess quantity. We shall denote Γ_i as the specific interfacial excess number of moles of component i or more simply as the adsorption coefficient of component i.

The Gibbs adsorption equation, written as $d \gamma = s^{\rm I} dT - \sum \Gamma_i d$ μ_i quantifies the variation of the interfacial free energy density γ with changes in T and the chemical potentials of species i, denoted as μ_i . Here, $s^{\rm I}$ is the specific interfacial excess entropy. At constant temperature, this becomes the equation for the Gibbs adsorption isotherm, which for a system with two components A and B is $d \gamma = -\Gamma_A d \mu_A - \Gamma_B d \mu_B$. Here, the two components A and A could be the polymer and the solvent, respectively. Using the Gibbs—Duhem equation, we can eliminate one of the chemical potentials. If A is the solvent, and we eliminate the chemical potential of the solvent, the Gibbs adsorption isotherm is written in terms of the solute A. If the coexisting phases are denoted as A and A then from the vantage point of the A phase, the Gibbs adsorption isotherm is rewritten in terms of the numbers of moles of A and A molecules in the A phase as A and A phase as A phase and A phase as A phase and A phase another than a phase and A phase and A phase and A phase and

 $(n_{\rm B}'/n_{\rm A}') - \Gamma_{\rm B}$. The interfacial free energy density γ is not proportional to adsorption. Instead, it is the slope $d \gamma/d \mu_{\rm B}$, i.e., the change in the interfacial free energy density with the chemical potential of the solute, that is proportional to adsorption.

8.3. Wetting Transitions and Phase Separation

Adsorption can give rise to wetting transitions. If we consider two condensed phases α' and α'' in contact and in equilibrium with a solid substrate s, as would be the case for phase separation occurring on the surface of a coverslip of a microscope, then the equation of Young gives us the following: $\gamma_{\alpha'\alpha''}\cos\theta = \gamma_{s\alpha''} - \gamma_{s\alpha'}$. The α' and α'' phases are in equilibrium below their critical point T_c . Assuming this is a system with an upper critical solution temperature, then as T_c is approached from below, the interfacial free energy density $\gamma_{\alpha'\alpha''}$ will scale as $(T_c - T)^{\beta}$. Here, β is expected to be between 0.3 and 0.4. Further, as T approaches T_o the difference $(\gamma_{s\alpha''} - \gamma_{s\alpha'})$ will approach zero and will scale as (T_c) $(T)^{1.3}$. The implication is that θ will tend to zero as Tapproaches T_c . The value of T at which $\theta = 0$ is the wetting temperature $T_{\rm W}$. Wetting transitions can either be first-order or critical. While $\cos\theta$ approaches unity continuously in both cases, in a first-order wetting transition, the derivative of $\cos\theta$ with respect to T will be discontinuous at T_{W} . In a critical wetting transition, the derivative of $\cos \theta$ with respect to T will be continuous at $T_{\rm W}$. 282

8.4. Adsorption Transitions, Prewetting, and the Connection to Prepercolation Clusters

The linkage of adsorption coupled to phase equilibria has been used to describe the condensation of a pioneer transcription factor on the surface of DNA.²⁸³ Morin et al. also invoked what they referred to as prewetting transitions. The review of Kaplan et al. 282 is very useful for understanding the underlying concepts and terminology. Here, we consider a wetting transition from the perspective of a two-component system, such as a macromolecule in a solvent, in contact with a vapor phase. This is readily realized for a one- or two-phase system in a cuvette that has an interface with air. Using the terminology of Kaplan et al., the α -phase for this system is the one-phase regime. 282 Conversely, the α' and α'' phases represent the two coexisting phases in the two-phase regime. If the α -phase is a polymer-solvent binary mixture, then α' and α'' are the polymer-rich and solvent-rich phases, respectively. If the α phase is a mixture of two distinct liquids, then α' and α'' are each rich in one of the liquids. We now consider adsorption from the vapor of one of the components, say the polymer in a binary mixture of polymer plus solvent, onto the α -phase. Note that all it takes is for either the polymer or solvent to be the volatile component for there to be a finite concentration of species in the vapor. The concentrations will be infinitesimally small away from the boiling point. Increasing the chemical potential of the polymer in the vapor phase will result in increased adsorption of the polymer onto the α phase. This increase will terminate at a finite value, which coincides with the separation of the α phase into α' and α'' . If the system happens to be above T_W , the separation of the α -phase into two coexisting phases α' and α'' will result in α' completely wetting α'' . If the system is below T_W , the separation of the α -phase into two coexisting phases α' and α'' will result in α' partially wetting α'' .

Above a threshold chemical potential of a macromolecule, the slope of the interfacial free energy density due to adsorption may change. This refers to an *adsorption transition* or the *crossing of a prewetting line*. This can happen either continuously or

discontinuously. For the former, the adsorption transition is a first-order process, whereas for the latter it is a higher-order process. When the coexistence line is approached from the one-phase regime, divergence of adsorption indicates the onset of phase separation and complete wetting. In contrast to divergent adsorption, conventional adsorption can prevail in the absence of phase separation or complete wetting. ²⁸²

In the preceding two paragraphs, adsorption of polymers from a vapor onto the interface of the one-phase system—the α phase—leads to either a partial wetting transition below $T_{\rm W}$ or a complete wetting transition above $T_{\rm W}$. If the one-phase system is not in contact with a vapor, then, at first glance, there is no adsorption possible. However, given the concept of prewetting, we see a direct connection between monotonic adsorptive transitions and the formation of prepercolation clusters given that both occur in subsaturated solutions. 190 If we replace molecules adsorbing from a vapor onto the interface between the vapor and the one-phase regime with molecules sticking to one another to give rise to clusters of different size, then we are describing physisorption via cohesion rather than adhesion. Clusters enable a partitioning of molecules from the bulk, and instead of adsorption or the extent of adsorption, we speak of clustering or the mean cluster size. When the cluster size diverges, we have phase separation that gives rise to two coexisting phases. As a result, there is a formal connection between prewetting and the formation of prepercolation clusters since both are realized in subsaturated solutions.

Within cells, there can be well-defined interfaces or surfaces that mimic solids. Prewetting can lower the threshold concentration for phase separation. This is what Morin et al. observed for the pioneer transcription factor in the presence of a DNA surface, leading to their invocation of the physics of prewetting. However, since they did not measure the change in the interfacial free energy density as a function of the chemical potential of the pioneer transcription factor, we regard their work as being suggestive of prewetting without formal proof of prewetting. Overall, the effects of adsorption, site-specific binding via ligands, prepercolation clusters, and the interplay between homotypic and heterotypic interactions among scaffolds must be accounted for in their entirety to understand the full complexities of spontaneous COAST-like processes.

8.5. Summary of Key Concepts Pertaining to Interfaces

We conclude this section by summarizing the concepts from the physics of adsorption at interfaces. We consider a system comprising macromolecules A and B that associate with one another and separate from the solvent. This gives rise to a dense phase, which is the condensate, that is enriched in macromolecules A and B. The condensate coexists with a solvent-rich phase that is dilute in terms of the concentrations of macromolecules A and B. Next, we add a third macromolecule, designated as C, that can associate with macromolecule A, and will have interactions with the solvent that are akin to those of macromolecule B. At low concentrations of macromolecule C, associations between macromolecules A and C drive adsorption of macromolecule C onto the interface between the condensate and the solvent-rich phase. If the concentration is increased, this adsorption may enable the creation of a nascent dense-phase, rich in macromolecule C, that partially wets the interface. One can measure a contact angle of the adsorbent phase rich in macromolecule C at the triple line defined by the three-way interface of the original condensate, the dilute phase, and the nascent phase. A contact angle that is less than 90° characterizes

a nascent phase that is a good wetter of the condensate. As the concentration of macromolecule C increases further, the nascent phase can grow via adsorption to lower the contact angle. When the contact angle becomes zero, the system has undergone a complete wetting transition, and the system is now characterized by three coexisting phases, viz., the original condensate, a dilute phase that is deficient in macromolecules and rich in solvent, and a new dense phase rich in macromolecule C that completely wets the condensate. At the interface of the original condensate and the new dense phase enriched in macromolecule C, there can be further adsorption leading to an equilibrium 2dimensional skin referred to as a complexion or grain boundary. 282 The role of complexions, namely, bona fide equilibrium 2-dimensional regions that are not coexisting bulk phases, needs special attention and consideration in the context of multilayered condensates such as nucleoli²⁸⁴ and nuclear speckles.1

The expectations summarized here, which are based on the physics of adsorption, and the cascade of wetting transitions it induces, are directly relevant to the spontaneous driving forces that determine the organization of several nuclear bodies, including the nucleolus. ²⁸⁴ The rules that govern the intrinsic driving forces for generating complex architectures of condensates, driven in part by interface-mediated interactions, are starting to come into focus. ²⁷⁵

8.6. Condensates Are Viscoelastic Materials

Within a condensate, the concentration of associative macromolecules that are scaffolds will be well above the percolation threshold. As a result, condensates are percolated networks of associative macromolecules. The structures of condensates are best described as being gel-like with a network structure These can be weak or strong gels. Further, condensates are expected to feature significant spatial inhomogeneities due to physical crosslinking, as has been shown by Farag et al.³ and Wu et al.¹⁹⁶ This gives rise to a distribution of mesh sizes, inhomogeneous molecular transport,²⁸⁵ and dynamic moduli characteristic of viscoelastic materials, such as Maxwell fluids or generalized Maxwell fluids with multiple relaxation times.²⁶ It is worth emphasizing that probing mesh sizes by querying the uptake or mobility of spherical particles in a complex matrix is fraught with numerous assumptions, as articulated in cautionary notes by Rubinstein and co-workers. There will likely be a coupling of hopping and diffusion,²⁸⁶ and regimes where the motions of even nonsticky molecules will either be diffusive or be confined within tubes. 287 Overall, the framework of the sticky Rouse model²⁸⁸ seems relevant for describing dynamics of condensates and the motions of probes within condensates.

On the topic of viscoelasticity, it is worth noting that a recent study, aided by a combination of atomic force microscopy and interferometry, has shown that intrinsically foldable domains are viscoelastic materials with intrinsic stiffness constants and internal friction. This has direct implications for modeling viscoelastic materials, where a network of molecules is organized in topologically distinct ways around the connections of underlying Maxwell (or other) elements that are viscoelastic in nature.

The material properties of viscoelastic materials, their aging, the internal stresses versus dissipation, the interplay between shear thinning versus shear thickening, and the possibility of a transition from a viscoelastic material to a viscoplastic material is only now coming into focus in the condensate field. These studies will require a treatise unto their own, and the rheological

characterization of condensates will require measurements that go well beyond what is currently in vogue. This much is clear: measurements based exclusively on fluorescence recovery after photobleaching are uninformative regarding the complex material properties of condensates.²⁴¹ It is also increasingly clear that macromolecules are inhomogeneously organized within condensates. 3,285 A uniform blob, which is what diffraction-limited microscopy suggests, is almost certainly not true of the organization of macromolecules within condensates. The spatial inhomogeneities will be direct determinants of the interplay between viscous versus elastic moduli. Since inhomogeneities arise from the extent and nature of crosslinking, it follows that aging properties of condensates, including changes to their terminal behaviors, will be tied to timedependent evolutions of collective material properties.²⁹⁰ These emergent, dynamical properties of condensates are likely to be regulated by active processes.

In recent work, Zhou and colleagues have studied the fusion dynamics of different types of condensates and proposed an interesting distinction that arises from analysis of the data using a "viscocapillary model". 291 They proposed the existence of a single stress relaxation rate and suggest that condensates organized around folded domains, i.e., patchy colloid-like domains show shear-thickening behavior. In contrast, Zhou and colleagues propose that condensates organized around IDRs show shear thinning behavior. 291,292 Here, shear thinning, and shear thickening refer, respectively, to the decrease versus increase of viscosity with time. The shear thinning behavior is what one conventionally expects for Maxwell fluids and related viscoelastic materials that feature terminal viscous behaviors. Zhou and co-workers have proposed that shear thickening behavior can arise from the stronger, site-specific interactions involving folded domains, which are apparently weakened and more distributed for IDRs. This is an intriguing proposal that calls for closer scrutiny. The key is to measure three distinct quantities, viz., the time scales for making and breaking crosslinks, the individual and correlated motions of molecules within condensates, and the speeds of fusion, paying attention to the possibility of metastable states defined by a balancing of viscous and elastic forces. ²⁹³ Recent work from Banerjee and co-workers has demonstrated the types of measurements that will be needed for proper adjudication of material properties of condensates. 6,294 Being able to adapt these measurements to complex condensates in vitro and in vivo remains a key challenge for the condensate field. However, such measurements are essential if we are to understand whether material properties are germane to biochemical functions of condensates in cells and in vitro.

8.7. Internal Environments of Condensates

Finally, and importantly, the current working assumption is that the internal environments within condensates, specifically the properties of solvents, are the same as those of the coexisting dilute phases *in vitro* or the coexisting cellular milieus *in vivo*. This implies that the strengths of interactions, the conformations of macromolecules, the valence of stickers, and the excluded volumes of spacers are the same across phase boundaries. There are a few studies²⁹⁵ that challenge this simplifying view. What is needed are measurements of the internal solvent properties of condensates. This will require a combination of time-resolved spectroscopies and/or chemical-biology-based approaches that can probe the internal solution environment of condensates as well as condensate interfaces. Of course, none of this will be trivial, but it is clearly essential. This

provides an opportunity for innovation at the intersection of multiple disciplines, including soft matter physics and physical as well as analytical chemistry. A useful starting point is the copious literature on partitioning of solutes and the considerations of solvent nonidealities in aqueous two-phase systems. ²⁹⁶ The recent work of Wu et al. ¹⁹⁶ shows that the interiors of condensates formed by intrinsically disordered low complexity domains are more hydrophobic than the coexisting dilute phases. Further, there are hotspots within interiors that are more hydrophobic than the background of condensates, suggesting that one cannot assume that molecules partitioning into condensates are crossing a boundary into materials of uniform hydrophobicity. ¹⁹⁶ These considerations and others need scrutiny, higher resolution investigations, ¹⁹⁶ and models for partitioning that rely on the tenets of inhomogeneous fluid solvation. ²⁹⁷

9.0. OVERALL SUMMARY AND CONCLUSIONS

9.1. Addressing Critiques of Phase Transitions in Cell Biology

Advances in structural biology and the ongoing technological revolution of cryo-electron tomography are yielding important insights regarding the arrangements of molecules in large complexes, wherein the molecules are flash-frozen in specific snapshots.²⁹⁸ By averaging over information collected for many particles, one can obtain a detailed picture of site-specific contacts forming in large complexes. The fact that such contacts exist in all manner of complexes cannot be denied. However, does what we see in a specific structural instantiation tell us what we need to know about the driving forces for forming assemblies that are often rather dynamic with components exchanging on a range of time scales? If the condensates are precise organizations of essentially rigid macromolecules, each networked to generate a perfectly elastic material, then a model based purely on sitespecific interactions seems reasonable. Even in this scenario, the cooperativity that gives rise to emergent properties of the assembly cannot be described purely as a sum of all site-specific contacts. These problems have been addressed over decades of work on the many complexities of binding polynomials, linkage effects, and cooperativity of binding.²⁴⁴

Cooperativity of conformational transitions or reversible associations is a defining hallmark of biomolecular systems that feature robustness and the ability to adapt. This is true even if the energetics of interest can be described using purely site-specific interactions. Unlike conformational transitions such as a protein folding/unfolding or binding, where cooperativity is tuned by considerations of site size, phase transitions are defined by unlimited or infinite cooperativity. This comes from the spectrum of interactions that go well beyond just site-specific contributions. IDRs, especially those that belong to specific regions on so-called diagrams-of-states, are likely to afford access to multiple energy and length scales, both in terms of interactions as well as fluctuations.

It is worth noting, as detailed below, that site-specific interactions enabled by the surfaces of folded domains and IDR-mediated interactions are describable by the same physicochemical principles. Salt bridges, $\pi-\pi$ interactions, associations of hydrophobic groups, and weakly polar interactions (first described for folded proteins 301) are shared by folded domains and IDRs. It is not as though folded domains and their site-specific interactions engage in mysterious forces that do not have a basis in physical chemistry. What is worth

noting is that while the interactions among IDRs may not be site-specific in the spirit of certain definitions, 109 they are exemplars of specificity in terms of the chemistries of species that contribute to the interactions. Further, the binding sites are distributed across IDRs, and the fluctuations engendered by conformational heterogeneity leads to changes in binding specificity, which one would quantify in terms of binding capacity, 303 a direct analog of heat capacity that quantifies enthalpy fluctuations. Accordingly, one suggestion is to refer to interactions among IDRs as being manifestations of *chemical specificity*. This specificity will vary with context and can be modulated by post-translational modifications as well as charge regulation effects. Importantly, there appear to be condensate-specific molecular grammars, and these are being uncovered using novel methods to identify distinguishing sequence features of IDRs. 182,201,216,305,306

Most critiques of phase separation as a route for condensate formation and dissolution are centered on the premise that current descriptions for the driving forces for phase transitions apparently invoke weak, nonspecific, and highly dynamic interactions driven solely by IDRs. 109 As highlighted throughout this review, a comprehensive accounting of the driving forces for segregative and associative transitions, and the coupling of these transitions, does not make any assertions about purely IDRdriven processes. However, it is also important to be clear in defining IDRs. Too often one reads about IDRs being "unstructured regions" that engage in weak, transient, and nonspecific interactions.³⁰⁷ This is incorrect, because the specificity, although distributed across sites and sequence regions, is clearly present. 42,212,304,308 The interactions may be on the order of k_BT , but these are interactions described by physical chemistry principles, as are interactions that are apparently specific and stoichiometric. Therefore, it does not follow that interactions mediated by IDRs are weak and nonspecific, and hence promiscuous. In fact, the purported promiscuity has never been rigorously demonstrated, although this is often the claim. Studies that strive to make the point about IDR interactions being "non-specific" often miss the essential definition of specificity ^{309,310} or how it must be quantified. ^{310,311} A single assay intended to query interoperability of IDRs is inadequate because the information written into the IDR sequences often controls more than one phenotype, 312,313 thus requiring the interrogation of the totality of functions and phenotypes that are influenced by the IDR of interest.

In much the same way that the structures of folded domains are determined by the precise linear sequence of amino acids, it follows that the conformational ensembles of IDRs are highly sequence specific. This sequence or chemical specificity can be challenging to uncover and often requires a combination of analytical, spectroscopic, and computational methods. The combinations of these methods have yielded a series of rules and heuristics that organize the sequence space of IDRs into distinct categories, each defined by distinct sequence-ensemble relationships. ^{32,42,314} Indeed, differences in sequence-specific IDR ensembles can be traced down to the atomic resolution. ³¹⁵

The functions of IDRs are driven by specific patterns of sequence-encoded interactions that enable specificity of molecular recognition. ^{308,316} Even fluctuations are sequence-specific, ³¹⁷ and so is the recognition of fluctuations. ^{250,308,316,318,319} It used to be argued that complexes formed by IDRs are weak when compared to complexes formed by folded domains. However, the distribution of affinities, quantified by Shammas et al. ³²⁰ in terms of the distributions of

apparent dissociation constants, show that complexes formed by folded domains, and IDRs span similar ranges of values. There, however, are clear differences in terms of the dissociation and association rates, and unlike folded domains, it appears that specificity in recognition, at least in some cases, is exerted through kinetic rather than thermodynamic considerations. ^{321,322}

In biology and biochemistry, complexes characterized by apparent dissociation constants that are in the nanomolar range are thought of as being strong complexes. By this criterion, recent studies have shown that the formation of conformationally heterogeneous complexes involves sequence-specific interactions that can be regarded as ultrastrong, ³¹⁸ giving rise to complexes whose dissociation constants are in the picomolar range. ^{250,254,318,319} Likewise, the barriers to interconversions between distinct conformations can also be heterogeneous. This gives rise to broad distributions of time scales for conformational interconversions³²³ that are mediated by local conformational preferences, long-range correlations, ³²⁴ and solvation. ³²⁵

Taken together, what has emerged is a description of distinct sequence families of IDRs, each defined by distinct sequence-ensemble relationships. While conformational heterogeneity is a defining hallmark of IDRs both as autonomous units and in complexes, 326 the extent of heterogeneity and the type of heterogeneity is highly sequence- and context-specific. 327 Indeed, all aspects of the charge states and conformational ensembles are governed by the combination of amino acid composition and the patterns of specific chemistries along the linear sequence.

Studies have shown that small differences in amino acid chemistries are of immense significance. As a result, Ser and Thr are not always interoperable, for nor are Arg and Lys, Col., 302, 329 Glu and Asp, 302, 329, 330 Gln and Asn, or Phe and Tyr. 66 Any interoperability is highly sequence- or contextspecific.⁶³ This is relevant because alignments of sequences of intrinsically foldable domains often consider the substitutions listed above as exemplars of sequence similarity. Further, until recently, the hypervariability of IDRs within functional families was seen as a challenge for describing the evolution of specificity in IDRs. The thinking continues to be that because IDRs cannot be aligned without the introduction and extensions of gaps using traditional multiple sequence alignment approaches, it must follow that IDRs are interoperable with random regions derived from orthogonal systems. This has been contradicted through studies that have introduced the concept of conformational buffering.313 Further, new methods that are being brought to bear for alignments of IDRs have helped uncover functionally relevant sequence features within orthologs and paralogs. 305,306 New alignment-free methods have also been introduced to uncover nonrandom patterns in IDRs. 182,316 The totality of these efforts has demonstrated that while IDRs may be evolving under different rates when compared to intrinsically folded domains, 316 their sequence features are also under evolutionary selection.

Overall, what has emerged is that one can reliably define IDRs as belonging to specific sequence families. There is specificity of "IDR structure", ³²¹ and the "structure" we speak of lies within the entirety of how we describe sequence-specific ensembles of conformational states and charge states that can be highly responsive to solution conditions and complementary interactions with other macromolecules.

Systems exhibiting conformational heterogeneity are defined by distribution functions. This description allows one to

incorporate the full range of complex hierarchies of time, length-, and energy-scales. These realizations pave the way for describing the phase behaviors of IDRs as autonomous units and of IDRs tethered to folded domains, both of which involve a blend of specific and solubility-mediating interactions. The emergent consequences of such interactions are encapsulated in processes that come under the rubric of COAST.

9.2. Concluding Remarks

The features that drive PSCP and related processes that come under the rubric of COAST include: (i) a combination of multivalence of stickers; (ii) a diversity of sticker types and a hierarchy of sticker-sticker interactions; (iii) the effective solvation volumes of spacers, be they linear or surface spacers; (iv) any effective attractions among stickers and spacers; (v) the stabilities of domains that encompass stickers; (vi) the conformational properties of the disordered regions; and (vii) the likelihood of emergent changes to each of these properties either through post-translational modifications or through coupled homotypic and heterotypic associations. While it is tempting to fixate on the specificity of sticker-sticker interactions, it is worth appreciating that stickers constitute less than 20% of the linear sequence, at least in IDRs studied to date. The important effects of spacers as drivers of phase separation, and their coevolution with stickers is beginning to be appreciated.^{3,47,66,156,260,261,332}

There undoubtedly are scenarios where large assemblies of precise molecularities can form via cooperative binding transitions that operate via a collective network of site-specific interactions. The emerging rules summarized to this point suggest that competing factors contribute to network-terminating binding reactions versus network-generating processes based on COAST. It does appear that, while binding via site-specific interactions of rigid or semirigid multivalent entities can explain the formation of assemblies with precise molecularities, such observations are special cases of general processes that come under the rubric of COAST.

In essence, the phase behaviors of interest are of associative macromolecules in a solvent itself comprising an assortment of associative small molecules. In addition to water, a typical aqueous buffer comprises an assortment of solution ions, including monovalent and multivalent inorganic ions, osmolytes, cosolutes or cosolvents, buffering agents, and a finite concentration of differently solvated hydronium and hydroxide ions. All these components can be regarded as associative small molecules. Further, as emphasized throughout this review, cellular milieus comprise finite concentrations of macromolecules beyond the ones of direct interest to this investigation. Therefore, if we disregard the possibility of associative transitions and focus purely on phase separation, then we neglect to capture much of the physics. The converse is also true because purely associative transitions will turn the entire system of interest into a single, system-spanning network. Such a scenario affords zero advantages from a functional or compartmentalization perspective. Associative and segregative phase transitions are of equal importance, and ignoring either will provide only a limited understanding of how evolution has enabled the practical realization of the full spectrum of COASTlike processes.

The current review has strived to put considerations of associative and segregative transitions on an equal footing. There is a lot of turf that we have not covered. Among the glaring omissions are discussions of complexities and advances in

complex coacervation, the impressive body of work that accounts for the role of active processes, the numerous complexities that contribute to the material properties or internal environments of condensates, and the crucial roles of RNA molecules.³³³ There clearly is a lot more to come. The hope is that the current review provides a useful starting point for understanding and appreciating the numerous complexities of associative macromolecules and their spontaneous phase transitions.

AUTHOR INFORMATION

Corresponding Author

Rohit V. Pappu — Department of Biomedical Engineering, Center for Biomolecular Condensates (CBC), Washington University in St. Louis, St. Louis, Missouri 63130, United States; orcid.org/0000-0003-2568-1378; Email: pappu@ wustl.edu

Authors

Samuel R. Cohen — Department of Biomedical Engineering, Center for Biomolecular Condensates (CBC), Washington University in St. Louis, St. Louis, Missouri 63130, United States; Center of Regenerative Medicine, Washington University in St. Louis, St. Louis, Missouri 63130, United States

Furqan Dar — Department of Biomedical Engineering, Center for Biomolecular Condensates (CBC), Washington University in St. Louis, St. Louis, Missouri 63130, United States

Mina Farag — Department of Biomedical Engineering, Center for Biomolecular Condensates (CBC), Washington University in St. Louis, St. Louis, Missouri 63130, United States;
ocid.org/0000-0002-6457-6848

Mrityunjoy Kar – Max Planck Institute of Cell Biology and Genetics, 01307 Dresden, Germany

Complete contact information is available at: https://pubs.acs.org/10.1021/acs.chemrev.2c00814

Author Contributions

CRediT: Rohit V Pappu conceptualization, formal analysis, supervision, writing-original draft, writing-review & editing; Samuel R Cohen conceptualization, formal analysis, visualization, writing-review & editing; Furqan Dar methodology, visualization, writing-review & editing; Mina Farag conceptualization, investigation, methodology, visualization, writing-original draft, writing-review & editing; Mrityunjoy Kar conceptualization, investigation, writing-review & editing.

Notes

The authors declare no competing financial interest.

Biographies

Rohit Pappu received his BSc. in Physics, Mathematics, and Electronics from St. Joseph's College, Bangalore University, India. In 1996, Pappu received his Ph.D. in Biological Physics from Tufts University. His thesis work with the late David L. Weaver focused on novel algorithms for Brownian dynamics simulations of polypeptides based on systematically coarse-grained and reversible coarse-graining models based on the use of electrostatic multipoles, and chemical kinetics approximations of the diffusion-collision model for protein folding. Pappu completed two postdoctoral stints, one in the lab of Jay W. Ponder at Washington University School of Medicine, working on potential smoothing algorithms for enhanced conformational sampling, and the second with George D. Rose at Johns Hopkins University

working on polymer physics descriptions of unfolded states of proteins. In 2001, Pappu joined the faculty of the Biomedical Engineering department at Washington University in St. Louis, where he continues as a faculty member. He is currently the Gene K. Beare Distinguished Professor of Engineering and Director of the Center for Biomolecular Condensates. Pappu's research program focuses on the biophysical principles underlying the form, function, and evolution of intrinsically disordered proteins. Pappu is also deeply interested in the physics of phase transitions of biopolymers and in the physio-chemical principles underlying the assembly and functions of biomolecular condensates.

Samuel Cohen is a postdoc in the lab of Rohit Pappu at Washington University in St. Louis. Cohen is working to understand the physical determinants of rheological properties of biomolecular condensates using theories of polymer dynamics and computational rheometry. He is also interested in the theory of liquids, the physics of phase transitions specifically complex coacervation, and biologically relevant spectroscopic and imaging techniques. Cohen did his Ph.D. work at the University of Maryland, training with John Fourkas and John Weeks. During his Ph.D., Cohen focused on the role of electrostatic forces in liquid structure and on modeling transport and spectroscopic phenomena in liquids at interfaces. He did some of his Ph.D. work as a Chateaubriand Fellow at the Laboratoire Interdisciplinaire de Physique in Grenoble, France.

Furqan Dar received his B.A. in Physics from Kenyon College in 2016. He then went on to receive his Ph.D. in Physics from Washington University in St. Louis in 2022 under the supervision of Rohit Pappu. Dar is currently a postdoctoral scientist in the Pappu Lab where his research focuses on understanding the multifaceted mechanisms driving the formation and modulation of biomolecular condensates. His specific focus is on the phase behaviors of multicomponent systems and the formation of heterogeneous distributions of clusters in subsaturated solutions. Dar is the lead developer of LaSSI, which is a lattice-based engine for simulations of architecture- and sequence-specific phase behaviors of associative biomacromolecules.

Mina Farag graduated from Johns Hopkins University with a B.A. in Biophysics and Mathematics. He is currently pursuing an M.D./Ph.D. dual degree from Washington University in St. Louis. His Ph.D. work is being performed under the supervision of Rohit Pappu with an expected graduation in 2023 and final graduation date with the M.D. and Ph.D. slated for May 2025. Farag's research focuses on the sequence-specific driving forces for, and the organizations of, biomolecular condensates that form via interactions involving intrinsically disordered proteins. Farag recently discovered that interfaces of condensates are defined by unique conformational properties when compared to the coexisting dilute and dense phases.

Mrityunjoy Kar received his BSc. Honors and MSc. degrees in Chemistry at Vidyasagar University, Midnapore, India. As a Ph.D. student, Kar studied Polymer Chemistry and Nanomaterial Science under the supervision of Sayam Sengupta at the CSIR-National Chemical Laboratory, Pune, India. He did postdoctoral research at the University of California San Diego, USA, for two years in the group of Shyni Varghese. Kar then moved to the Max Planck Institute of Molecular Cell Biology (MPI-CBG) in Dresden, Germany where is currently a postdoc in the lab of Anthony A. Hyman. Kar also works in close collaboration with Rohit Pappu. Kar has focused on the physicochemical mechanisms underlying the driving forces for phase transitions of RNA-binding proteins. He made the key discovery of heterogeneous distributions of clusters forming in subsaturated solutions of these proteins.

ACKNOWLEDGMENTS

Mrityunjoy Kar is a postdoctoral scientist in the lab of Anthony Hyman at the Max Planck Institute for Cell Biology and Genetics in Dresden, Germany. Work in the Pappu lab is currently supported by grants from the US National Institutes of Health, the Air Force Office of Scientific Research, the US National Science Foundation, and the St. Jude Children's Research Hospital. S. R. Cohen acknowledges support via T32 EB028092 from the US National Institutes of Health. We are grateful to alumni and current colleagues in the Pappu lab, specifically Jeong-Mo Choi, Nadia Erkamp, Martin Fossat, Alex Holehouse, Matthew King, Ammon Posey, Kiersten Ruff, and Xiangze Zeng for stimulating discussions. Our thinking regarding condensates and the physics of associative macromolecules has benefited immensely from discussions with colleagues and collaborators including Priya Banerjee, Clifford Brangwynne, Anthony Hyman, Amy Gladfelter, Tuomas Knowles, Tanja Mittag, Michael Rosen, and Geraldine Seydoux.

REFERENCES

- (1) Banani, S. F.; Lee, H. O.; Hyman, A. A.; Rosen, M. K. Biomolecular Condensates: Organizers of Cellular Biochemistry. *Nature Rev. Cell Mol. Biol.* **2017**, *18*, 285–298.
- (2) Shin, Y.; Brangwynne, C. P. Liquid Phase Condensation in Cell Physiology and Disease. *Science* **2017**, *357*, No. eaaf4382.
- (3) Farag, M.; Cohen, S. R.; Borcherds, W. M.; Bremer, A.; Mittag, T.; Pappu, R. V. Condensates of Disordered Proteins Have Small-World Network Structures and Interfaces Defined by Expanded Conformations. *Nature Commun.* **2022**, *13*, 7722.
- (4) Powers, S. K.; Holehouse, A. S.; Korasick, D. A.; Schreiber, K. H.; Clark, N. M.; Jing, H.; Emenecker, R.; Han, S.; Tycksen, E.; Hwang, I.; et al. Nucleo-Cytoplasmic Partitioning of Arf Proteins Controls Auxin Responses in Arabidopsis Thaliana. *Mol. Cell* **2019**, *76*, 177–190.
- (5) Keizer, V. I. P.; Grosse-Holz, S.; Woringer, M.; Zambon, L.; Aizel, K.; Bongaerts, M.; Delille, F.; Kolar-Znika, L.; Scolari, V. F.; Hoffmann, S.; et al. Live-Cell Micromanipulation of a Genomic Locus Reveals Interphase Chromatin Mechanics. *Science* **2022**, *377*, 489–495.
- (6) Alshareedah, I.; Kaur, T.; Banerjee, P. R. Methods for Characterizing the Material Properties of Biomolecular Condensates. *Meth. Enzymol.* **2021**, *646*, 143–183.
- (7) Berry, J.; Brangwynne, C. P.; Haataja, M. Physical Principles of Intracellular Organization Via Active and Passive Phase Transitions. *Rep. Prog. Phys.* **2018**, *81*, 046601.
- (8) Walter, H.; Brooks, D. E. Phase Separation in Cytoplasm, Due to Macromolecular Crowding, Is the Basis for Microcompartmentation. *FEBS Lett.* **1995**, *361*, 135–139.
- (9) Choi, J.-M.; Holehouse, A. S.; Pappu, R. V. Physical Principles Underlying the Complex Biology of Intracellular Phase Transitions. *Annu. Rev. Biophys.* **2020**, *49*, 107–133.
- (10) Fritsch, A. W.; Diaz-Delgadillo, A. F.; Adame-Arana, O.; Hoege, C.; Mittasch, M.; Kreysing, M.; Leaver, M.; Hyman, A. A.; Jülicher, F.; Weber, C. A. Local Thermodynamics Govern Formation and Dissolution of Caenorhabditis Elegans P Granule Condensates. *Proc. Natl. Acad. Sci. U. S. A.* **2021**, *118*, No. e2102772118.
- (11) Guillen-Boixet, J.; Kopach, A.; Holehouse, A. S.; Wittmann, S.; Jahnel, M.; Schlussler, R.; Kim, K.; Trussina, I.; Wang, J.; Mateju, D.; et al. Rna-Induced Conformational Switching and Clustering of G3bp Drive Stress Granule Assembly by Condensation. *Cell* **2020**, *181*, 346–361
- (12) Yang, P.; Mathieu, C.; Kolaitis, R. M.; Zhang, P.; Messing, J.; Yurtsever, U.; Yang, Z.; Wu, J.; Li, Y.; Pan, Q.; et al. G3bp1 Is a Tunable Switch That Triggers Phase Separation to Assemble Stress Granules. *Cell* **2020**, *181*, 325–345.
- (13) Flory, P. J. Molecular Size Distribution in Three Dimensional Polymers. I. Gelation 1. *J. Am. Chem. Soc.* **1941**, *63*, 3083–3090.
- (14) Broadbent, S. R.; Hammersley, J. M. Percolation Processes: I. Crystals and Mazes. *Math. Proc. Cambridge Philos. Soc.*; Cambridge

University Press Cambridge Core, 1957, 53, 629–641, DOI: 10.1017/S0305004100032680.

- (15) Frey, S.; Richter, R. P.; Görlich, D. Fg-Rich Repeats of Nuclear Pore Proteins Form a Three-Dimensional Meshwork with Hydrogel-Like Properties. *Science* **2006**, *314*, 815–817.
- (16) Rubinstein, M.; Colby, R. H. *Polymer Physics*; Oxford University Press, 2003.
- (17) Tanaka, F. Theory of Thermoreversible Gelation. *Macromolecules* **1989**, 22, 1988–1994.
- (18) Ribbeck, K.; Görlich, D. The Permeability Barrier of Nuclear Pore Complexes Appears to Operate Via Hydrophobic Exclusion. *EMBO J.* **2002**, *21*, 2664–2671.
- (19) Schmidt, H. B.; Görlich, D. Nup98 Fg Domains from Diverse Species Spontaneously Phase-Separate into Particles with Nuclear Pore-Like Permselectivity. *eLife* **2015**, *4*, No. e04251.
- (20) Ng, S. C.; Görlich, D. A Simple Thermodynamic Description of Phase Separation of Nup98 Fg Domains. *Nature Commun.* **2022**, *13*, 6172.
- (21) Schneider, J. P.; Pochan, D. J.; Ozbas, B.; Rajagopal, K.; Pakstis, L.; Kretsinger, J. Responsive Hydrogels from the Intramolecular Folding and Self-Assembly of a Designed Peptide. *J. Am. Chem. Soc.* **2002**, *124*, 15030–15037.
- (22) Grove, T. Z.; Osuji, C. O.; Forster, J. D.; Dufresne, E. R.; Regan, L. Stimuli-Responsive Smart Gels Realized Via Modular Protein Design. *J. Am. Chem. Soc.* **2010**, *132*, 14024–14026.
- (23) Aggeli, A.; Boden, N.; Carrick, L. M.; Mcleish, T. C. B.; Nyrkova, I. A.; Semenov, A. N. Self-Assembling Peptide Gels. In *Molecular Gels: Materials with Self-Assembled Fibrillar Networks*; Weiss, R. G., Terech, P., Eds.; Springer Netherlands, 2006; pp 99–130.
- (24) Kato, M.; Han, T. W.; Xie, S.; Shi, K.; Du, X.; Wu, L. C.; Mirzaei, H.; Goldsmith, E. J.; Longgood, J.; Pei, J.; et al. Cell-Free Formation of Rna Granules: Low Complexity Sequence Domains Form Dynamic Fibers within Hydrogels. *Cell* **2012**, *149*, 753–767.
- (25) Boeynaems, S.; Alberti, S.; Fawzi, N. L.; Mittag, T.; Polymenidou, M.; Rousseau, F.; Schymkowitz, J.; Shorter, J.; Wolozin, B.; Van Den Bosch, L.; et al. Protein Phase Separation: A New Phase in Cell Biology. *Trend. Cell Biol.* **2018**, 28, 420–435.
- (26) Jawerth, L.; Fischer-Friedrich, E.; Saha, S.; Wang, J.; Franzmann, T.; Zhang, X.; Sachweh, J.; Ruer, M.; Ijavi, M.; Saha, S.; et al. Protein Condensates as Aging Maxwell Fluids. *Science* **2020**, *370*, 1317–1323.
- (27) Choi, J. M.; Hyman, A. A.; Pappu, R. V. Generalized Models for Bond Percolation Transitions of Associative Polymers. *Phys. Rev. E* **2020**, *102*, 042403.
- (28) Kumar, S. K.; Douglas, J. F. Gelation in Physically Associating Polymer Solutions. *Phys. Rev. Lett.* **2001**, 87, 188301.
- (29) Singh, K.; Rabin, Y. Aging of Thermoreversible Gel of Associating Polymers. *Macromolecules* **2020**, *53*, 3883–3890.
- (30) Franks, F. Water: A Matrix of Life; Royal Society of Chemistry, 2000.
- (31) Kriwacki, R. W.; Hengst, L.; Tennant, L.; Reed, S. I.; Wright, P. E. Structural Studies of P21waf1/Cip1/Sdi1 in the Free and Cdk2-Bound State: Conformational Disorder Mediates Binding Diversity. *Proc. Natl. Acad. Sci. U. S. A.* **1996**, *93*, 11504–11509.
- (32) Mao, A. H.; Lyle, N.; Pappu, R. V. Describing Sequence-Ensemble Relationships for Intrinsically Disordered Proteins. *Biochem. J.* **2013**, *449*, 307–318.
- (33) Crick, S. L.; Jayaraman, M.; Frieden, C.; Wetzel, R.; Pappu, R. V. Fluorescence Correlation Spectroscopy Shows That Monomeric Polyglutamine Molecules Form Collapsed Structures in Aqueous Solutions. *Proc. Natl. Acad. Sci. U. S. A.* **2006**, *103*, 16764–16769.
- (34) Tran, H. T.; Mao, A.; Pappu, R. V. Role of Backbone-Solvent Interactions in Determining Conformational Equilibria of Intrinsically Disordered Proteins. *J. Am. Chem. Soc.* **2008**, *130*, 7380–7392.
- (35) Holehouse, A. S.; Garai, K.; Lyle, N.; Vitalis, A.; Pappu, R. V. Quantitative Assessments of the Distinct Contributions of Polypeptide Backbone Amides Versus Side Chain Groups to Chain Expansion Via Chemical Denaturation. *J. Am. Chem. Soc.* **2015**, *137*, 2984–2995.
- (36) Mukhopadhyay, S.; Krishnan, R.; Lemke, E. A.; Lindquist, S.; Deniz, A. A. A Natively Unfolded Yeast Prion Monomer Adopts an

- Ensemble of Collapsed and Rapidly Fluctuating Structures. *Proc. Natl. Acad. Sci. U. S. A.* **2007**, *104*, 2649–2654.
- (37) Pappu, R. V.; Wang, X.; Vitalis, A.; Crick, S. L. A Polymer Physics Perspective on Driving Forces and Mechanisms for Protein Aggregation. *Arch. Biochem. Biophys.* **2008**, *469*, 132–141.
- (38) Posey, A. E.; Ruff, K. M.; Harmon, T. S.; Crick, S. L.; Li, A.; Diamond, M. I.; Pappu, R. V. Profilin Reduces Aggregation and Phase Separation of Huntingtin N-Terminal Fragments by Preferentially Binding to Soluble Monomers and Oligomers. *J. Biol. Chem.* **2018**, 293, 3734–3746.
- (39) Mao, A. H.; Crick, S. L.; Vitalis, A.; Chicoine, C. L.; Pappu, R. V. Net Charge Per Residue Modulates Conformational Ensembles of Intrinsically Disordered Proteins. *Proc. Natl. Acad. Sci. U. S. A.* **2010**, 107, 8183–8188.
- (40) Marsh, J. A.; Forman-Kay, J. D. Sequence Determinants of Compaction in Intrinsically Disordered Proteins. *Biophys. J.* **2010**, *98*, 2383–2390.
- (41) Müller-Späth, S.; Soranno, A.; Hirschfeld, V.; Hofmann, H.; Rüegger, S.; Reymond, L.; Nettels, D.; Schuler, B. Charge Interactions Can Dominate the Dimensions of Intrinsically Disordered Proteins. *Proc. Natl. Acad. Sci. U. S. A.* **2010**, *107*, 14609–14614.
- (42) Das, R. K.; Ruff, K. M.; Pappu, R. V. Relating Sequence Encoded Information to Form and Function of Intrinsically Disordered Proteins. *Curr. Opin. Struct. Biol.* **2015**, 32, 102–112.
- (43) Holehouse, A. S.; Pappu, R. V. Collapse Transitions of Proteins and the Interplay among Backbone, Sidechain, and Solvent Interactions. *Annu. Rev. Biophys.* **2018**, *47*, 19–39.
- (44) Hyman, A. A.; Weber, C. A.; Jülicher, F. Liquid-Liquid Phase Separation in Biology. *Annu. Rev. Cell Dev. Biol.* **2014**, *30*, 39–58.
- (45) Brangwynne, C. P.; Eckmann, C. R.; Courson, D. S.; Rybarska, A.; Hoege, C.; Gharakhani, J.; Juelicher, F.; Hyman, A. A. Germline P Granules Are Liquid Droplets That Localize by Controlled Dissolution/Condensation. *Science* **2009**, 324, 1729–1732.
- (46) Li, P.; Banjade, S.; Cheng, H. C.; Kim, S.; Chen, B.; Guo, L.; Llaguno, M.; Hollingsworth, J. V.; King, D. S.; Banani, S. F.; et al. Phase Transitions in the Assembly of Multivalent Signalling Proteins. *Nature* **2012**, *483*, 336–340.
- (47) Harmon, T. S.; Holehouse, A. S.; Rosen, M. K.; Pappu, R. V. Intrinsically Disordered Linkers Determine the Interplay between Phase Separation and Gelation in Multivalent Proteins. *eLife* **2017**, *6*, 30294.
- (48) Banjade, S.; Wu, Q.; Mittal, A.; Peeples, W. B.; Pappu, R. V.; Rosen, M. K. Conserved Interdomain Linker Promotes Phase Separation of the Multivalent Adaptor Protein Nck. *Proc. Natl. Acad. Sci. U. S. A.* **2015**, *112*, e6426—e6435.
- (49) Brangwynne, C. P.; Tompa, P.; Pappu, R. V. Polymer Physics of Intracellular Phase Transitions. *Nat. Phys.* **2015**, *11*, 899–904.
- (50) Flory, P. J. Thermodynamics of High Polymer Solutions. *J. Chem. Phys.* **1942**, *10*, 51–61.
- (51) Huggins, M. L. Some Properties of Solutions of Long-Chain Compounds. *J. Phys. Chem.* **1942**, *46*, 151–158. Huggins, M. L. Solutions of Long Chain Compounds. *J. Chem. Phys.* **1941**, *9*, 440–440.
- (52) Tanaka, F. Theory of Molecular Association and Thermoreversible Gelation. In *Molecular Gels: Materials with Self-Assembled Fibrillar Networks*; Springer, 2006; pp 17–78.
- (53) Tanaka, F. Polymer Physics: Applications to Molecular Association and Thermoreversible Gelation; Cambridge University Press, 2011.
- (54) Stockmayer, W. H. Theory of Molecular Size Distribution and Gel Formation in Branched-Chain Polymers. *J. Chem. Phys.* **1943**, *11*, 45–55.
- (55) Semenov, A. N.; Rubinstein, M. Thermoreversible Gelation in Solutions of Associative Polymers. 1. Statics. *Macromolecules* **1998**, *31*, 1373–1385.
- (56) Kratky, K. W. Is the Percolation Transition of Hard Spheres a Thermodynamic Phase Transition? *J. Sta. Phys.* **1988**, 52, 1413–1421. (57) Mathieu, C.; Pappu, R. V.; Taylor, J. P. Beyond Aggregation: Pathological Phase Transitions in Neurodegenerative Disease. *Science* **2020**, 370, 56–60.

- (58) Posey, A. E.; Ruff, K. M.; Lalmansingh, J. M.; Kandola, T. S.; Lange, J. J.; Halfmann, R.; Pappu, R. V. Mechanistic Inferences from Analysis of Measurements of Protein Phase Transitions in Live Cells. *J. Mol. Biol.* **2021**, 433, 166848.
- (59) Minton, A. P. Simple Calculation of Phase Diagrams for Liquid-Liquid Phase Separation in Solutions of Two Macromolecular Solute Species. *J. Phys. Chem. B* **2020**, 124, 2363–2370.
- (60) Tanaka, F. Theoretical Study of Molecular Association and Thermoreversible Gelation in Polymers. *Polymer J.* **2002**, 34, 479–509.
- (61) Rubinstein, M.; Dobrynin, A. V. Solutions of Associative Polymers. *Trend. Polym. Sci.* **1997**, *5*, 181–186.
- (62) Bianchi, E.; Blaak, R.; Likos, C. N. Patchy Colloids: State of the Art and Perspectives. *Phys. Chem. Chem. Phys.* **2011**, *13*, 6397–6410.
- (63) Ruff, K. M.; Choi, Y. H.; Cox, D.; Ormsby, A. R.; Myung, Y.; Ascher, D. B.; Radford, S. E.; Pappu, R. V.; Hatters, D. M. Sequence Grammar Underlying the Unfolding and Phase Separation of Globular Proteins. *Mol. Cell* **2022**, *82*, 3193–3208.
- (64) Martin, E. W.; Holehouse, A. S.; Peran, I.; Farag, M.; Incicco, J. J.; Bremer, A.; Grace, C. R.; Soranno, A.; Pappu, R. V.; Mittag, T. Valence and Patterning of Aromatic Residues Determine the Phase Behavior of Prion-Like Domains. *Science* **2020**, *367*, 694–699.
- (65) Wang, J.; Choi, J.-M.; Holehouse, A. S.; Lee, H. O.; Zhang, X.; Jahnel, M.; Maharana, S.; Lemaitre, R.; Pozniakovsky, A.; Drechsel, D.; et al. A Molecular Grammar Governing the Driving Forces for Phase Separation of Prion-Like Rna Binding Proteins. *Cell* **2018**, *174*, 688–699.
- (66) Bremer, A.; Farag, M.; Borcherds, W. M.; Peran, I.; Martin, E. W.; Pappu, R. V.; Mittag, T. Deciphering How Naturally Occurring Sequence Features Impact the Phase Behaviours of Disordered Prion-Like Domains. *Nat. Chem.* **2022**, *14*, 196–207.
- (67) Kaur, T.; Raju, M.; Alshareedah, I.; Davis, R. B.; Potoyan, D. A.; Banerjee, P. R. Sequence-Encoded and Composition-Dependent Protein-Rna Interactions Control Multiphasic Condensate Morphologies. *Nature Commun.* **2021**, *12*, 872.
- (68) Riback, J. A.; Katanski, C. D.; Kear-Scott, J. L.; Pilipenko, E. V.; Rojek, A. E.; Sosnick, T. R.; Drummond, D. A. Stress-Triggered Phase Separation Is an Adaptive, Evolutionarily Tuned Response. *Cell* **2017**, *168*, 1028–1040.
- (69) Mao, Y. S.; Zhang, B.; Spector, D. L. Biogenesis and Function of Nuclear Bodies. *Trend. Genet.* **2011**, *27*, 295–306.
- (70) Seim, I.; Roden, C. A.; Gladfelter, A. S. Role of Spatial Patterning of N-Protein Interactions in Sars-Cov-2 Genome Packaging. *Biophys. J.* **2021**, *120*, 2771–2784.
- (71) Roden, C. A.; Dai, Y.; Giannetti, C. A.; Seim, I.; Lee, M.; Sealfon, R.; McLaughlin, G. A.; Boerneke, M. A.; Iserman, C.; Wey, S. A.; et al. Double-Stranded Rna Drives Sars-Cov-2 Nucleocapsid Protein to Undergo Phase Separation at Specific Temperatures. *Nucleic Acids Res.* **2022**, *50*, 8168–8192.
- (72) Boeynaems, S.; Holehouse, A. S.; Weinhardt, V.; Kovacs, D.; Van Lindt, J.; Larabell, C.; Van Den Bosch, L.; Das, R.; Tompa, P. S.; Pappu, R. V.; et al. Spontaneous Driving Forces Give Rise to Protein-Rna Condensates with Coexisting Phases and Complex Material Properties. *Proc. Natl. Acad. Sci. U. S. A.* **2019**, *116*, 7889–7898.
- (73) Bracha, D.; Walls, M. T.; Wei, M.-T.; Zhu, L.; Kurian, M.; Avalos, J. L.; Toettcher, J. E.; Brangwynne, C. P. Mapping Local and Global Liquid Phase Behavior in Living Cells Using Photo-Oligomerizable Seeds. *Cell* **2018**, *175*, 1467–1480.
- (74) Yeomans, J. M. Statistical Mechanics of Phase Transitions; Oxford University Press, 1992.
- (75) Mittag, T.; Pappu, R. V. A Conceptual Framework for Understanding Phase Separation and Addressing Open Questions and Challenges. *Mol. Cell* **2022**, *82*, 2201–2214.
- (76) Sing, C. E.; Perry, S. L. Recent Progress in the Science of Complex Coacervation. *Soft Matt.* **2020**, *16*, 2885–2914.
- (77) Kim, J. Y.; Cho, C. H.; Palffy-Muhoray, P.; Kyu, T. Polymerization-Induced Phase Separation in a Liquid-Crystal-Polymer Mixture. *Phys. Rev. Lett.* **1993**, *71*, 2232–2235.
- (78) Phillips, J. N. The Energetics of Micelle Formation. *Trans. Farad. Soc.* **1955**, *51*, 561–569.

- (79) Khalatur, P. G.; Khokhlov, A. R.; Nyrkova, I. A.; Semenov, A. N. Aggregation Processes in Self-Associating Polymer Systems: A Comparative Analysis of Theoretical and Computer Simulation Data for Micelles in the Superstrong Segregation Regime. *Macromol. Theor. Simul.* **1996**, *5*, 749–757.
- (80) Cuylen, S.; Blaukopf, C.; Politi, A. Z.; Müller-Reichert, T.; Neumann, B.; Poser, I.; Ellenberg, J.; Hyman, A. A.; Gerlich, D. W. Ki-67 Acts as a Biological Surfactant to Disperse Mitotic Chromosomes. *Nature* **2016**, 535, 308–312.
- (81) Leibler, L. Theory of Microphase Separation in Block Copolymers. *Macromolecules* **1980**, *13*, 1602–1617.
- (82) Rana, U.; Brangwynne, C. P.; Panagiotopoulos, A. Z. Phase Separation Vs Aggregation Behavior for Model Disordered Proteins. *J. Chem. Phys.* **2021**, *155*, 125101.
- (83) Cates, M. E.; Tailleur, J. Motility-Induced Phase Separation. Annu. Rev. Cond. Matt. Phys. 2015, 6, 219–244.
- (84) Weber, C. A.; Zwicker, D.; Jülicher, F.; Lee, C. F. Physics of Active Emulsions. *Rep. Prog. Phys.* **2019**, 82, 064601.
- (85) Sweatman, M. B.; Lue, L. The Giant Salr Cluster Fluid: A Review. Adv. Theor. Simul. 2019, 2, 1900025.
- (86) Martin, E. W.; Harmon, T. S.; Hopkins, J. B.; Chakravarthy, S.; Incicco, J. J.; Schuck, P.; Soranno, A.; Mittag, T. A Multi-Step Nucleation Process Determines the Kinetics of Prion-Like Domain Phase Separation. *Nature Commun.* **2021**, *12*, 4513.
- (87) Shimobayashi, S. F.; Ronceray, P.; Sanders, D. W.; Haataja, M. P.; Brangwynne, C. P. Nucleation Landscape of Biomolecular Condensates. *Nature* **2021**, *599*, 503–506.
- (88) Boyd-Shiwarski, C. R.; Shiwarski, D. J.; Griffiths, S. E.; Beacham, R. T.; Norrell, L.; Morrison, D. E.; Wang, J.; Mann, J.; Tennant, W.; Anderson, E. N.; et al. Wnk Kinases Sense Molecular Crowding and Rescue Cell Volume Via Phase Separation. *Cell* **2022**, *185*, 4488.
- (89) Tanaka, H. Viscoelastic Phase Separation. J. Phys. Cond. Mater. 2000, 12, R207-R264.
- (90) Bertrand, T.; Lee, C. F. Diversity of Phase Transitions and Phase Separations in Active Fluids. *Phys. Rev. Res.* **2022**, *4*, L022046.
- (91) Henninger, J. E.; Oksuz, O.; Shrinivas, K.; Sagi, I.; LeRoy, G.; Zheng, M. M.; Andrews, J. O.; Zamudio, A. V.; Lazaris, C.; Hannett, N. M.; et al. Rna-Mediated Feedback Control of Transcriptional Condensates. *Cell* **2021**, *184*, 207–225.
- (92) Riback, J. A.; Zhu, L.; Ferrolino, M. C.; Tolbert, M.; Mitrea, D. M.; Sanders, D. W.; Wei, M. T.; Kriwacki, R. W.; Brangwynne, C. P. Composition-Dependent Thermodynamics of Intracellular Phase Separation. *Nature* **2020**, *581*, 209–214.
- (93) Alder, B. J.; Wainwright, T. E. Phase Transition for a Hard Sphere System. *J. Chem. Phys.* **1957**, *27*, 1208–1209.
- (94) Wood, W. W.; Jacobson, J. D. Preliminary Results from a Recalculation of the Monte Carlo Equation of State of Hard Spheres. *J. Chem. Phys.* **1957**, *27*, 1207–1208.
- (95) Barker, J. A.; Henderson, D. What Is "Liquid"? Understanding the States of Matter. Rev. Mod. Phys. 1976, 48, 587–671.
- (96) Bolhuis, P. G.; Frenkel, D.; Mau, S.-C.; Huse, D. A. Entropy Difference between Crystal Phases. *Nature* **1997**, 388, 235–236.
- (97) Onsager, L. The Effects of Shape on the Interaction of Colloidal Particles. *Ann. N.Y. Acad. Sci.* **1949**, *51*, 627–659.
- (98) Speranza, A.; Sollich, P. Simplified Onsager Theory for Isotropic-Nematic Phase Equilibria of Length Polydisperse Hard Rods. *J. Chem. Phys.* **2002**, *117*, 5421–5436.
- (99) Yu, L. J.; Saupe, A. Observation of a Biaxial Nematic Phase in Potassium Laurate-1-Decanol-Water Mixtures. *Phys. Rev. Lett.* **1980**, 45, 1000–1003.
- (100) Camp, P. J.; Allen, M. P. Hard Ellipsoid Rod-Plate Mixtures: Onsager Theory and Computer Simulations. *Physica A* **1996**, 229, 410–427.
- (101) Weeks, J. D.; Chandler, D.; Andersen, H. C. Perturbation Theory of the Thermodynamic Properties of Simple Liquids. *J. Chem. Phys.* **1971**, *55*, 5422–5423.
- (102) Chandler, D.; Weeks, J. D.; Andersen, H. C. Van Der Waals Picture of Liquids, Solids, and Phase Transformations. *Science* **1983**, 220, 787–794.

- (103) Hoover, W. G.; Gray, S. G.; Johnson, K. W. Thermodynamic Properties of the Fluid and Solid Phases for Inverse Power Potentials. *J. Chem. Phys.* **1971**, *55*, 1128–1136.
- (104) Widom, B. Intermolecular Forces and the Nature of the Liquid State. *Science* **1967**, *157*, 375–382.
- (105) Jun, S.; Wright, A. Entropy as the Driver of Chromosome Segregation. *Nature Rev. Microbiol.* **2010**, *8*, 600–607.
- (106) Mitra, D.; Pande, S.; Chatterji, A. Polymer Architecture Orchestrates the Segregation and Spatial Organization of Replicating E. Coli Chromosomes in Slow Growth. *Soft Matt.* **2022**, *18*, 5615–5631.
- (107) Denisov, I. G.; McLean, M. A.; Shaw, A. W.; Grinkova, Y. V.; Sligar, S. G. Thermotropic Phase Transition in Soluble Nanoscale Lipid Bilayers. *J. Phys. Chem. B* **2005**, *109*, 15580–15588.
- (108) Ogston, A. G. On the Interaction of Solute Molecules with Porous Networks. J. Phys. Chem. 1970, 74, 668-669.
- (109) Musacchio, A. On the Role of Phase Separation in the Biogenesis of Membraneless Compartments. *EMBO J.* **2022**, *41*, No. e109952.
- (110) Kirschbaum, J.; Zwicker, D. Controlling Biomolecular Condensates Via Chemical Reactions. *J. Royal Soc. Interfac.* **2021**, *18*, 20210255.
- (111) Bechinger, C.; Di Leonardo, R.; Löwen, H.; Reichhardt, C.; Volpe, G.; Volpe, G. Active Particles in Complex and Crowded Environments. *Rev. Mod. Phys.* **2016**, *88*, 045006.
- (112) Tran-Cong-Miyata, Q.; Nakanishi, H. Phase Separation of Polymer Mixtures Driven by Photochemical Reactions: Current Status and Perspectives. *Polym. Int.* **2017**, *66*, 213–222.
- (113) Hildebrand, J. H. A History of Solution Theory. *Annu. Rev. Phys. Chem.* **1981**, 32, 1–24.
- (114) Welton, T. Room-Temperature Ionic Liquids. Solvents for Synthesis and Catalysis. *Chem. Rev.* **1999**, *99*, 2071–2084.
- (115) Raos, G.; Allegra, G. Chain Collapse and Phase Separation in Poor-Solvent Polymer Solutions: A Unified Molecular Description. *J. Chem. Phys.* **1996**, *104*, 1626–1645.
- (116) Raos, G.; Allegra, G. Macromolecular Clusters in Poor-Solvent Polymer Solutions. *J. Chem. Phys.* **1997**, *107*, 6479–6490.
- (117) Handwerger, K. E.; Cordero, J. A.; Gall, J. G. Cajal Bodies, Nucleoli, and Speckles in the Xenopus Oocyte Nucleus Have a Low-Density, Sponge-Like Structure. *Mol. Biol. Cell* **2005**, *16*, 202–211.
- (118) Wei, M. T.; Elbaum-Garfinkle, S.; Holehouse, A. S.; Chen, C. C.; Feric, M.; Arnold, C. B.; Priestley, R. D.; Pappu, R. V.; Brangwynne, C. P. Phase Behaviour of Disordered Proteins Underlying Low Density and High Permeability of Liquid Organelles. *Nat. Chem.* **2017**, *9*, 1118–1125.
- (119) Seim, I.; Posey, A. E.; Snead, W. T.; Stormo, B. M.; Klotsa, D.; Pappu, R. V.; Gladfelter, A. S. Dilute Phase Oligomerization Can Oppose Phase Separation and Modulate Material Properties of a Ribonucleoprotein Condensate. *Proc. Natl. Acad. Sci. U. S. A.* **2022**, *119*, No. e2120799119.
- (120) Hill, T. L. An Introduction to Statistical Thermodynamics; Addison-Wesley, 1960.
- (121) Neal, B. L.; Asthagiri, D.; Lenhoff, A. M. Molecular Origins of Osmotic Second Virial Coefficients of Proteins. *Biophys. J.* **1998**, *75*, 2469–2477.
- (122) Zimm, B. H. Application of the Methods of Molecular Distribution to Solutions of Large Molecules. *J. Chem. Phys.* **1946**, *14*, 164–179.
- (123) Ma, Y.; Acosta, D. M.; Whitney, J. R.; Podgornik, R.; Steinmetz, N. F.; French, R. H.; Parsegian, V. A. Determination of the Second Virial Coefficient of Bovine Serum Albumin under Varying Ph and Ionic Strength by Composition-Gradient Multi-Angle Static Light Scattering. *J. Biol. Phys.* **2015**, *41*, 85–97.
- (124) Safari, M. S.; King, M. R.; Brangwynne, C. P.; Petry, S. Interaction of Spindle Assembly Factor Tpx2 with Importins-Alpha/Beta Inhibits Protein Phase Separation. *J. Biol. Chem.* **2021**, 297, 100998.
- (125) Ellis, R. J. Macromolecular Crowding: Obvious but Underappreciated. *Trend. Biochem. Sci.* **2001**, *26*, 597–604.

- (126) Banani, S. F.; Rice, A. M.; Peeples, W. B.; Lin, Y.; Jain, S.; Parker, R.; Rosen, M. K. Compositional Control of Phase-Separated Cellular Bodies. *Cell* **2016**, *166*, *651*–*663*.
- (127) Prausnitz, J. M.; Lichtenthaler, R.; Gomes de Azevedo, E. *Molecular Thermodynamics of Fluid Phase Equilibria*; Prentice Hall, Inc., 1999
- (128) Jacobs, W. M.; Frenkel, D. Phase Transitions in Biological Systems with Many Components. *Biophys. J.* **2017**, *112*, 683–691.
- (129) Iqbal, M.; Tao, Y.; Xie, S.; Zhu, Y.; Chen, D.; Wang, X.; Huang, L.; Peng, D.; Sattar, A.; Shabbir, M. A. B.; et al. Aqueous Two-Phase System (Atps): An Overview and Advances in Its Applications. *Biological Procedures Online* **2016**, *18*, 18.
- (130) Esquena, J. Water-in-Water (W/W) Emulsions. Curr. Opin. Struct. Biol. 2016, 25, 109-119.
- (131) Fei, J.; Jadaliha, M.; Harmon, T. S.; Li, I. T.; Hua, B.; Hao, Q.; Holehouse, A. S.; Reyer, M.; Sun, Q.; Freier, S. M.; et al. Quantitative Analysis of Multilayer Organization of Proteins and Rna in Nuclear Speckles at Super Resolution. *J. Cell Sci.* **2017**, *130*, 4180–4192.
- (132) Feric, M.; Vaidya, N.; Harmon, T. S.; Mitrea, D. M.; Zhu, L.; Richardson, T. M.; Kriwacki, R. W.; Pappu, R. V.; Brangwynne, C. P. Coexisting Liquid Phases Underlie Nucleolar Subcompartments. *Cell* **2016**, *165*, 1686–1697.
- (133) Feric, M.; Sarfallah, A.; Dar, F.; Temiakov, D.; Pappu, R. V.; Misteli, T. Mesoscale Structure-Function Relationships in Mitochondrial Transcriptional Condensates. *Proc. Natl. Acad. Sci. U. S. A.* **2022**, *119*, No. e2207303119.
- (134) Lafontaine, D. L. J.; Riback, J. A.; Bascetin, R.; Brangwynne, C. P. The Nucleolus as a Multiphase Liquid Condensate. *Nature Rev. Cell Mol. Biol.* **2021**, 22, 165–182.
- (135) Yewdall, N. A.; André, A. A. M.; Lu, T.; Spruijt, E. Coacervates as Models of Membraneless Organelles. *Curr. Opin. Struct. Biol.* **2021**, 52, 101416.
- (136) Simon, J. R.; Carroll, N. J.; Rubinstein, M.; Chilkoti, A.; López, G. P. Programming Molecular Self-Assembly of Intrinsically Disordered Proteins Containing Sequences of Low Complexity. *Nat. Chem.* **2017**, *9*, 509–515.
- (137) Scatchard, G. The Gibbs Adsorption Isotherm. *J. Phys. Chem.* **1962**, *66*, *618*–*620*.
- (138) Ruff, K. M.; Roberts, S.; Chilkoti, A.; Pappu, R. V. Advances in Understanding Stimulus-Responsive Phase Behavior of Intrinsically Disordered Protein Polymers. *J. Mol. Biol.* **2018**, *430*, 4619–4635.
- (139) Wadsworth, G. M.; Zahurancik, W. J.; Zeng, X.; Pullara, P.; Lai, L. B.; Sidharthan, V.; Pappu, R. V.; Gopalan, V.; Banerjee, P. R. Rnas Undergo Phase Transitions with Lower Critical Solution Temperatures. *bioRxiv* 2022.
- (140) Sommer, J.-U. Gluonic and Regulatory Solvents: A Paradigm for Tunable Phase Segregation in Polymers. *Macromolecules* **2018**, *51*, 3066–3074.
- (141) Garcia Quiroz, F.; Li, N. K.; Roberts, S.; Weber, P.; Dzuricky, M.; Weitzhandler, I.; Yingling, Y. G.; Chilkoti, A. Intrinsically Disordered Proteins Access a Range of Hysteretic Phase Separation Behaviors. *Sci. Adv.* **2019**, *5*, No. eaax5177.
- (142) Bharadwaj, S.; Nayar, D.; Dalgicdir, C.; van der Vegt, N. F. A. An Interplay of Excluded-Volume and Polymer-(Co) Solvent Attractive Interactions Regulates Polymer Collapse in Mixed Solvents. *J. Chem. Phys.* **2021**, *154*, 134903.
- (143) Schellman, J. A. Macromolecular Binding. *Biopolymers* 1975, 14, 999–1018.
- (144) Woodbury, C. P. Introduction to Macromolecular Binding Equilibria; CRC Press, 2007. DOI: 10.1201/b12823.
- (145) Sciortino, F.; Zaccarelli, E. Reversible Gels of Patchy Particles. Curr. Opin. Solid Stat. Mater. Sci. 2011, 15, 246–253.
- (146) Oh, J. S.; Lee, S.; Glotzer, S. C.; Yi, G.-R.; Pine, D. J. Colloidal Fibers and Rings by Cooperative Assembly. *Nature Commun.* **2019**, *10*, 3936
- (147) Vissers, T.; Smallenburg, F.; Munao, G.; Preisler, Z.; Sciortino, F. Cooperative Polymerization of One-Patch Colloids. *J. Chem. Phys.* **2014**, *140*, 144902.

- (148) Hong, L.; Jiang, S.; Granick, S. Simple Method to Produce Janus Colloidal Particles in Large Quantity. *Langmuir* **2006**, 22, 9495–9499.
- (149) Gallegos, J. A. S.; Perdomo-Pérez, R.; Valadez-Pérez, N. E.; Castañeda-Priego, R. Location of the Gel-Like Boundary in Patchy Colloidal Dispersions: Rigidity Percolation, Structure, and Particle Dynamics. *Phys. Rev. E* **2021**, *104*, 064606.
- (150) Schmit, J. D.; Bouchard, J. J.; Martin, E. W.; Mittag, T. Protein Network Structure Enables Switching between Liquid and Gel States. *J. Am. Chem. Soc.* **2020**, *142*, 874–883.
- (151) Rubinstein, M.; Semenov, A. N. Thermoreversible Gelation in Solutions of Associating Polymers. 2. Linear Dynamics. *Macromolecules* **1998**, *31*, 1386–1397.
- (152) Marzahn, M. R.; Marada, S.; Lee, J.; Nourse, A.; Kenrick, S.; Zhao, H.; Ben-Nissan, G.; Kolaitis, R. M.; Peters, J. L.; Pounds, S.; et al. Higher-Order Oligomerization Promotes Localization of Spop to Liquid Nuclear Speckles. *EMBO J.* **2016**, 35, 1254–1275.
- (153) Smulders, M. M. J.; Nieuwenhuizen, M. M. L.; de Greef, T. F. A.; van der Schoot, P.; Schenning, A. P. H. J.; Meijer, E. W. How to Distinguish Isodesmic from Cooperative Supramolecular Polymerisation. *Chemistry* **2010**, *16*, 362–367.
- (154) De Greef, T. F. A.; Smulders, M. M. J.; Wolffs, M.; Schenning, A. P. H. J.; Sijbesma, R. P.; Meijer, E. W. Supramolecular Polymerization. *Chem. Rev.* **2009**, *109*, 5687–5754.
- (155) Bianchi, E.; Largo, J.; Tartaglia, P.; Zaccarelli, E.; Sciortino, F. Phase Diagram of Patchy Colloids: Towards Empty Liquids. *Phys. Rev. Lett.* **2006**, *97*, 168301.
- (156) Harmon, T. S.; Holehouse, A. S.; Pappu, R. V. Differential Solvation of Intrinsically Disordered Linkers Drives the Formation of Spatially Organized Droplets in Ternary Systems of Linear Multivalent Proteins. *New J. Phys.* **2018**, 20, 045002.
- (157) Hubatsch, L.; Jawerth, L. M.; Love, C.; Bauermann, J.; Tang, T. Y. D.; Bo, S.; Hyman, A. A.; Weber, C. A. Quantitative Theory for the Diffusive Dynamics of Liquid Condensates. *eLife* **2021**, *10*, No. e68620.
- (158) Ying, Q.; Chu, B. Overlap Concentration of Macromolecules in Solution. *Macromolecules* **1987**, *20*, 362–366.
- (159) Uematsu, T.; Svanberg, C.; Jacobsson, P. A Unified Picture of Static and Dynamic Length Scales in Polymer Solutions. *Macromolecules* **2005**, *38*, 6227–6230.
- (160) Zmpitas, W.; Gross, J. Detailed Pedagogical Review and Analysis of Wertheim's Thermodynamic Perturbation Theory. *Fluid Phase Equilib.* **2016**, 428, 121–152.
- (161) Prigogine, I.; Bellemans, A.; Mathot, V. *The Molecular Theory of Solutions*; North-Holland, 1957.
- (162) Lundberg, R. D.; Makowski, H. S. A Comparison of Sulfonate and Carboxylate Ionomers. In *Ions in Polymers*, Advances in Chemistry, Vol. 187; American Chemical Society, 1980; pp 21–36.
- (163) Rubinstein, M.; Semenov, A. N. Dynamics of Entangled Solutions of Associating Polymers. *Macromolecules* **2001**, *34*, 1058–1068.
- (164) Weiss, R. A.; Zhao, H. Rheological Behavior of Oligomeric Ionomers. *J. Rheol.* **2009**, 53, 191–213.
- (165) Wertheim, M. S. Fluids with Highly Directional Attractive Forces. Iii. Multiple Attraction Sites. *J. Sta. Phys.* **1986**, *42*, 459–476.
- (166) Kudlay, A.; Erukhimovich, I. Phase Behavior of Solutions of Polymers with Multiply Aggregating Groups. *Macromol. Theor. Simul.* **2001**, *10*, 542–552.
- (167) Wertheim, M. S. Fluids with Highly Directional Attractive Forces. Iv. Equilibrium Polymerization. *J. Sta. Phys.* **1986**, 42, 477–492.
- (168) Han, X.-G.; Zhang, C.-X. Self-Consistent Field Lattice Model Study on the Phase Behavior of Physically Associating Polymer Solutions. *J. Chem. Phys.* **2010**, *132*, 164905.
- (169) Ermoshkin, A. V.; Olvera De La Cruz, M. Gelation in Strongly Charged Polyelectrolytes. *J. Polym. Sci., Part B* **2004**, 42, 766–776.
- (170) Cates, M. E.; Witten, T. A. Chain Conformation and Solubility of Associating Polymers. *Macromolecules* **1986**, *19*, 732–739.
- (171) Dudowicz, J.; Freed, K. F.; Douglas, J. F. Lattice Cluster Theory of Associating Polymers. Iv. Phase Behavior of Telechelic Polymer Solutions. *J. Chem. Phys.* **2012**, *136*, 194903.

- (172) Borisov, O. V.; Halperin, A. Polysoaps within the P-Cluster Model: Solutions and Brushes. *Macromolecules* **1999**, 32, 5097–5105.
- (173) Clément, F.; Johner, A.; Joanny, J. F.; Semenov, A. N. Stress Relaxation in Telechelic Gels. 1. Sticker Extraction. *Macromolecules* **2000**, 33, 6148–6158.
- (174) Khalatur, P. G.; Khokhlov, A. R.; Mologin, D. A. Simulation of Self-Associating Polymer Systems. I. Shear-Induced Structural Changes. *J. Chem. Phys.* **1998**, *109*, 9602–9613.
- (175) Tanaka, F.; Edwards, S. F. Viscoelastic Properties of Physically Crosslinked Networks. 1. Transient Network Theory. *Macromolecules* **1992**, 25, 1516–1523.
- (176) Wertheim, M. S. Fluids with Highly Directional Attractive Forces. I. Statistical Thermodynamics. J. Sta. Phys. 1984, 35, 19–34.
- (177) Witten, T. A. Heterogeneous Polymers and Self-Organization. *J. Phys. Cond. Mater.* **1990**, *2*, SA1.
- (178) Singh, K.; Rabin, Y. Sequence Effects on Internal Structure of Droplets Of associative Polymers. *Biophys. J.* **2021**, *120*, 1210–1218.
- (179) Mahmad Rasid, I.; Do, C.; Holten-Andersen, N.; Olsen, B. D. Effect of Sticker Clustering on the Dynamics of Associative Networks. *Soft Matt.* **2021**, *17*, 8960–8972.
- (180) Lyubartsev, A. P.; Laaksonen, A. Calculation of Effective Interaction Potentials from Radial Distribution Functions: A Reverse Monte Carlo Approach. *Phys. Rev. E* **1995**, *52*, 3730–3737.
- (181) Mohan, A.; Oldfield, C. J.; Radivojac, P.; Vacic, V.; Cortese, M. S.; Dunker, A. K.; Uversky, V. N. Analysis of Molecular Recognition Features (Morfs). *J. Mol. Biol.* **2006**, *362*, 1043–1059.
- (182) Cohan, M. C.; Shinn, M. K.; Lalmansingh, J. M.; Pappu, R. V. Uncovering Non-Random Binary Patterns within Sequences of Intrinsically Disordered Proteins. *J. Mol. Biol.* **2022**, *434*, 167373.
- (183) Yamazaki, T.; Yamamoto, T.; Yoshino, H.; Souquere, S.; Nakagawa, S.; Pierron, G.; Hirose, T. Paraspeckles Are Constructed as Block Copolymer Micelles. *EMBO J.* **2021**, *40*, No. e107270.
- (184) Roberts, S.; Harmon, T. S.; Schaal, J. L.; Miao, V.; Li, K.; Hunt, A.; Wen, Y.; Oas, T. G.; Collier, J. H.; Pappu, R. V.; et al. Injectable Tissue Integrating Networks from Recombinant Polypeptides with Tunable Order. *Nat. Mater.* **2018**, *17*, 1154–1163.
- (185) Protter, D. S. W.; Rao, B. S.; Van Treeck, B.; Lin, Y.; Mizoue, L.; Rosen, M. K.; Parker, R. Intrinsically Disordered Regions Can Contribute Promiscuous Interactions to Rnp Granule Assembly. *Cell Rep.* 2018, 22, 1401–1412.
- (186) Record, M. T.; Guinn, E.; Pegram, L.; Capp, M. Introductory Lecture: Interpreting and Predicting Hofmeister Salt Ion and Solute Effects on Biopolymer and Model Processes Using the Solute Partitioning Model. *Faraday Discus.* **2013**, *160*, 9–44.
- (187) Banjade, S.; Rosen, M. K. Phase Transitions of Multivalent Proteins Can Promote Clustering of Membrane Receptors. *eLife* **2014**, 3, No. e04123.
- (188) Mittal, A.; Holehouse, A. S.; Cohan, M. C.; Pappu, R. V. Sequence-to-Conformation Relationships of Disordered Regions Tethered to Folded Domains of Proteins. *J. Mol. Biol.* **2018**, 430, 2403–2421.
- (189) Choi, J.-M.; Dar, F.; Pappu, R. V. Lassi: A Lattice Model for Simulating Phase Transitions of Multivalent Proteins. *PLOS Comput. Biol.* **2019**, *15*, No. e1007028.
- (190) Kar, M.; Dar, F.; Welsh, T. J.; Vogel, L.; Kuhnemuth, R.; Majumdar, A.; Krainer, G.; Franzmann, T. M.; Alberti, S.; Seidel, C. M.; et al. Phase Separating Rna Binding Proteins Form Heterogeneous Distributions of Clusters in Subsaturated Solutions. *Proc. Natl. Acad. Sci. U. S. A.* 2022, *119*, No. e2202222119.
- (191) Krainer, G.; Saar, K. L.; Arter, W. E.; Welsh, T. J.; Czekalska, M. A.; Jacquat, R. P. B.; Peter, Q.; Traberg, W. C.; Pujari, A.; Jayaram, A. K.; et al. Direct Digital Sensing of Protein Biomarkers in Solution. *Nat. Commun.* **2023**, *14*, 653.
- (192) Widengren, J.; Kudryavtsev, V.; Antonik, M.; Berger, S.; Gerken, M.; Seidel, C. A. M. Single-Molecule Detection and Identification of Multiple Species by Multiparameter Fluorescence Detection. *Anal. Chem.* **2006**, *78*, 2039–2050.

- (193) He, G.; GrandPre, T.; Wilson, H.; Zhang, Y.; Jonikas, M. C.; Wingreen, N. S.; Wang, Q. Phase-Separating Pyrenoid Proteins Form Complexes in the Dilute Phase. *Commun. Biol.* **2023**, *6*, 19.
- (194) Rawat, P.; Boehning, M.; Hummel, B.; Aprile-Garcia, F.; Pandit, A. S.; Eisenhardt, N.; Khavaran, A.; Niskanen, E.; Vos, S. M.; Palvimo, J. J.; et al. Stress-Induced Nuclear Condensation of Nelf Drives Transcriptional Downregulation. *Mol. Cell* **2021**, *81*, 1013–1026.
- (195) Lan, C.; Kim, J.; Ulferts, S.; Aprile-Garcia, F.; Anandamurugan, A.; Grosse, R.; Sawarkar, R.; Reinhardt, A.; Hugel, T. Quantitative Real-Time in-Cell Imaging Reveals Heterogeneous Clusters of Proteins Prior to Condensation. *bioRxiv* 2022.
- (196) Wu, T.; King, M. R.; Farag, M.; Pappu, R. V.; Lew, M. D. Single Fluorogen Imaging Reveals Spatial Inhomogeneities within Biomolecular Condensates. *bioRxiv* 2023.
- (197) Narayanan, A.; Meriin, A.; Andrews, J. O.; Spille, J.-H.; Sherman, M. Y.; Cisse, I. I. A First Order Phase Transition Mechanism Underlies Protein Aggregation in Mammalian Cells. *eLife* **2019**, *8*, No. e39695.
- (198) Cho, N. H.; Cheveralls, K. C.; Brunner, A.-D.; Kim, K.; Michaelis, A. C.; Raghavan, P.; Kobayashi, H.; Savy, L.; Li, J. Y.; Canaj, H.; et al. Opencell: Endogenous Tagging for the Cartography of Human Cellular Organization. *Science* **2022**, *375*, No. eabi6983.
- (199) Yang, Y.; Jones, H. B.; Dao, T. P.; Castañeda, C. A. Single Amino Acid Substitutions in Stickers, but Not Spacers, Substantially Alter Ubqln2 Phase Transitions and Dense Phase Material Properties. *J. Phys. Chem. B* **2019**, *123*, 3618–3629.
- (200) Guo, Y. E.; Manteiga, J. C.; Henninger, J. E.; Sabari, B. R.; Dall'Agnese, A.; Hannett, N. M.; Spille, J.-H.; Afeyan, L. K.; Zamudio, A. V.; Shrinivas, K.; et al. Pol ii Phosphorylation Regulates a Switch between Transcriptional and Splicing Condensates. *Nature* **2019**, *572*, 543–548.
- (201) Greig, J. A.; Nguyen, T. A.; Lee, M.; Holehouse, A. S.; Posey, A. E.; Pappu, R. V.; Jedd, G. Arginine-Enriched Mixed-Charge Domains Provide Cohesion for Nuclear Speckle Condensation. *Mol. Cell* **2020**, 77, 1237–1250.
- (202) Bock, A. S.; Murthy, A. C.; Tang, W. S.; Jovic, N.; Shewmaker, F.; Mittal, J.; Fawzi, N. L. N-Terminal Acetylation Modestly Enhances Phase Separation and Reduces Aggregation of the Low-Complexity Domain of Rna-Binding Protein Fused in Sarcoma. *Protein Sci.* **2021**, 30, 1337–1349.
- (203) Qamar, S.; Wang, G.; Randle, S. J.; Ruggeri, F. S.; Varela, J. A.; Lin, J. Q.; Phillips, E. C.; Miyashita, A.; Williams, D.; Ströhl, F.; et al. Fus Phase Separation Is Modulated by a Molecular Chaperone and Methylation of Arginine Cation-Pi; Interactions. *Cell* **2018**, *173*, 720–734.
- (204) Timilsena, Y. P.; Akanbi, T. O.; Khalid, N.; Adhikari, B.; Barrow, C. J. Complex Coacervation: Principles, Mechanisms and Applications in Microencapsulation. *Int. J. Biol. Macromol.* **2019**, *121*, 1276–1286.
- (205) Neitzel, A. E.; Fang, Y. N.; Yu, B.; Rumyantsev, A. M.; de Pablo, J. J.; Tirrell, M. V. Polyelectrolyte Complex Coacervation across a Broad Range of Charge Densities. *Macromolecules* **2021**, *54*, 6878–6890.
- (206) Knoerdel, A. R.; Blocher McTigue, W. C.; Sing, C. E. Transfer Matrix Model of Ph Effects in Polymeric Complex Coacervation. *J. Phys. Chem. B* **2021**, *125*, 8965–8980.
- (207) Priftis, D.; Megley, K.; Laugel, N.; Tirrell, M. Complex Coacervation of Poly(Ethylene-Imine)/Polypeptide Aqueous Solutions: Thermodynamic and Rheological Characterization. *J. Colloid Interface Sci.* **2013**, 398, 39–50.
- (208) Overbeek, J. T. G.; Voorn, M. J. Phase Separation in Polyelectrolyte Solutions. Theory of Complex Coacervation. *J. Cell. Compar. Physiol.* **1957**, 49, 7–26.
- (209) Perry, S. L.; Sing, C. E. Prism-Based Theory of Complex Coacervation: Excluded Volume Versus Chain Correlation. *Macromolecules* **2015**, *48*, 5040–5053.
- (210) Lytle, T. K.; Sing, C. E. Transfer Matrix Theory of Polymer Complex Coacervation. *Soft Matter* **2017**, *13*, 7001–7012.

- (211) Chang, L.-W.; Lytle, T. K.; Radhakrishna, M.; Madinya, J. J.; Vélez, J.; Sing, C. E.; Perry, S. L. Sequence and Entropy-Based Control of Complex Coacervates. *Nature Commun.* **2017**, *8*, 1273.
- (212) Das, R. K.; Pappu, R. V. Conformations of Intrinsically Disordered Proteins Are Influenced by Linear Sequence Distributions of Oppositely Charged Residues. *Proc. Natl. Acad. Sci. U. S. A.* **2013**, *110*, 13392–13397.
- (213) Fossat, M. J.; Posey, A. E.; Pappu, R. V. Quantifying Charge State Heterogeneity for Proteins with Multiple Ionizable Residues. *Biophys. J.* **2021**, *120*, 5438–5453.
- (214) Aumiller, W. M., Jr.; Pir Cakmak, F.; Davis, B. W.; Keating, C. D. Rna-Based Coacervates as a Model for Membraneless Organelles: Formation, Properties, and Interfacial Liposome Assembly. *Langmuir* **2016**, 32, 10042–10053.
- (215) Pak, C. W.; Kosno, M.; Holehouse, A. S.; Padrick, S. B.; Mittal, A.; Ali, R.; Yunus, A. A.; Liu, D. R.; Pappu, R. V.; Rosen, M. K. Sequence Determinants of Intracellular Phase Separation by Complex Coacervation of a Disordered Protein. *Mol. Cell* **2016**, *63*, 72–85.
- (216) King, M. R.; Lin, A. Z.; Ruff, K. M.; Farag, M.; Ouyang, W.; Vahey, M. D.; Lundberg, E.; Pappu, R. V. Uncovering Molecular Grammars of Intrinsically Disordered Regions That Organize Nucleolar Fibrillar Centers. *bioRxiv* 2022.
- (217) Lin, M. Y.; Lindsay, H. M.; Weitz, D. A.; Klein, R.; Ball, R. C.; Meakin, P. Universal Diffusion-Limited Colloid Aggregation. *J. Phys. Cond. Mater.* **1990**, *2*, 3093.
- (218) Lin, M. Y.; Lindsay, H. M.; Weitz, D. A.; Ball, R. C.; Klein, R.; Meakin, P. Universal Reaction-Limited Colloid Aggregation. *Phys. Rev.* A **1990**, *41*, 2005–2020.
- (219) Setru, S. U.; Gouveia, B.; Alfaro-Aco, R.; Shaevitz, J. W.; Stone, H. A.; Petry, S. A Hydrodynamic Instability Drives Protein Droplet Formation on Microtubules to Nucleate Branches. *Nat. Phys.* **2021**, *17*, 493–498.
- (220) Mitchison, T. J. Colloid Osmotic Parameterization and Measurement of Subcellular Crowding. *Mol. Biol. Cell* **2019**, *30*, 173–180.
- (221) Potemkin, I. I.; Vasilevskaya, V. V.; Khokhlov, A. R. Associating Polyelectrolytes: Finite Size Cluster Stabilization Versus Physical Gel Formation. *J. Chem. Phys.* **1999**, *111*, 2809–2817.
- (222) Brady, J. P.; Farber, P. J.; Sekhar, A.; Lin, Y.-H.; Huang, R.; Bah, A.; Nott, T. J.; Chan, H. S.; Baldwin, A. J.; Forman-Kay, J. D.; et al. Structural and Hydrodynamic Properties of an Intrinsically Disordered Region of a Germ Cell-Specific Protein on Phase Separation. *Proc. Natl. Acad. Sci. U. S. A.* 2017, 114, No. E8194-E8203.
- (223) Shin, Y.; Berry, J.; Pannucci, N.; Haataja, M. P.; Toettcher, J. E.; Brangwynne, C. P. Spatiotemporal Control of Intracellular Phase Transitions Using Light-Activated Optodroplets. *Cell* **2017**, *168*, 159–171
- (224) Qian, D.; Welsh, T. J.; Erkamp, N. A.; Qamar, S.; Nixon-Abell, J.; Krainer, G.; George-Hyslop, P. S.; Michaels, T. C. T.; Knowles, T. P. J. Tie-Lines Reveal Interactions Driving Heteromolecular Condensate Formation. *Phys. Rev. X* **2022**, *12*, 041038.
- (225) André, A. A. M.; Yewdall, N. A.; Spruijt, E. Crowding-Induced Phase Separation and Solidification by Co-Condensation of Peg in Npm1-Rrna Condensates. *Biophys. J.* **2023**, *122*, 397.
- (226) Bremer, A.; Posey, A. E.; Borgia, M. B.; Borcherds, W. M.; Farag, M.; Pappu, R. V.; Mittag, T. Quantifying Coexistence Concentrations in Multi-Component Phase-Separating Systems Using Analytical Hplc. *Biomol.* 2022, *12*, 1480.
- (227) Zeng, X.; Holehouse, A. S.; Chilkoti, A.; Mittag, T.; Pappu, R. V. Connecting Coil-to-Globule Transitions to Full Phase Diagrams for Intrinsically Disordered Proteins. *Biophys. J.* **2020**, *119*, 402–418.
- (228) Honerkamp-Smith, A. R.; Veatch, S. L.; Keller, S. L. An Introduction to Critical Points for Biophysicists; Observations of Compositional Heterogeneity in Lipid Membranes. *Biochim. Biophys. Acta* **2009**, *1788*, 53–63.
- (229) Dignon, G. L.; Zheng, W.; Kim, Y. C.; Best, R. B.; Mittal, J. Sequence Determinants of Protein Phase Behavior from a Coarse-Grained Model. *PLOS Comput. Biol.* **2018**, *14*, No. e1005941.

- (230) Joseph, J. A.; Reinhardt, A.; Aguirre, A.; Chew, P. Y.; Russell, K. O.; Espinosa, J. R.; Garaizar, A.; Collepardo-Guevara, R. Physics-Driven Coarse-Grained Model for Biomolecular Phase Separation with near-Quantitative Accuracy. *Nature Comput. Sci.* **2021**, *1*, 732–743.
- (231) Landau, L. The Theory of Phase Transitions. *Nature* **1936**, *138*, 840–841.
- (232) Dignon, G. L.; Zheng, W.; Best, R. B.; Kim, Y. C.; Mittal, J. Relation between Single-Molecule Properties and Phase Behavior of Intrinsically Disordered Proteins. *Proc. Natl. Acad. Sci. U. S. A.* **2018**, 115, 9929–9934.
- (233) Lin, Y.-H.; Forman-Kay, J. D.; Chan, H. S. Sequence-Specific Polyampholyte Phase Separation in Membraneless Organelles. *Phys. Rev. Lett.* **2016**, *117*, 178101.
- (234) Dobashi, T.; Nakata, M.; Kaneko, M. Coexistence Curve of Polystyrene in Methylcyclohexane. I. Range of Simple Scaling and Critical Exponents. *J. Chem. Phys.* **1980**, 72, 6685–6691.
- (235) Su, X.; Ditlev, J. A.; Hui, E.; Xing, W.; Banjade, S.; Okrut, J.; King, D. S.; Taunton, J.; Rosen, M. K.; Vale, R. D. Phase Separation of Signaling Molecules Promotes T Cell Receptor Signal Transduction. *Science* **2016**, *352*, 595–599.
- (236) Langdon, E. M.; Qiu, Y.; Ghanbari Niaki, A.; McLaughlin, G. A.; Weidmann, C. A.; Gerbich, T. M.; Smith, J. A.; Crutchley, J. M.; Termini, C. M.; Weeks, K. M.; et al. Mrna Structure Determines Specificity of a Polyq-Driven Phase Separation. *Science* **2018**, *360*, 922–927.
- (237) McSwiggen, D. T.; Mir, M.; Darzacq, X.; Tjian, R. Evaluating Phase Separation in Live Cells: Diagnosis, Caveats, and Functional Consequences. *Genes Dev.* **2019**, 33, 1619–1634.
- (238) Sanders, D. W.; Kedersha, N.; Lee, D. S. W.; Strom, A. R.; Drake, V.; Riback, J. A.; Bracha, D.; Eeftens, J. M.; Iwanicki, A.; Wang, A.; et al. Competing Protein-Rna Interaction Networks Control Multiphase Intracellular Organization. *Cell* **2020**, *181*, 306–324.
- (239) Xing, W.; Muhlrad, D.; Parker, R.; Rosen, M. K. A Quantitative Inventory of Yeast P Body Proteins Reveals Principles of Composition and Specificity. *eLife* **2020**, *9*, No. e56525.
- (240) Zwicker, D.; Laan, L. Evolved Interactions Stabilize Many Coexisting Phases in Multicomponent Liquids. *Proc. Natl. Acad. Sci. U. S. A.* **2022**, *119*, No. e2201250119.
- (241) Emenecker, R. J.; Holehouse, A. S.; Strader, L. C. Sequence Determinants of in Cell Condensate Morphology, Dynamics, and Oligomerization as Measured by Number and Brightness Analysis. *Cell Commun. Signal.* **2021**, *19*, 65.
- (242) Robert, C. H.; Decker, H.; Richey, B.; Gill, S. J.; Wyman, J. Nesting: Hierarchies of Allosteric Interactions. *Proc. Natl. Acad. Sci. U. S. A.* 1987, 84, 1891–1895.
- (243) Wyman, J.; Gill, S. J. Conversations with Jeffries Wyman. Annu. Rev. Biophys. Biophys. Chem. 1987, 16, 1–24.
- (244) Wyman, J.; Gill, S. J. Binding and Linkage: Functional Chemistry of Biological Macromolecules; University Science Books, 1990.
- (245) Sugar, I. P. Cooperativity and Classification of Phase Transitions. Application to One- and Two-Component Phospholipid Membranes. *J. Phys. Chem.* **1987**, *91*, 95–101.
- (246) Xu, B.; He, G.; Weiner, B. G.; Ronceray, P.; Meir, Y.; Jonikas, M. C.; Wingreen, N. S. Rigidity Enhances a Magic-Number Effect in Polymer Phase Separation. *Nature Commun.* **2020**, *11*, 1561.
- (247) Jang, S.; Xuan, Z.; Lagoy, R. C.; Jawerth, L. M.; Gonzalez, I. J.; Singh, M.; Prashad, S.; Kim, H. S.; Patel, A.; Albrecht, D. R.; et al. Phosphofructokinase Relocalizes into Subcellular Compartments with Liquid-Like Properties in Vivo. *Biophys. J.* 2021, 120, 1170–1186.
- (248) Bouchard, J. J.; Otero, J. H.; Scott, D. C.; Szulc, E.; Martin, E. W.; Sabri, N.; Granata, D.; Marzahn, M. R.; Lindorff-Larsen, K.; Salvatella, X.; et al. Cancer Mutations of the Tumor Suppressor Spop Disrupt the Formation of Active, Phase-Separated Compartments. *Mol. Cell* **2018**, 72, 19–36.
- (249) Emenecker, R. J.; Holehouse, A. S.; Strader, L. C. Biological Phase Separation and Biomolecular Condensates in Plants. *Annu. Rev. Plant Biol.* **2021**, 72, 17–46.
- (250) Borgia, A.; Borgia, M. B.; Bugge, K.; Kissling, V. M.; Heidarsson, P. O.; Fernandes, C. B.; Sottini, A.; Soranno, A.; Buholzer, K. J.; Nettels,

- D.; et al. Extreme Disorder in an Ultrahigh-Affinity Protein Complex. *Nature* **2018**, *555*, 61–66.
- (251) Heidarsson, P. O.; Mercadante, D.; Sottini, A.; Nettels, D.; Borgia, M. B.; Borgia, A.; Kilic, S.; Fierz, B.; Best, R. B.; Schuler, B. Release of Linker Histone from the Nucleosome Driven by Polyelectrolyte Competition with a Disordered Protein. *Nat. Chem.* **2022**, *14*, 224–231.
- (252) Tompa, P.; Fuxreiter, M. Fuzzy Complexes: Polymorphism and Structural Disorder in Protein—Protein Interactions. *Trend. Biochem. Sci.* **2008**, 33, 2–8.
- (253) Galvanetto, N.; Ivanović, M. T.; Chowdhury, A.; Sottini, A.; Nüesch, M. F.; Nettels, D.; Best, R. B.; Schuler, B. Ultrafast Molecular Dynamics Observed within a Dense Protein Condensate. *bioRxiv* **2022**.
- (254) Turner, A. L.; Watson, M.; Wilkins, O. G.; Cato, L.; Travers, A.; Thomas, J. O.; Stott, K. Highly Disordered Histone H1-DNA Model Complexes and Their Condensates. *Proc. Natl. Acad. Sci. U. S. A.* **2018**, *115*, 11964–11969.
- (255) Decker, C. J.; Parker, R. P-Bodies and Stress Granules: Possible Roles in the Control of Translation and Mrna Degradation. *Cold Spring Harb. Persp. Biol.* **2012**, *4*, a012286.
- (256) Klein, I. A.; Boija, A.; Afeyan, L. K.; Hawken, S. W.; Fan, M.; Dall'Agnese, A.; Oksuz, O.; Henninger, J. E.; Shrinivas, K.; Sabari, B. R.; et al. Partitioning of Cancer Therapeutics in Nuclear Condensates. *Science* **2020**, *368*, 1386–1392.
- (257) Felitsky, D. J.; Record, M. T. Application of the Local-Bulk Partitioning and Competitive Binding Models to Interpret Preferential Interactions of Glycine Betaine and Urea with Protein Surface. *Biochemistry* **2004**, *43*, 9276–9288.
- (258) Kozlov, A. G.; Cheng, X.; Zhang, H.; Shinn, M. K.; Weiland, E.; Nguyen, B.; Shkel, I. A.; Zytkiewicz, E.; Finkelstein, I. J.; Record, M. T.; et al. How Glutamate Promotes Liquid-Liquid Phase Separation and DNA Binding Cooperativity of E. Coli Ssb Protein. *J. Mol. Biol.* **2022**, 434, 167562.
- (259) Wyman, J.; Gill, S. J. Ligand-Linked Phase Changes in a Biological System: Applications to Sickle Cell Hemoglobin. *Proc. Natl. Acad. Sci. U. S. A.* **1980**, *77*, 5239–5242.
- (260) Ruff, K. M.; Dar, F.; Pappu, R. V. Ligand Effects on Phase Separation of Multivalent Macromolecules. *Proc. Natl. Acad. Sci. U. S. A.* **2021**, *118*, No. e2017184118.
- (261) Ruff, K. M.; Dar, F.; Pappu, R. V. Polyphasic Linkage and the Impact of Ligand Binding on the Regulation of Biomolecular Condensates. *Biophys. Rev.* **2021**, *2*, 021302.
- (262) Ghosh, A.; Mazarakos, K.; Zhou, H.-X. Three Archetypical Classes of Macromolecular Regulators of Protein Liquid-Liquid Phase Separation. *Proc. Natl. Acad. Sci. U. S. A.* **2019**, *116*, 19474–19483.
- (263) Dao, T. P; Yang, Y.; Presti, M. F; Cosgrove, M. S; Hopkins, J. B; Ma, W.; Loh, S. N; Castaneda, C. A Mechanistic Insights into the Enhancement or Inhibition of Phase Separation by Polyubiquitin Chains of Different Lengths or Linkages. *EMBO Rep.* **2022**, 23, No. e55056.
- (264) Ali, S.; Prabhu, V. M. Characterization of the Ultralow Interfacial Tension in Liquid-Liquid Phase Separated Polyelectrolyte Complex Coacervates by the Deformed Drop Retraction Method. *Macromolecules* **2019**, *52*, 7495–7502.
- (265) Bergeron-Sandoval, L. P.; Kumar, S.; Heris, H. K.; Chang, C. L. A.; Cornell, C. E.; Keller, S. L.; Francois, P.; Hendricks, A. G.; Ehrlicher, A. J.; Pappu, R. V.; et al. Endocytic Proteins with Prion-Like Domains Form Viscoelastic Condensates That Enable Membrane Remodeling. *Proc. Natl. Acad. Sci. U. S. A.* **2021**, *118*, No. e2113789118.
- (266) Wang, H.; Kelley, F. M.; Milovanovic, D.; Schuster, B. S.; Shi, Z. Surface Tension and Viscosity of Protein Condensates Quantified by Micropipette Aspiration. *Biophys. Rep.* **2021**, *1*, 100011.
- (267) Widom, B. Some Topics in the Theory of Fluids. *J. Chem. Phys.* **1963**, *39*, 2808–2812.
- (268) Schrader, M. E. Young-Dupre Revisited. *Langmuir* **1995**, *11*, 3585–3589.
- (269) Mukherjee, S.; Bagchi, B. Entropic Origin of the Attenuated Width of the Ice-Water Interface. *J. Phys. Chem. C* **2020**, *124*, 7334–7340.

- (270) Baldi, E.; Ceriotti, M.; Tribello, G. A. Extracting the Interfacial Free Energy and Anisotropy from a Smooth Fluctuating Dividing Surface. *J. Phys. Cond. Mater.* **2017**, *29*, 445001.
- (271) Ranganathan, S.; Shakhnovich, E. I. Dynamic Metastable Long-Living Droplets Formed by Sticker-Spacer Proteins. *eLife* **2020**, *9*, No. e56159.
- (272) Ma, W.; Zhen, G.; Xie, W.; Mayr, C. In Vivo Reconstitution Finds Multivalent Rna-Rna Interactions as Drivers of Mesh-Like Condensates. *eLife* **2021**, *10*, No. e64252.
- (273) Law, J. O.; Jones, C. M.; Stevenson, T.; Turner, M. S.; Kusumaatmaja, H.; Grellscheid, S. N. Using Shape Fluctuations to Probe the Mechanics of Stress Granules. *bioRxiv* 2022.
- (274) Taylor, N. O.; Wei, M. T.; Stone, H. A.; Brangwynne, C. P. Quantifying Dynamics in Phase-Separated Condensates Using Fluorescence Recovery after Photobleaching. *Biophys. J.* **2019**, *117*, 1285–1300.
- (275) Erkamp, N. A.; Farag, M.; Qian, D.; Sneideris, T.; Welsh, T. J.; Ausserwöger, H.; Weitz, D. A.; Pappu, R. V.; Knowles, T. P. J. Adsorption of Rna to Interfaces of Biomolecular Condensates Enables Wetting Transitions. *bioRxiv* 2023.
- (276) Aarts, D. G. A. L.; Schmidt, M.; Lekkerkerker, H. N. W. Direct Visual Observation of Thermal Capillary Waves. *Science* **2004**, *304*, 847–850.
- (277) Böddeker, T. J.; Rosowski, K. A.; Berchtold, D.; Emmanouilidis, L.; Han, Y.; Allain, F. H. T.; Style, R. W.; Pelkmans, L.; Dufresne, E. R. Non-Specific Adhesive Forces between Filaments and Membraneless Organelles. *Nat. Phys.* **2022**, *18*, 571–578.
- (278) Fisk, S.; Widom, B. Structure and Free Energy of the Interface between Fluid Phases in Equilibrium near the Critical Point. *J. Chem. Phys.* **1969**, *50*, 3219–3227.
- (279) Linsenmeier, M.; Faltova, L.; Palmiero, U. C.; Seiffert, C.; Küffner, A. M.; Pinotsi, D.; Zhou, J.; Mezzenga, R.; Arosio, P. The Interface of Condensates of the Hnrnpal Low Complexity Domain Promotes Formation of Amyloid Fibrils. *bioRxiv* 2022.
- (280) Stroberg, W.; Schnell, S. Do Cellular Condensates Accelerate Biochemical Reactions? Lessons from Microdroplet Chemistry. *Biophys. J.* **2018**, *115*, 3–8.
- (281) Tolman, R. C. Consideration of the Gibbs Theory of Surface Tension. J. Chem. Phys. 1948, 16, 758-774.
- (282) Kaplan, W. D.; Chatain, D.; Wynblatt, P.; Carter, W. C. A Review of Wetting Versus Adsorption, Complexions, and Related Phenomena: The Rosetta Stone of Wetting. J. Mater. Sci. 2013, 48, 5681–5717.
- (283) Morin, J. A.; Wittmann, S.; Choubey, S.; Klosin, A.; Golfier, S.; Hyman, A. A.; Jülicher, F.; Grill, S. W. Sequence-Dependent Surface Condensation of a Pioneer Transcription Factor on DNA. *Nat. Phys.* **2022**, *18*, 271.
- (284) Pederson, T. The Nucleolus. Cold Spring Harb. Persp. Biol. 2011, 3, a000638.
- (285) Shayegan, M.; Tahvildari, R.; Kisley, L.; Metera, K.; Michnick, S. W.; Leslie, S. R. Probing Inhomogeneous Diffusion in the Microenvironments of Phase-Separated Polymers under Confinement. *J. Am. Chem. Soc.* **2019**, *141*, 7751–7757.
- (286) Cai, L.-H.; Panyukov, S.; Rubinstein, M. Hopping Diffusion of Nanoparticles in Polymer Matrices. *Macromolecules* **2015**, *48*, 847–862.
- (287) Cai, L.-H.; Panyukov, S.; Rubinstein, M. Mobility of Nonsticky Nanoparticles in Polymer Liquids. *Macromolecules* **2011**, 44, 7853–7863.
- (288) Jiang, N.; Zhang, H.; Tang, P.; Yang, Y. Linear Viscoelasticity of Associative Polymers: Sticky Rouse Model and the Role of Bridges. *Macromolecules* **2020**, *53*, 3438–3451.
- (289) Deopa, S. P. S.; Rajput, S. S.; Kumar, A.; Patil, S. Direct and Simultaneous Measurement of the Stiffness and Internal Friction of a Single Folded Protein. *J. Phys. Chem. Lett.* **2022**, *13*, 9473–9479.
- (290) Shen, Y.; Ruggeri, F. S.; Vigolo, D.; Kamada, A.; Qamar, S.; Levin, A.; Iserman, C.; Alberti, S.; George-Hyslop, P. S.; Knowles, T. P. J. Biomolecular Condensates Undergo a Generic Shear-Mediated Liquid-to-Solid Transition. *Nat. Nanotechnol.* **2020**, *15*, 841–847.

- (291) Ghosh, A.; Kota, D.; Zhou, H.-X. Shear Relaxation Governs Fusion Dynamics of Biomolecular Condensates. *Nature Commun.* **2021**, *12*, 5995.
- (292) Zhou, H.-X. Viscoelasticity of Biomolecular Condensates Conforms to the Jeffreys Model. J. Chem. Phys. 2021, 154, 041103.
- (293) Dahiya, P.; Caggioni, M.; Spicer, P. T. Arrested Coalescence of Viscoelastic Droplets: Polydisperse Doublets. *Philos. Trans. Royal Soc. A* **2016**, *374*, 20150132.
- (294) Alshareedah, I.; Moosa, M. M.; Pham, M.; Potoyan, D. A.; Banerjee, P. R. Programmable Viscoelasticity in Protein-Rna Condensates with Disordered Sticker-Spacer Polypeptides. *Nature Commun.* **2021**, *12*, 6620.
- (295) Nott, T. J.; Craggs, T. D.; Baldwin, A. J. Membraneless Organelles Can Melt Nucleic Acid Duplexes and Act as Biomolecular Filters. *Nat. Chem.* **2016**, *8*, 569–575.
- (296) Zaslavsky, B. Y. Bioanalytical Applications of Partitioning in Aqueous Polymer Two-Phase Systems. *Anal. Chem.* **1992**, *64*, 765A–773A.
- (297) Huggins, D. J. Application of Inhomogeneous Fluid Solvation Theory to Model the Distribution and Thermodynamics of Water Molecules around Biomolecules. *Phys. Chem. Chem. Phys.* **2012**, *14*, 15106–15117.
- (298) Callaway, E. The Revolution Will Not Be Crystallized: A New Method Sweeps through Structural Biology. *Nature* **2015**, *525*, 172–174.
- (299) Di Cera, E. Site-Specific Thermodynamics: Understanding Cooperativity in Molecular Recognition. *Chem. Rev.* **1998**, *98*, 1563–1502
- (300) Schmid, F. Understanding and Modeling Polymers: The Challenge of Multiple Scales. ACS Polymers Au 2023, 3, 28.
- (301) Burley, S. K.; Petsko, G. A. Weakly Polar Interactions in Proteins. *Adv. Protein Chem.* **1988**, 39, 125–189.
- (302) Zeng, X.; Ruff, K. M.; Pappu, R. V. Competing Interactions Give Rise to Two-State Behavior and Switch-Like Transitions in Charge-Rich Intrinsically Disordered Proteins. *Proc. Natl. Acad. Sci. U. S. A.* **2022**, *119*, No. e2200559119.
- (303) Di Cera, E.; Gill, S. J.; Wyman, J. Binding Capacity: Cooperativity and Buffering in Biopolymers. *Proc. Natl. Acad. Sci. U. S. A.* 1988, 85, 449–452.
- (304) Martin, E. W.; Holehouse, A. S. Intrinsically Disordered Protein Regions and Phase Separation: Sequence Determinants of Assembly or Lack Thereof. *Emerging Topics in Life Sciences* **2020**, *4*, 307–329.
- (305) Zarin, T.; Strome, B.; Peng, G.; Pritišanac, I.; Forman-Kay, J. D.; Moses, A. M. Identifying Molecular Features That Are Associated with Biological Function of Intrinsically Disordered Protein Regions. *eLife* **2021**, *10*, No. e60220.
- (306) Sangster, A. G.; Zarin, T.; Moses, A. M. Evolution of Short Linear Motifs and Disordered Proteins Topic: Yeast as Model System to Study Evolution. *Curr. Opin. Gen. Dev.* **2022**, *76*, 101964.
- (307) Feng, Z.; Jia, B.; Zhang, M. Liquid-Liquid Phase Separation in Biology: Specific Stoichiometric Molecular Interactions Vs Promiscuous Interactions Mediated by Disordered Sequences. *Biochemistry* **2021**, *60*, 2397–2406.
- (308) Sherry, K. P.; Das, R. K.; Pappu, R. V.; Barrick, D. Control of Transcriptional Activity by Design of Charge Patterning in the Intrinsically Disordered Ram Region of the Notch Receptor. *Proc. Natl. Acad. Sci. U. S. A.* **2017**, *114*, No. E9243-E9252.
- (309) Das, R. K.; Mittal, A.; Pappu, R. V. How Is Functional Specificity Achieved through Disordered Regions of Proteins? *BioEssays* **2013**, *35*, 17–22.
- (310) Kozlov, A. G.; Jezewska, M. J.; Bujalowski, W.; Lohman, T. M. Binding Specificity of Escherichia Coli Single-Stranded DNA Binding Protein for the X Subunit of DNA Pol Iii Holoenzyme and Pria Helicase. *Biochemistry* **2010**, *49*, 3555–3566.
- (311) Randles, L. G.; Batey, S.; Steward, A.; Clarke, J. Distinguishing Specific and Nonspecific Interdomain Interactions in Multidomain Proteins. *Biophys. J.* **2008**, *94*, *622*–*628*.
- (312) Staller, M. V.; Ramirez, E.; Kotha, S. R.; Holehouse, A. S.; Pappu, R. V.; Cohen, B. A. Directed Mutational Scanning Reveals a

- Balance between Acidic and Hydrophobic Residues in Strong Human Activation Domains. *Cell Sys.* **2022**, *13*, 334–345.
- (313) González-Foutel, N. S.; Glavina, J.; Borcherds, W. M.; Safranchik, M.; Barrera-Vilarmau, S.; Sagar, A.; Estaña, A.; Barozet, A.; Garrone, N. A.; Fernandez-Ballester, G.; et al. Conformational Buffering Underlies Functional Selection in Intrinsically Disordered Protein Regions. *Nature Struc. Mol. Biol.* **2022**, *29*, 781–790.
- (314) Adamski, W.; Salvi, N.; Maurin, D.; Magnat, J.; Milles, S.; Jensen, M. R.; Abyzov, A.; Moreau, C. J.; Blackledge, M. A Unified Description of Intrinsically Disordered Protein Dynamics under Physiological Conditions Using Nmr Spectroscopy. *J. Am. Chem. Soc.* **2019**, *141*, 17817–17829.
- (315) Jensen, M. R.; Ruigrok, R. W. H.; Blackledge, M. Describing Intrinsically Disordered Proteins at Atomic Resolution by Nmr. *Curr. Opin. Struct. Biol.* **2013**, 23, 426–435.
- (316) Shinn, M. K.; Cohan, M. C.; Bullock, J. L.; Ruff, K. M.; Levin, P. A.; Pappu, R. V. Connecting Sequence Features within the Disordered C-Terminal Linker of Bacillus Subtilis Ftsz to Functions and Bacterial Cell Division. *Proc. Natl. Acad. Sci. U. S. A.* **2022**, *119*, No. e2211178119.
- (317) Cohan, M. C.; Ruff, K. M.; Pappu, R. V. Information Theoretic Measures for Quantifying Sequence-Ensemble Relationships of Intrinsically Disordered Proteins. *Protein Eng. Des. Selec.* **2019**, 32, 191–202.
- (318) Wiggers, F.; Wohl, S.; Dubovetskyi, A.; Rosenblum, G.; Zheng, W.; Hofmann, H. Diffusion of a Disordered Protein on Its Folded Ligand. *Proc. Natl. Acad. Sci. U. S. A.* **2021**, *118*, No. e2106690118.
- (319) Vancraenenbroeck, R.; Harel, Y. S.; Zheng, W.; Hofmann, H. Polymer Effects Modulate Binding Affinities in Disordered Proteins. *Proc. Natl. Acad. Sci. U. S. A.* **2019**, *116*, 19506–19512.
- (320) Shammas, S. L.; Rogers, J. M.; Hill, S. A.; Clarke, J. Slow, Reversible, Coupled Folding and Binding of the Spectrin Tetramerization Domain. *Biophys. J.* **2012**, *103*, 2203–2214.
- (321) Ferrie, J. J.; Karr, J. P.; Tjian, R.; Darzacq, X. Structure"-Function Relationships in Eukaryotic Transcription Factors: The Role of Intrinsically Disordered Regions in Gene Regulation. *Mol. Cell* **2022**, 82, 3970–3984.
- (322) Rogers, J. M.; Oleinikovas, V.; Shammas, S. L.; Wong, C. T.; De Sancho, D.; Baker, C. M.; Clarke, J. Interplay between Partner and Ligand Facilitates the Folding and Binding of an Intrinsically Disordered Protein. *Proc. Natl. Acad. Sci. U. S. A.* **2014**, *111*, 15420–15425.
- (323) Salvi, N.; Abyzov, A.; Blackledge, M. Multi-Timescale Dynamics in Intrinsically Disordered Proteins from Nmr Relaxation and Molecular Simulation. *J. Phys. Chem. Lett.* **2016**, 7, 2483–2489.
- (324) Parigi, G.; Rezaei-Ghaleh, N.; Giachetti, A.; Becker, S.; Fernandez, C.; Blackledge, M.; Griesinger, C.; Zweckstetter, M.; Luchinat, C. Long-Range Correlated Dynamics in Intrinsically Disordered Proteins. *J. Am. Chem. Soc.* **2014**, *136*, 16201–16209.
- (325) Salvi, N.; Abyzov, A.; Blackledge, M. Solvent-Dependent Segmental Dynamics in Intrinsically Disordered Proteins. *Sci. Adv.* **2019**, *5*, No. eaax2348.
- (326) Borg, M.; Mittag, T.; Pawson, T.; Tyers, M.; Forman-Kay, J. D.; Chan, H. S. Polyelectrostatic Interactions of Disordered Ligands Suggest a Physical Basis for Ultrasensitivity. *Proc. Natl. Acad. Sci. U. S. A.* **2007**, *104*, 9650–9655.
- (327) Lyle, N.; Das, R. K.; Pappu, R. V. A Quantitative Measure for Protein Conformational Heterogeneity. *J. Chem. Phys.* **2013**, *139*, 121907.
- (328) Choi, J.-M.; Pappu, R. V. Experimentally Derived and Computationally Optimized Backbone Conformational Statistics for Blocked Amino Acids. J. Chem. Theory Comput.h 2019, 15, 1355–1366.
- (329) Fossat, M. J.; Zeng, X.; Pappu, R. V. Uncovering Differences in Hydration Free Energies and Structures for Model Compound Mimics of Charged Side Chains of Amino Acids. *J. Phys. Chem. B* **2021**, *125*, 4148–4161.
- (330) Roesgaard, M. A.; Lundsgaard, J. E.; Newcombe, E. A.; Jacobsen, N. L.; Pesce, F.; Tranchant, E. E.; Lindemose, S.; Prestel, A.; Hartmann-Petersen, R.; Lindorff-Larsen, K.; et al. Deciphering the

- Alphabet of Disorder-Glu and Asp Act Differently on Local but Not Global Properties. *Biomol.* **2022**, *12*, 1426.
- (331) Chakraborty, A. K.; Bratko, D. A Simple Theory and Monte Carlo Simulations for Recognition between Random Heteropolymers and Disordered Surfaces. *J. Chem. Phys.* **1998**, *108*, 1676–1682.
- (332) Holehouse, A. S.; Ginell, G. M.; Griffith, D.; Böke, E. Clustering of Aromatic Residues in Prion-Like Domains Can Tune the Formation, State, and Organization of Biomolecular Condensates. *Biochemistry* **2021**, *60*, 3566–3581.
- (333) Maharana, S.; Wang, J.; Papadopoulos, D. K.; Richter, D.; Pozniakovsky, A.; Poser, I.; Bickle, M.; Rizk, S.; Guillén-Boixet, J.; Franzmann, T. M.; et al. Rna Buffers the Phase Separation Behavior of Prion-Like Rna Binding Proteins. *Science* **2018**, *360*, 918–921.